UNIVERSITÀ DEGLI STUDI DI MILANO
FACOLTÀ DI MEDICINA E CHIRURGIA

Dipartimento di Scienze Cliniche e di Comunità
Scuola di Dottorato in Scienze Biomediche Cliniche e Sperimentali

CORSO DI DOTTORATO
Biotecnologie Applicate alle Scienze Mediche
XXVI CICLO

TESI DI DOTTORATO DI RICERCA
p53 and Microtubules Targeting as a Novel Strategy with Potential for Treatment of Aggressive Poorly Differentiated Thyroid Cancer

Settori Scientifico Disciplinari
BIO/13 - BIO/14 - MED/06 - MED/13

Elisa Stellaria Grassi
Matricola Nr R09281

Relatore: Chiar.mo Prof. Luca Persani

Coordinatore: Chiar.mo Prof. Alessandro Gianni

Anno Accademico
2012/2013

To all the people who keep asking me when I will be a "real doctor"

A tutte le persone che continuano a chiedermi quando saro' un "medico vero"

ABSTRACT

Thyroid cancer is the most common endocrine malignancy and his global incidence has rapidly increased in last decades. Despite the major part of thyroid cancer is represented by well differentiated hystotypes, the acquisition of additional mutations, such as p53 and β-catenin ones, causes loss of differentiation and confer high malignancy. Current treatment for undifferentiated thyroid cancers is regarded as almost ineffective, with a median survival of 3- 4 months, somewhat better in localized and worse in metastatic disease.

SP600125 is a multi-kinase inhibitor that has recently been shown to be a promising anticancer drug. In the last five years it has been proved able to induce endoreduplication and subsequent polyploidization, but there are contrasting results about its intracellular actions and there is no evidence on the specific mechanism of action. Moreover, in 2012, SP600125 has been found to be the most effective against p53 deficient cells among more than 300 screened compounds. However, opposite results have also been obtained depending on cell type, concentration and time of incubation.

In the current study the effects of micromolar doses of SP600125 have been characterized in six thyroid cancer cell lines with different p53 status. The results show that at low concentrations SP600125 dramatically reduces the proliferation of p53 mutated cells, with lesser effects on p53 null and no effects on the wild-type ones. In p53 mutated cells it has been proved able to induce p53 nuclear translocation and phosphorylation at serine 15; this modification resulted to be responsible of increased levels of p21.

Importantly other considerable novel effects have been revealed. Firstly, SP600125 caused alterations of microtubule dynamics in p53 mutated cells, with increase of acetylation levels and loss of Microtubule Organizing Center (MTOC)-periphery organization. These effects were accompanied by alterations in cellular morphology and in late endosome/lysosome trafficking. Endoreduplication and alteration of microtubule dynamics finally resulted in aberrant mitosis and cell death. The second mechanism involves alteration of cellular motility: different kinases involved in this process are affected by SP600125 treatment and β-catenin remains at the intercellular junctions in affected cells,consistent with a failure of cell detachment (a figure consistent with inhibition of cell migration/motility). Microtubule alterations concomitantly also account for motility alterations. Both tubulin and β-catenin variations are due to HDAC6 activity alterations. This enzyme regulates the levels of acetylation of these proteins and is profoundly inhibited following SP600125 in p53 deficient cells. Alteration of HDAC6 activity is

hypothesized to be the result of SP600125 direct inhibition of ROCK2, an upstream kinase regulator of HDAC6 activity.

In conclusion SP600125 is a promising drug particularly active on p53-mutated cancers at concentrations unable to affect normal cell viability. The effects of SP600125 action include arrest of tumor growth, and importantly induction of tumor cell death and metastatic diffusion inhibition.

TABLE

OF

CONTENTS

Chapters' Index

Figures' Index - Introduction

Figures' Index - Results

Tables' Index

INTRODUCTION

I

THYROID CANCER

1.1 THYROID CANCER: EPIDEMIOLOGY AND CLASSIFICATION

Thyroid cancer is the most common endocrine malignancy and his global incidence has rapidly increased in last decades [1]; every year it is responsible of more deaths than all other endocrine cancers combined [2]. Although the death rate is relatively low, disease recourrence or persistence is high, particularly for more advanced ones. It is estimated that in US 62,980 men and women will be diagnosed with and 1,890 men and women will die of cancer of the thyroid in 2014 [3-4]. There is a significant prevalence in female vs. male incidence with a 3:1 ratio; incidence rates reach a peak around 50 years of age for women and 60 years for men.
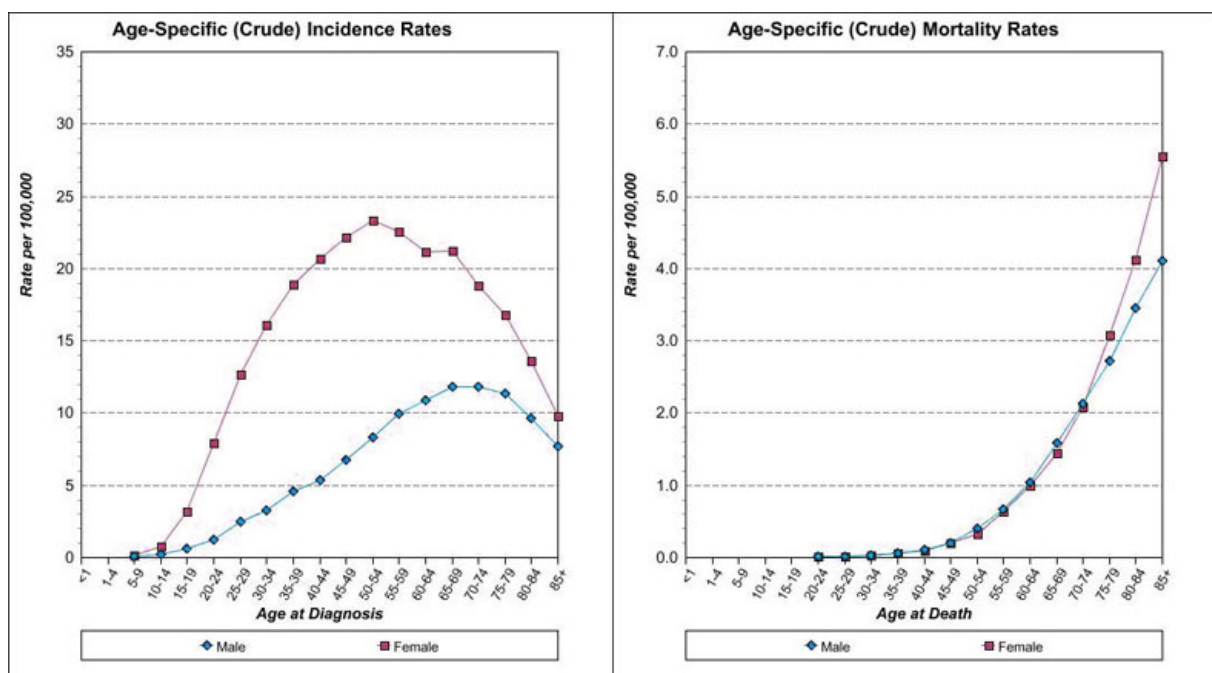
Fig 1. Thyroid cancer incidence and mortality rates. SEER epidemiological data [3].
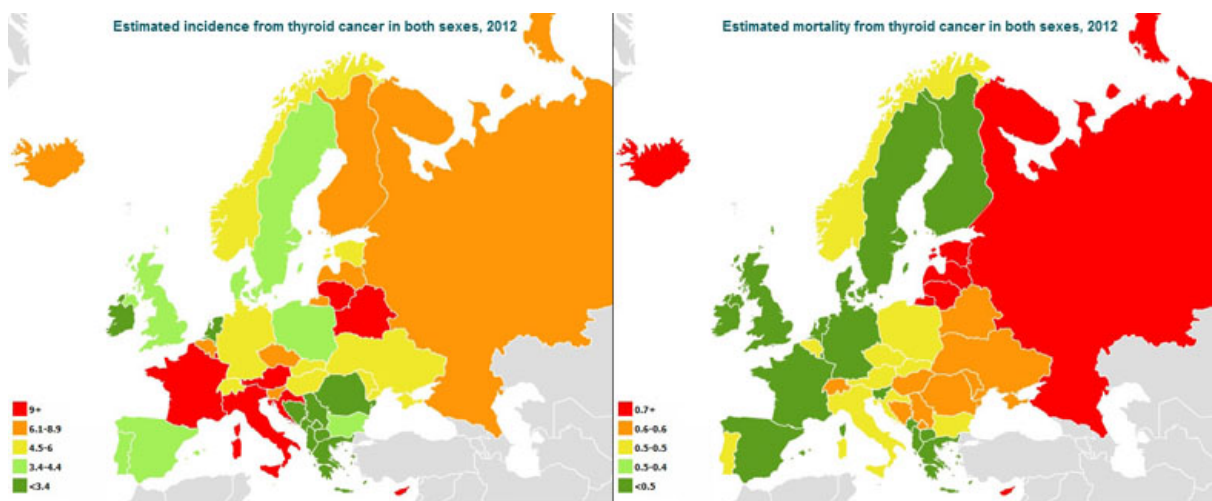
Fig 2. Thyroid cancer incidence and mortality rates in European Countries. IARC epidemiological data [5].

3

Worldwide incidence rates are highly variable probably as a result of local environment, age, sex and ethnical influences [2]. Rates have been observed to be high in certain geographic areas such as Hawaii, particularly among Chinese and Filipinos, while rates in Poland are among the lowest recorded [2, 6].

In the last 50 years thyroid cancer incidence has more than doubled, with highest increase in papillary histotype, mainly due to new small sized tumors diagnoses; There was no significant change in the incidence of the less common histological categories: follicular, medullary, and anaplastic [7-8]. Despite increasing incidence, the mortality from thyroid cancer has remained stable through years.

There are different types and subtypes of thyroid cancers, classified by cellular origins, characteristics and prognoses [9]. Follicular thyroid cells derived tumors include papillary thyroid cancer (PTC), follicular thyroid cancer (FTC), poorly differentiated thyroid cancer (PDTC) and anaplastic thyroid cancer (ATC); parafollicular C cells derived cancers are medullary thyroid cancers (MTC).

origin	Tumor type	Standard care and prognosis	Characteristics
Follicular thyroid cells	Papillary Thyroid Cancer (PTC)	Thyroidectomy and, in selected cases, radioiodine ablation; novel drugs for resistant disease. Good overall prognosis.	Well differentiated, with papillary architecture and characteristic nuclear features that include enlargement, oval shape, elongation, overlapping and clearing, inclusions and grooves; propensity for lymphatic metastasis; PTC subtypes include conventional PTC (CPTC), follicular-variant PTC (FVPTC), tall-cell PTC (TCPTC) and a few rare variants.
	Follicular Thyroid Cancer (FTC)	Thyroidectomy and radioiodine ablation; novel drugs for resistant cases. Good overall prognosis.	Well differentiated, hypercellular, microfollicular patterns, lacking nuclear features of PTC; vascular or capsular invasion; propensity for metastasis via the blood stream; Hürthle cell thyroid cancer is a unique subtype of FTC that accounts for 2–3% of thyroid cancers and is characterized by large, mitochondria-rich oncocytic cells and dense nuclei and nucleoli, as well as a high propensity for metastasis and a poor prognosis.
	Poorly Differentiated Thyroid Cancer (PDTC)	Surgery, chemotherapy, radiotherapy, novel drugs. Poor prognosis.	Poorly differentiated, often overlapping with PTC and FTC; intermediate aggressiveness between differentiated and undifferentiated thyroid cancers.
	Anaplastic Thyroid Cancer (ATC)	Surgery, chemotherapy, radiotherapy, novel drugs, palliative care. Highly and rapidly lethal.	Undifferentiated; admixture of spindle, pleomorphic giant and epithelioid cells; extremely invasive and metastatic; highly lethal; may occur de novo or derive from PTC, FTC or PDTC.
C cells	Medullary Thyroid Cancer (MTC)	Surgery, chemotherapy, radiotherapy, novel drugs.	Moderate aggressiveness, high propensity for lymphatic metastasis; RET mutation; occurring in familial, MEN2 or sporadic forms.

Table 1. Main thyroid tumors and their characteristics. Adapted from [10]
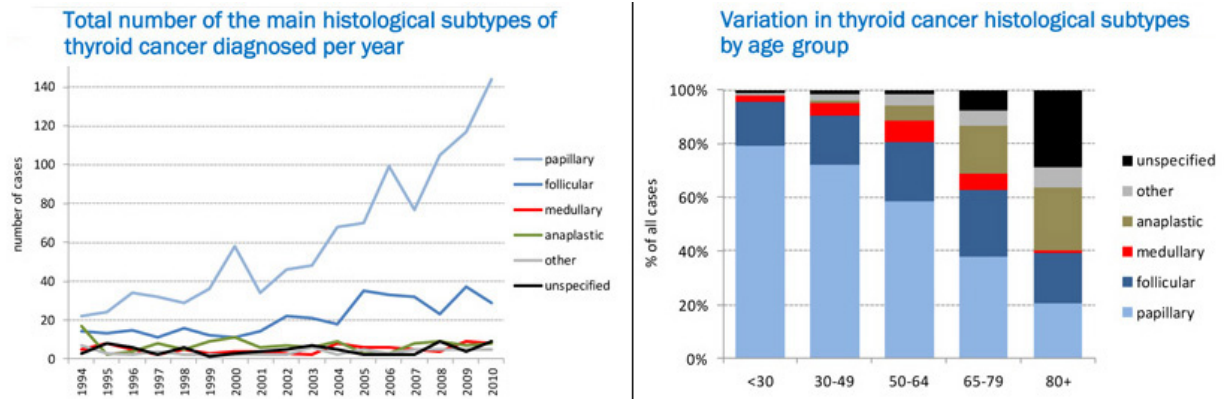
Fig 3. Histological subtypes statistics. Epidemiological data from [3, 5].

1.2 THYROID CANCER: PATHOGENESIS AND GENETIC ALTERATIONS

Thyroid cells proliferation depends on the combined activation of cAMP/PKA, MAPK and PI3K pathways, as a result of TSH or Growth Factors stimulation; it is well known that alterations in genes involved in these signalling pathways play a prominent role in the development of thyroid cancer.
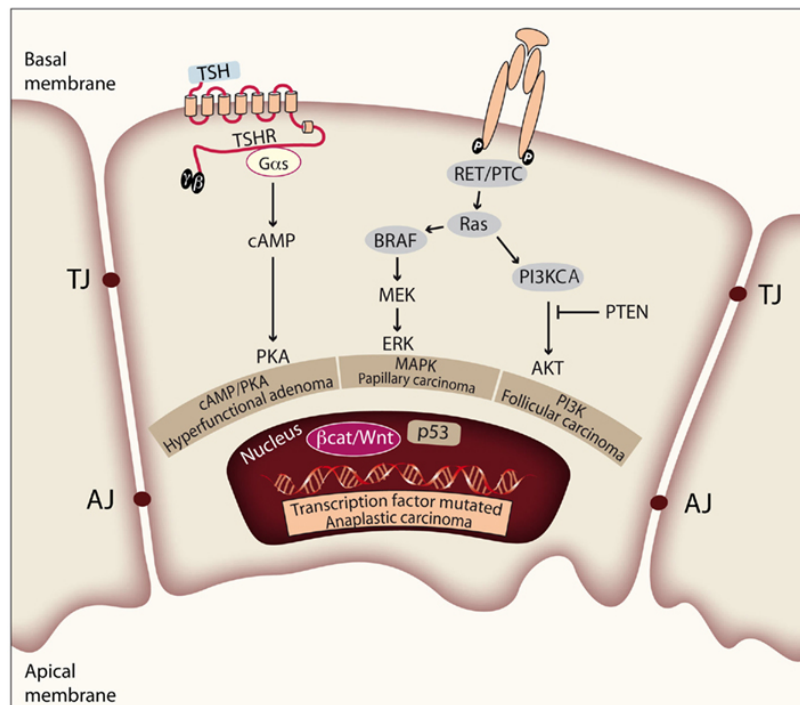
Fig 4. Pathways involved in thyroid tumorigenesis. Thyroid cell proliferation depends on the combined activation of cAMP/PKA, MAPK, and PI3K pathways, induced by TSH and other growth factors. Mutations of effectors along these signaling pathways play prominent roles in the pathogenesis of thyroid neoplasia. Adapted from [11].

Thyroid cancer pathogenesis is classically view as an accumulation of different genetic alterations that drive progression through a dedifferentiation process [11-12].
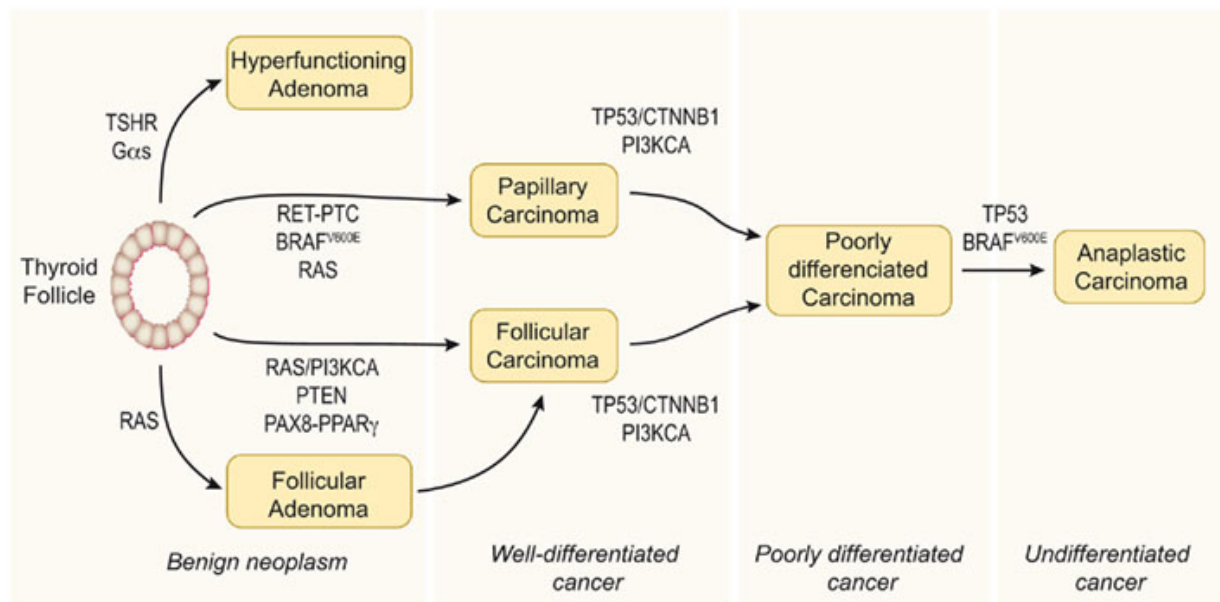
Fig 5. Step model of thyroid carcinogenesis. The well-differentiated thyroid follicular cell may give rise to both benign and malignant tumors. After gaining mutations in different oncogenes and tumor suppressor genes, the differentiated thyroid follicle can give rise to well-differentiated papillary or follicular carcinomas, poorly differentiated carcinoma, and anaplastic carcinoma. Adapted from [11]

Numerous genetic alterations that have a fondamental role in the pathogenesis of thyroid cancer have been identified. The most frequent point mutation is BRAF T1799A which results in the constitutional active protein BRAF^{V600E}; it occours in half of the PTCs and it's associated with poor clinico-pathological outcomes [13-16]. RAS isoforms activating mutations play a consistent role in FTCs pathogenesis although additional genetic alterations are required for cancer development [10, 17]. PTEN deletions results in PI3K-AKT pathway activation and are primarily responsible of FTCs development. PI3CA, CTNNB1 and p53 mutations are mainly responsible of thyroid cancer progression toward less differentiated and most aggressive histotypes [10].

In addition to point mutation, copy number gains are common for genes encoding RTKs and PI3K-AKT family members; they are prevalent in PDTC and ATC, suggesting a predominant role in progression of thyroid cancers [10, 17]. The most frequent oncogenic rearrangement in thyroid cancer is RET-PTC, which can occur in PTC [10, 18]. Another important rearrangement is PAX8-PPARG, often found in FTC [10].

Mutations	Primary signalling pathways affected	Functional impact on the protein and tumor
BRAF[V600E]	MAPK	Activating; promoting tumorigenesis, invasion, metastasis, recurrence and mortality
HRAS, KRAS, NRAS	MAPK PI3K–AKT	Activating; promoting tumorigenesis, invasion and metastasis of PDTC and FTC
PTEN (mutation)	PI3K–AKT	Inactivating the gene but activating the PI3K pathway; promoting tumorigenesis and invasiveness
PTEN (deletion)	PI3K–AKT	Inactivating the gene but activating the PI3K pathway; promoting tumorigenesis and invasiveness
PIK3CA	PI3K–AKT	Activating; promoting tumorigenesis and invasiveness
AKT1	PI3K–AKT	Unclear; seems to favour metastasis
CTNNB1	WNT–β-catenin	Activating; promoting tumour progression
TP53	p53-coupled pathways	Inactivating; promoting tumour progression
IDH1	IDH1-associated metabolic pathways	Inactivating; impact on tumours is unclear

Table 2. Principal mutations in thyroid cancer.
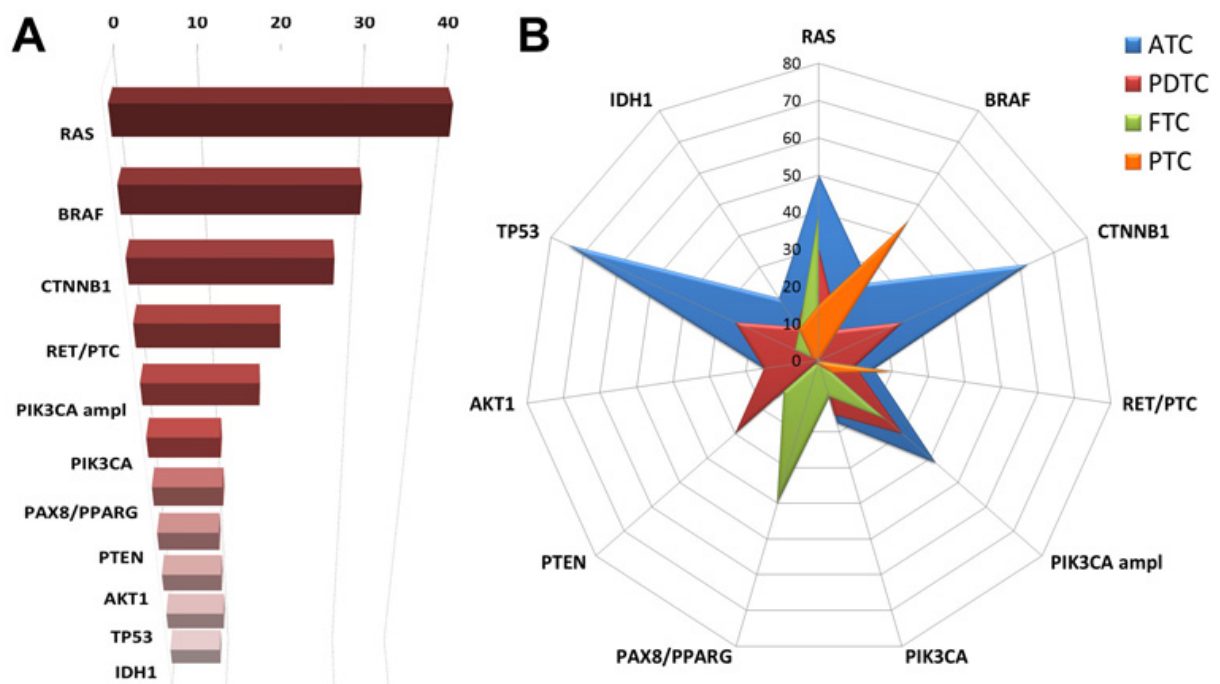
Fig 6. Principal mutations in thyroid cancer. A: overall prevalence; B: prevalence in thyroid cancer histological types.

7

Almost all the mutations involved in thyroid cancer insorgence influence mainly two intracellular signalling pathways, MAPK and PI3K-AKT.

The MAPK pathway play a fundamental role in the regulation of cell proliferation and survival and it is mainly involved in PTC tumorigenesis; mutations in RAS and BRAF result in constitutional activation of this pathway and confer tranformed cell growth advantage. Carcinogenesis often implies a wide range of secondary molecular alterations that amplify the oncogenic activity of primary ones.

PI3K-AKT pathway plays a fundamental role in FTC evolution as well as in the acquisition of metastatic potential; hyperactivation is mainly due to PTEN deletions and PIK3CA and AKT copy gain.

The signalling pathways involved in progression toward undifferentiated types are mainly WNT-b-catenin and p53; aberrant activation of WNT signalling can be a direct consequence of PI3K-AKT pathway hyperactivation or result from mutations in CTNNB1 gene.

1.3 THYROID CANCER: CONVENTIONAL THERAPIES AND NEW DRUGS

In general, treatment of DTC consists of three strategies, depending on disease extent:

- thyroid surgery with or without neck dissection;
- treatment with radioactive iodine (^{131}I);
- thyrotropin (TSH) suppression by levothyroxine to avoid growth stimulation of remaining thyroid cells by TSH.

These approaches achieved a 10-year disease-free survival in more than 90% of the cases, with a complete remission in 60% of the patients with local recurrence and in 30% of the patients with distant metastases. The overall prognosis of thyroid cancer is excellent; however, overall survival falls dramatically when standard therapies fail and the 5-year survival rate decreases to less than 50% when radioactive iodine therapy loses its activity due to loss of cellular differentiation [19-20].

Current treatment for PDTC and ATC is regarded as almost ineffective and patients with ATC show the worst prognosis. The median survival is about 3–4 months and the 5-year survival rate is approximately 10%, somewhat better in localized and worse in metastatic disease [20]. The

sudden onset and evolution of ATC necessitates immediate involvement by surgeons, radiation oncologists, medical oncologists, and palliative care teams. Chemotherapy is often added concurrently with radiation but in most studies it appears to have a limited effect on survival [20-22].

Cytotoxic therapy

For patients with PDTCs, ATCs or metastatic DTCs that progress despite these standard therapies, systemic chemotherapy has traditionally been a limited option [23].

Bleomycin was the first drug used in thyroid cancer treatment; contrasting results and long-term toxicities led to gradual abandon [23-24]. Doxorubicin has shown partial response and disease stabilization in large cohort studies with best response in patients with lung metastases and high performance status [25]. Platinum compounds were able to induce minor clinical responses and symptomatic palliation with various degrees of adverse events [23].

Due to limited efficacy of monotherapy, different combined treatment have been explored; best outcomes are usually obtained when doxorubicin is included.

New molecules

Among the new drugs, proteasome and Aurora kinase inhibitors were demonstrated to be effective in both preclinical and clinical investigations [26]. Bortezomib is a proteasome inhibitor that has been shown to induce apoptosis and necrosis in relapsing thyroid tumors; Aurora Kinase Inhibitors exert proapoptotic and antiproliferative effects through impairment of chromosome segregation during the mitotic phase of the cell cycle. There is new evidence that proteasome and aurora kinase ihibitors can synergize and exert relevant antitumoral activity in thyroid neoplasia [22].

Histone deacetylase inhibitors (HDACs) are a promising class of antineoplastic agents that induce differentiation and apoptosis. Moreover, they may enhance the cytotoxicity of DNA-targeting drugs through hyperacetylation of histones [21].

Targeted therapy

In last years there has been large evidence that, among several aberrant molecular mechanisms, one specific oncogene or a particular pathway may be sufficient to maintain the malignant phenotype, a mechanism defined as 'oncogene addiction'. Inhibition of cancer growth and/or apoptosis acting on these pathways is the rationale for targeted therapy [27-28].

Among all the alterations involved in thyroid cancer development, MAPK and the PI3K-AKT signaling pathways are the most exploited for targeted therapy; moreover, most of them act against TK receptors involved in angiogenesis thus having a good potential in well vascularized thyroid carcinomas [29].

Nevertheless, taking into consideration the rapid process of tumor progression and adaptation, interfering with oncogenic alterations might not be sufficient in the majority of tumors and combination therapies to block multiple pathways may be necessary [30].

Antisense drugs, monoclonal antibodies and small-molecule drugs are examples of therapies intercepting important molecules in oncogenic pathways.

Antisense drugs are small synthetic single-stranded DNA sequences of 13-25 oligonucleotides complementary to a particular targeted mRNA. When hybridised to the corresponding mRNA, RNAse H recognizes the complex and cleaves the mRNA, leaving the antisense drug intact. These substances also interfere with ribosomal assembly, blocking gene expression and inhibiting protein synthesis. Systemic treatment with antisense drugs is generally well tolerated [31].

Side effects are dose-dependent and include thrombocytopenia, hypotension, fever, complement activation, prolonged partial thromboplastin time, asthenia, and increased concentration of hepatic enzymes [32].

Most small-molecule are kinase inhibitors that obstruct the binding of ATP to the ATP pocket within the catalytic domain and thus are known as ATP mimetics. Other compounds target regions outside the ATP-binding site of the enzyme, for example the substrate-binding domain. These drugs obstruct auto-phosphorylation and signal transduction downstream from the targeted kinase [31].
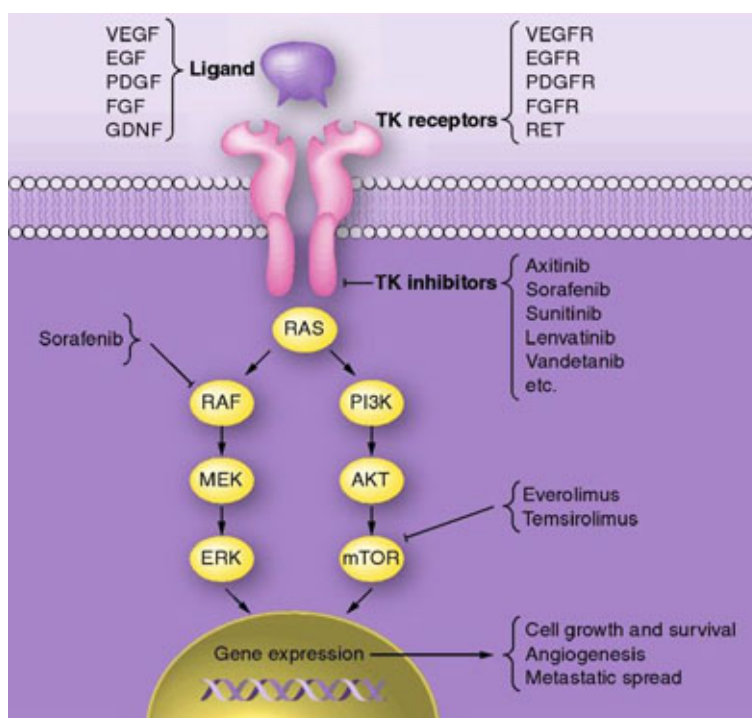
Fig 7. Thyroid cancer molecular pathways and targeted drugs. Represented are most frequent mutated pathways in thyroid cancer and levels of action of targeted drugs. Adapted from [29]

Drug	Target	Mechanism of action
Zactima (ZD6474)	RET, VEGFR, EGFR	Kinase Inhibitor
Pyrazolopyrimidine (PP1, PP2)	RET, SRC family kinase	Kinase Inhibitor
Iodocarbazole (CEP-701, -751)	RET, NTRK	Kinase Inhibitor
2-indolinone (RPI-1)	RET	Kinase Inhibitor
Benzamide (STI571)	RET, ABL, C-KIT, PDGFR	Kinase Inhibitor
Sorafenib (BAY43-9006)	BRAF, CRAF, VEGFR, RET, PDGFR	Kinase Inhibitor
Geldanamycin and derivatives	BRAF, CRAF, EGF-R, Her-2, AKT, p53, cdk4	Hsp90 inhibitor
Macrolide radicicol and derivatives	BRAF, CRAF, EGF-R, Her-2, AKT, p53, cdk4	Hsp90 inhibitor
Purine-scaffold derivatives	BRAF, CRAF, EGF-R, Her-2, AKT, p53, cdk4	Hsp90 inhibitor
ISIS 5132	CRAF	Antisense oligonucleotide
Tipifarnib (R115777)	RAS	Farnesyl transf. inhibitor
L-778123	RAS	Farnesyl transf. inhibitor
Lonafarnib (SCH66336)	RAS	Farnesyl transf. inhibitor
BMS-214662	RAS	Farnesyl transf. inhibitor

11

FTI-277	RAS	Farnesyl transf. inhibitor
L744832	RAS	Farnesyl transf. inhibitor
ISIS2503	RAS	Antisense oligonucleotide
CI-1040 (PD184352)	MEK1, MEK2	Kinase Inhibitor
PD0325901	MEK1, MEK2	Kinase Inhibitor
ARRY-142886	MEK1, MEK2	Kinase Inhibitor
LY294002	PI3 kinase	Kinase Inhibitor
KP372-1	AKT	Kinase Inhibitor
CCI-779	mTOR	Kinase Inhibitor
RAD001	mTOR	Kinase Inhibitor
Vatalenib (PTK787)	VEGFR, PDGFR, C-KIT	Kinase Inhibitor
AG013736	VEGFR, PDGFR, C-KIT	Kinase Inhibitor
NVP-AEE788	VEGFR, EGFR	Kinase Inhibitor
Gefitinib (Iressa)	EGFR	Kinase Inhibitor
Erlotinib (OSI-774)	EGFR	Kinase Inhibitor
Lapatinib (GW-572016)	EGFR, Her-2	Kinase Inhibitor
Canertinib (CI-1033)	EGFR, Her-2, Her-3, Her-4	Kinase Inhibitor
Mab 4253	EGFR	Antibody
NVP-ADW742	IGF-1R	Kinase Inhibitor
PD173074	FGFR4	Kinase Inhibitor

Table 3. Targeted therapy for thyroid cancer. [31]

2
SP600125

1,9-Pyrazoloanthrone (SP600125) is a chemical compound, derivate of anthrones, that can be synthesized by the condensation of 2-chloroanthraquinone with anhydrous hydrazine in pyridine at 100 °C. Purification is achieved via conversion to the *N*-acetyl derivative which is crystallized from acetic acid, followed by hydrolysis of the acetyl group with ammonium hydroxide in methanol.

CAS No.	129-56-6
Chemical Name:	1,9-Pyrazoloanthrone
EPA Substance Registry System:	Anthra[1,9-cd]pyrazol- 6(2H)-one(129-56-6)
Synonyms:	SP600125; JNK INHIBITOR II; SAPK INHIBITOR II; Nsc75890; c.i.70300; pyrazolanthrone; ANTHRAPYRAZOLONE;
CBNumber:	CB6354608
Molecular Formula:	C14H8N2O
Formula Weight:	220.23.00
Melting Point:	281~282℃
Storage Temperature:	2-8°C
Solubility:	H2O: insoluble
Color:	yellow

Table 4. SP600125 properties

Anthrapyrazoles have been first synthetized in 1984 [33] in the attempt to find a novel class of highly active anticancer DNA-complexing agents with diminished or absent cardiotoxicity compared to the anthracycline antitumor antibiotics daunorubicin and doxorubicin and anthracenediones. In the following years a various amount of anthrapyrazoles has been sintesized [34-36] and part of them reached phase I and II clinical trials [37-39]. In these studies anyway millimolar dosages were used to obtain DNA damage activity leading to relevant toxic effects. Due to toxicity profile and to development of new promising anticancer drugs, further studies on SP600125 were not performed.
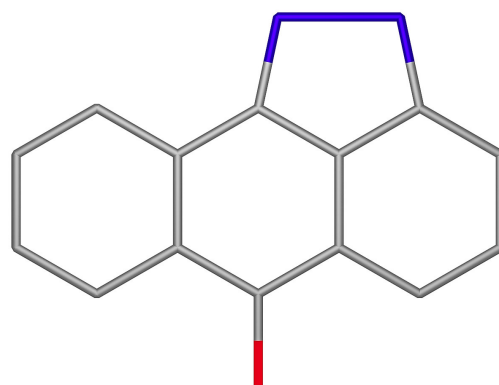
Fig 8. SP600125 structure.

In 2001 anyway Bennet group reported the inhibitory effect on Jun N-terminal kinase (JNK) by

different anthrapyrazolones, most powerful of them being SP600125 [40]. It's noteworthy that all the subsequent studies were performed with much lower concentrations than DNA-damage inducing ones. In the last decades SP600125 was then commercialized and widely used as JNK inhibitor, with reported minimal effects on many different kinases. Particular efficacy was shown in reducing ischemia-reperfusion injury in different animal models [41-47].

A	Compound	Structure	JNK2, μM	JNK3, μM
	SP600125		0.11	0.19
	Compound A		18	24
	Compound B		6	7
	Compound C		3.0	6.1
	Compound D		0.05	0.11
	Compound E		0.18	0.43

B

C

Enzyme	IC50 (μM)	Enzyme	IC50 (μM)
JNK1	0.04	MEKK1	>10
JNK2	0.04	MKK3	1.5
JNK3	0.09	MKK4	0.4
ERK2	>10	MKK6	1.0
p38-2	>10	MKK7	5.1
p56Lck	4.3	PKA	>10
Chk1	>10	PKB/AKT	1.0
EGF-TK	>10	PKC (mix)	>10
IKK-1	>10	PKCα	1.5
IKK-2	>10	PKCθ	>10
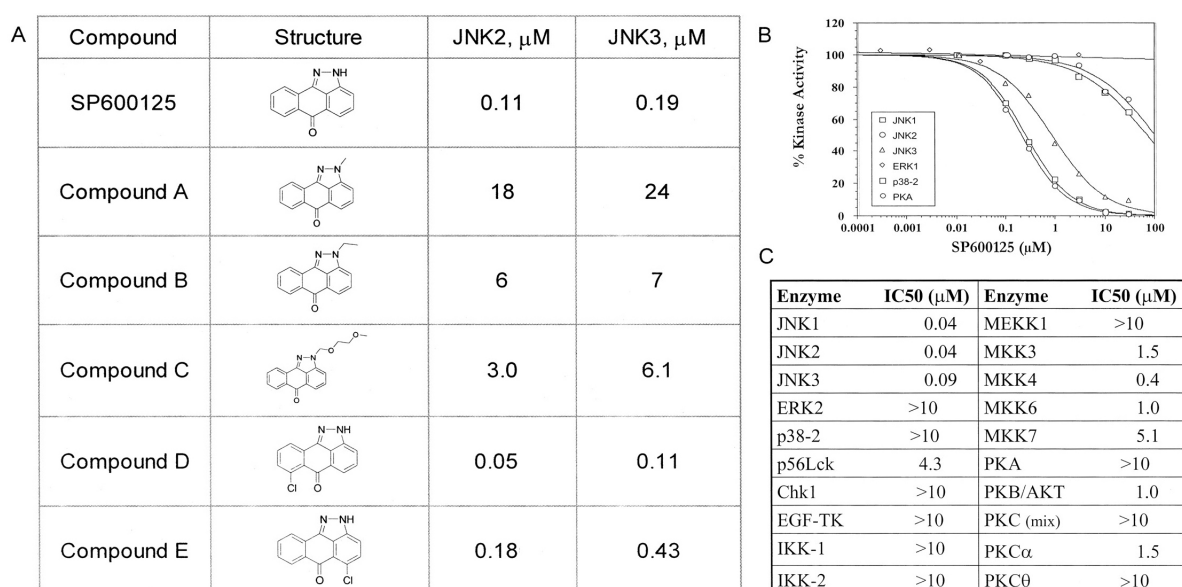
Fig. 9 Bennet's syntesized compounds. A: different compounds screened for JNK inhibitory activity and relative IC50 values; B:inhibition profiles of SP600125 vs. related MAP kinases (ERK2 and p38–2) and an unrelated serine threonine kinase (PKA) performed at *K*mlevels of substrates; C: kinase selectivity data for SP600125. Adapted from [40].

Despite the general acceptance of SP600125 being mainly a JNK inhibitor, in 2003, in a wide range kinase inhibitor specificity screening study, it was shown to be highly specific for many different other enzymes [48].

Protein Kinase	PP1 (10μM)	PP2 (10μM)	PP3 (10μM)	SU 6656 (10μM)	SP 600125 (10μM)	KT 5823 (10μM)	EGCG (10μM)	ML-7 (20μM)	ML-9 (100μM)
MKK1	52±4	55±6	89±8	82±3	89±3	99±3	94±3	102±2	95±3
MAPK2/ERK2	75±1	61±3	92±6	102±6	55±3	106±3	53±6	85±6	101±3
JNK/SAPK1c	98±3	98±1	99±2	103±2	38±5	99±1	76±7	97±3	102±3
SAPK2a/p38	13±1	21±0	100±5	70±7	86±3	102±4	105±5	100±7	94±1
SAPK2b/p38b	22±1	26±0	84±2	90±7	75±1	100±5	87±3	89±3	98±1
SAPK3/p38g	92±5	90±8	83±2	75±5	82±1	103±1	85±4	95±4	98±2
SAPK4/p38d	102±2	96±1	95±2	78±1	98±3	105±6	60±1	75±3	86±3
MAPKAP-K1a	69±6	114±2	115±2	27±6	46±3	105±6	109±0	99±2	44±2
MAPKAP-K2	96±5	106±0	98±2	96±5	72±6	71±5	79±6	93±5	106±7
MSK1	55±2	57±3	93±2	94±6	51±7	74±2	88±0	59±1	14±1

PRAK	85±7	85±8	97±3	95±2	39±1	83±8	10±2	78±5	91±2
PKA	76±3	74±3	89±5	73±3	82±1	102±5	109±4	85±1	71±4
PKCa	80±3	66±3	100±0	90±4	79±8	102±2	76±1	85±4	80±1
PDK1	97±2	99±3	82±3	94±2	62±5	114±5	50±1	107±6	113±4
PKBa	97±8	77±7	108±1	100±3	95±2	83±2	87±3	88±2	76±1
SGK	94±6	111±1	94±2	70±5	22±7	72±5	104±5	101±0	84±4
S6K1	43±0	70±3	93±3	71±0	22±4	90±4	87±5	74±1	27±3
GSK3b	86±1	113±8	99±0	83±5	60±5	52±1	78±2	107±2	107±5
ROCK-II	65±4	75±4	93±2	43±6	59±3	97±8	53±7	74±1	23±2
AMPK	93±2	84±2	94±2	14±2	26±1	90±2	101±2	82±1	61±1
CHK1	91±4	93±1	96±1	66±5	39±0	93±3	79±2	94±2	103±4
CK2	96±7	90±1	76±7	93±2	63±1	98±5	105±4	83±0	69±1
PHK	70±6	93±4	99±5	21±1	34±1	99±6	78±8	85±3	79±1
LCK	0±0	1±0	77±2	8±4	53±1	94±1	89±6	87±1	116±6
CSK	3±0	3±1	96±7	89±4	71±6	93±1	76±3	94±8	96±4
CDK2/Cyc A	75±4	68±3	84±0	54±7	20±1	94±4	97±0	73±1	75±1
CK1	8±1	6±1	54±1	66±5	10±1	83±1	105±7	106±6	103±4
DYRK1A	101±4	94±4	60±5	23±5	16±6	112±4	9±1	66±8	38±3

Table 5. Inhibition of protein kinases by commercially available inhibitors (% of residual activity); Highlighted are kinases on which SP600125 has similar or more efficacy than on JNK. Adapted from [48].

Considering only kinases on which SP600125 has more than 50% inhibitory effect, a functional protein interactions network analysis through a dedicated software [49] highlights three main areas, all of them involved in cell proliferation.
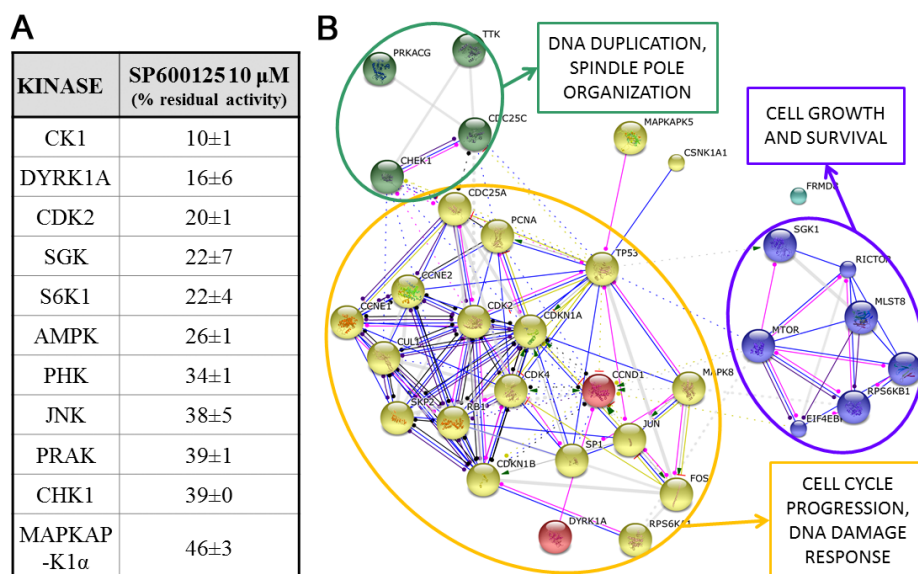
Fig 10. STRING 9.1 protein protein interaction pathway analysis. A: input kinases; B network expansion and clustering [49].

By these datas it can be seen that SP600125 is able to deeply influence intracellular processes with a more complicated mechanism of action than mere JNK inhibition. Moreover effects on cell cycle progression have recently been reported [50-53] and SP600125 has been shown to influence mitotic spindle organization [54] even if only in last years this effect has been attributed to a direct interaction with Mps1 and not to JNK inhibition [55-56].
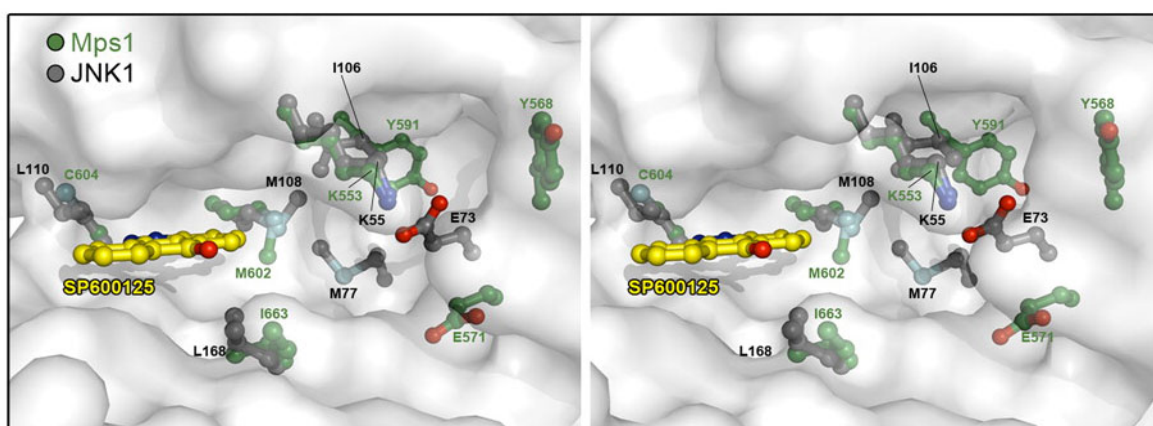
Fig 11. Stereo view of the inhibitor-binding site in Mps1 and JNK1 with SP600125. Important differences in the composition and orientation of key residues are shown. Adapted from [55].

A turning point was 2012 work by Jemaà et al. in which a drug screening was performed to identify compounds selectively killing p53-deficient cancer cells; SP600125 demonstrated to be the most selective upon 480 compounds [57].
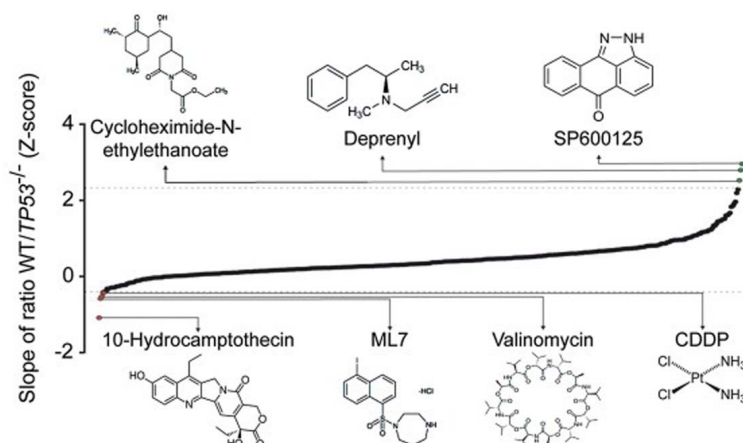
Fig 12. p53-deficient cells inhibitory activity of screened compounds. Variations in the p53 wt/null cells ratio after different drug treatments for 48h compared to the initial 1:1 ratio. SP600125 appears to be the most selective one. Adapted from [57].

In this study SP600125 was shown to preferentially inhibit p53-null cell growth inducing cell cycle perturbations and polyploization. Anyway, the effect on p53-mutated cells were not investigated as well as the possible mechanisms of action.

17

3

P53,

CELL CYCLE &

CELL DEATH

p53, frequently called the guardian of the genome, is the most often mutated gene in human cancers. It is involved in a large amount of signaling pathways that control the cell cycle and maintain the integrity of the human genome. p53 plays a fundamental role in the response to cellular stress, acute DNA damage and hyper-proliferative signals caused by oncogene expression by inducing apoptosis or cell-cycle arrest and senescence; it is an important safeguard against tumorigenesis preventing the genomic instability and the increased risk for carcinogenesis associated with propagation of damaged cells [58-59].

The best characterized molecular function of p53 in driving apoptosis, cell-cycle arrest, or senescence is as a transcriptional factor; in addition it has other important non-nuclear activities as the ability to repress transcription and to promote apoptosis through direct interaction with apoptotic regulators in the mitochondria and cytosol. Although the major part of its targets have clear links to apoptosis and cell-cycle arrest, some are implicated in other cellular

Fig 13. p53 responses to different stimuli. In response to a wide variety of noxious stimuli p53 is able to trigger different cellular responses depending on the intensity and duration of the stimulus itself.

processes including metabolism and cell migration, which can also contribute to tumor suppression [60].

Human p53 is a nuclear phosphoprotein of 53 kDa, encoded by a 20 Kb gene containing 11 exons and 10 introns which is located on the small arm of chromosome 17 [61-62]. It consists of 393 amino acids assembled into five structurally and functionally different domains: an acidic N-terminal region which contains the transactivation domain (amino acids 1-42), a hydrophobic, proline-rich region (amino acids 64-92), a central sequence-specific DNA-binding domain (amino acids 102-292), a tetramerization domain (amino acids 324-355), a highly basic C-terminal region regulatory domain (amino acids 363-393) with a nuclear localization signal and 3 nuclear export signal sequences. Of all p53 domains, the DNA-binding one is the most frequently mutated in human cancers.
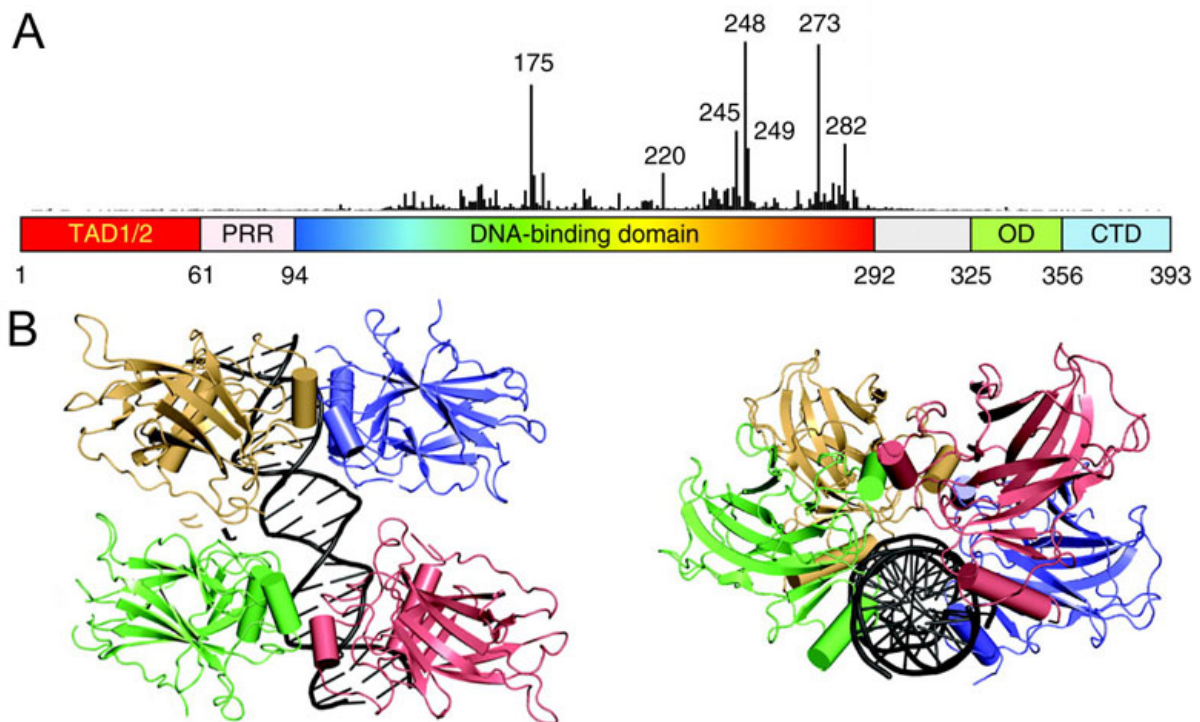
Fig 14. p53 structure. A: p53 structure and point mutation incidence in human cancers; B: p53 homotetramer interacting with DNA. TAD transactivation domain, PRR proline rich region, OD omotetramerization domain, CTD C-terminal domain. Adapted from [63].

3.1 P53 REGULATION

Under normal circumstances, wild type p53 is maintained at very low concentrations within the cells; it exists mainly in an inactive latent form with half-life limited to minutes; anyway cellular stresses or exposure to DNA damaging agents can prolong it to hours.

p53 activity and stability are tightly regulated through complex networks of post-translational modifications, including phosphorylation, acetylation, ADP-ribosylation, ubiquitylation, sumoylation, neddylation, and cytoplasmic sequestration. Most of these modifications occur in the N- and C-terminal regions.

Post-translational modifications generally result in nuclear translocation and stabilization of p53, where,
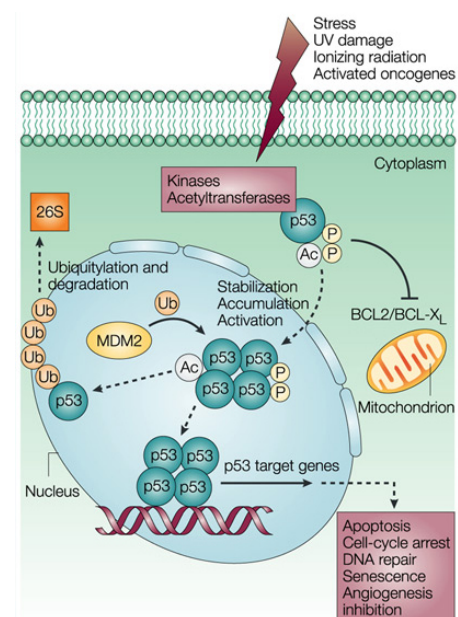
Fig 15. p53 regulation. Different post-translational modification influence p53 stability through modulation of the interaction with MDM2.

20

after activation, it interacts with its target genes. The transcriptional activation leads to diverse cellular responses such as apoptosis, cell-cycle arrest or DNA repair. Activated p53 also act outside of the nucleus to induce apoptosis by binding with anti-apoptotic proteins such as BCL2.

Phosphorylation and acetylation are the main modifications enhancing the transcription activating ability of p53 because they generally result in p53 stabilization and accumulation in the nucleus; they also prevent p53 from being targeted for degradation [64].

Phosphorylation of p53 generally results an increase in its sequence-specific DNA binding. Many protein kinases have been shown to act on p53. Different protein kinases phosphorylate several sites on p53, and in some instances the same site can be phosphorylated by more than one protein kinase. Twenty serine and threonine sites have been identified to be phosphorylated in human cells; these include serines 6, 9, 15, 20, 33, 37 and 46 and Thr18 and Thr81 in the amino-terminal region; Ser315 and Ser392 in the C-terminal domain; and Thr150, Thr155 and Ser149 in the central core. In addition, Thr55, Ser376 and Ser378 seem to be constitutively phosphorylated in unstressed cells [64-65] .

Variations in p53 phosphorylation are physiologically found in cell cycle progression: phosphorylation of serines 9, 15, 20 and 372 peaks during G1, whereas phosphorylation of Ser37 and Ser392 peaks during G2/M phase. Ser37 is the only site phosphorylated during S phase and acetylation of p53 is highest at G0 [66].

Acetylation also have a crucial role in stabilization transcriptional activation of p53. Almost every type of cellular stress increases acetylation levels of several lysines, all of them located in the C-terminal region, in the regulatory domains adjacent to the tetramerization domain, including Lys305, Lys320, Lys372, Lys373, Lys381, Lys382, and Lys386. Two histone acetyltransferases (HATs) are known to acetylate p53: p300/CBP acetylates the C terminus of p53 at Lys305, Lys372, Lys373, Lys381, and Lys382, whereas PCAF (p300/CBP-associated factor) acetylates Lys320. The consensus is that the recruitment of the co-activators CBP and p300 stabilizes p53 and increase the sequence-specific DNA binding following DNA damage, possibly as a result of an acetylation-induced conformational changes [67-68].

Acetylation may also regulate the stability of p53 by inhibiting its ubiquitylation induced by MDM2. Inhibition of p53 deacetylation leads to a longer half-life of endogenous p53 suggesting that acetylation of p53 may also contribute to p53 stabilization [67].
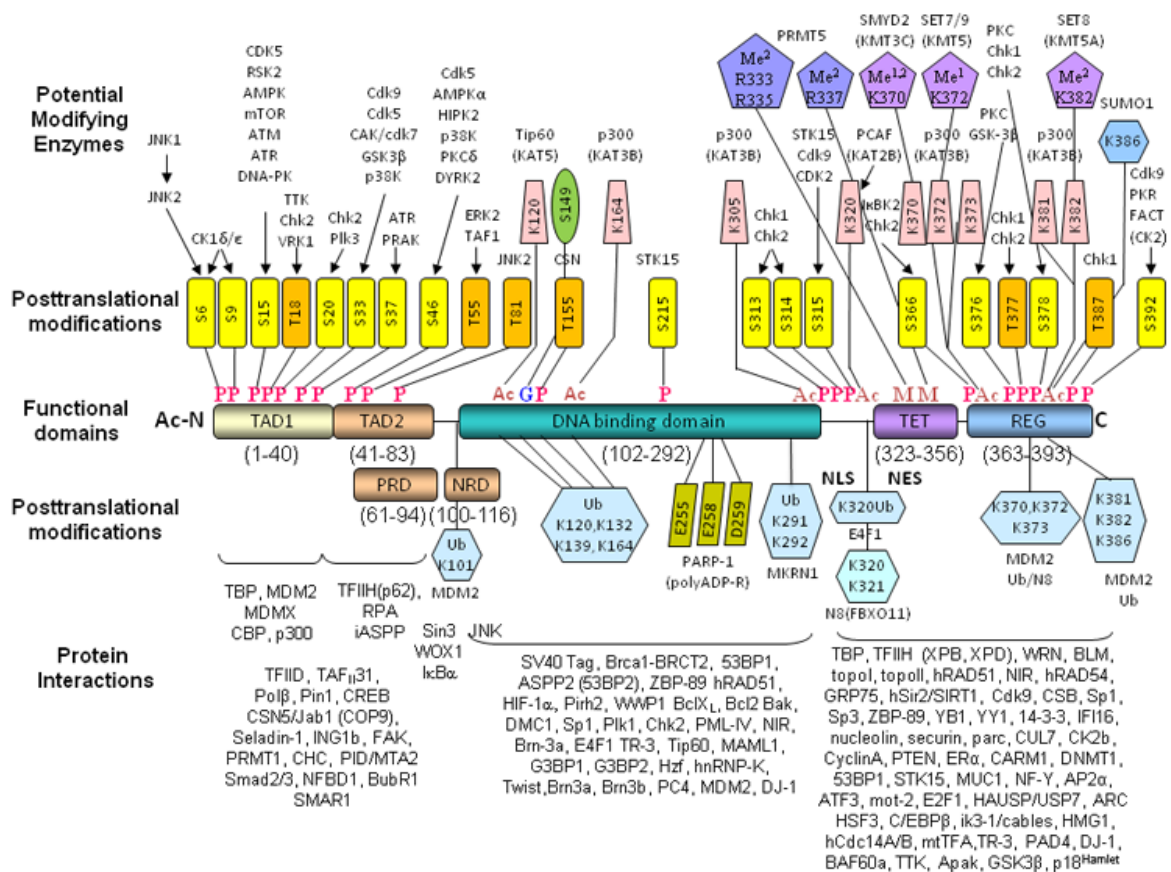
Fig 16. p53 post-translational modifications, enzymes and interacting proteins. TAD transactivation damain, TET tetramerization domain, REG regulatory domain; P, phosphorylation; Ac, acetylation; G, glycosylation; Me, mono(1) or di-(2) methylation, N8, neddylation; Ub, ubiquitination; polyADP-R, poly-ADP-ribosylation. Adapted from [69]

p53 is degraded through an ubiquitin-dependent process primarily mediated by MDM2. The p53 protein regulates the MDM2 gene at the level of transcription, and the MDM2 protein regulates the p53 protein at the level of its activity. This creates a feedback loop that regulates both the activity of the p53 protein and the levels of MDM2. MDM2 seems to have roles in both localization and degradation of p53. Recent data indicate that monoubiquitylation might act as a signal in nuclear export for p53 and that different levels of MDM2 can induce both mono and polyubiquitylation in a dose-dependent manner, so determining the fate of p53 [64].

MDM2 is also regulated by ATM, a protein that has a key role in the cellular response to DNA damage. ATM is normally rapidly activated by DNA damage and can phosphorylate MDM2, resulting in MDM2 deactivation, which leads to increased p53 levels.

As well as ATM, MDM2 is also regulated by ARF; ARF might facilitate accumulation of p53 by binding to MDM2 and inhibiting its association with p53 or by promoting sumoylation of

MDM2. Recent evidence indicates that this and the MDM2 pathways are structured very differently in normal cells versus stressed cells: in normal, unstressed cells, MDM2 levels are independent of p53 activity as a transcription factor, but this feedback pathway becomes active under stress. A relative of MDM2, MDMX, is also a key negative regulator of p53 and is also upregulated in many tumours that express wild-type p53, providing still another potential mechanism for deactivating p53.
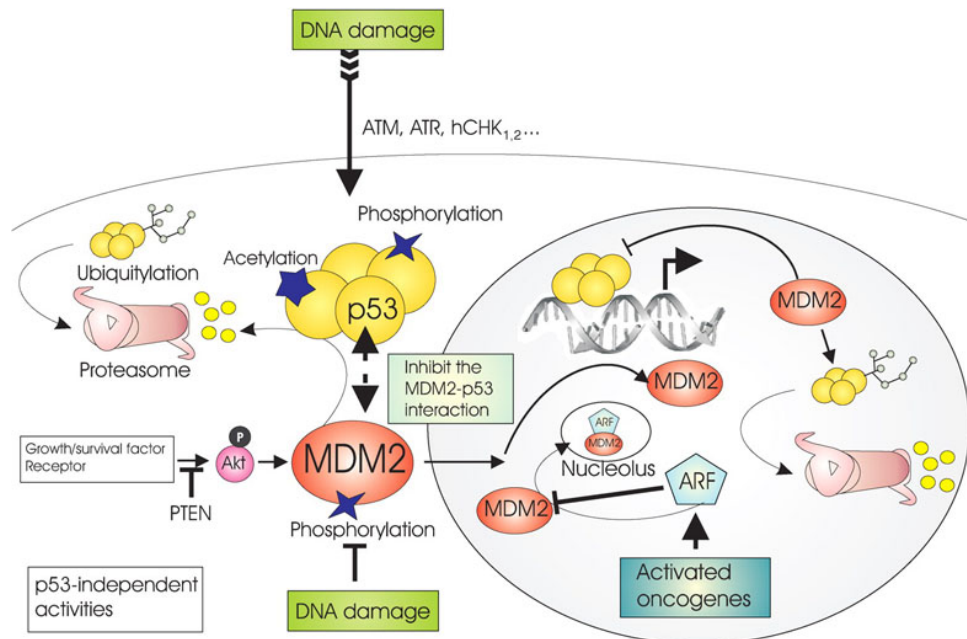
Fig 17. p53-MDM2 interactions. p53 and MDM2 form an auto-regulatory feedback loop. p53 stimulates the expression of MDM2; MDM2 inhibits p53 activity because it blocks its transcriptional activity, favours its nuclear export and stimulates its degradation.

In addition to this pathways, p53 is negatively regulated by several other proteins. JNK was one of the first MDM2-independent p53 degradation pathways to be identified and actually seems to have a dual role: under unstressed conditions, JNK binds to p53 preferentially in the G0/G1cell-cycle phase resulting in ubiquitylation and degradation while under stress conditions JNK phosphorylates p53 at threonine 81, resulting in stabilization and activation [70-71].

Other proteins that act as E3 ligases to promote p53 degradation include PIRH2, which is a p53 target gene, COP1 protein and TAF1 [72-74].

3.2 p53 EFFECTS: CELL CYCLE ARREST, MITOTIC CATASTROPHE OR APOPTOSIS?

It is known that DNA-damaging stimuli and stressful environmental conditions lead to either growth arrest or cell death. p53 responds in various modes, depending on several factors; the most important ones are cell type, growth factors avalaibility, stress duration and intensity .

The classical view implies that low levels of p53 induce cell cycle arrest, whereas high levels of p53 induce apoptosis. This way of action is usually explained with the fact that p53 binds to proarrest genes with high affinities but associates with proapoptotic genes with low affinities.

It has been recently reported that p53 levels can vary in a series of discrete pulses, the number of p53 pulses being positively related to the amount of DNA damage. The p53-Mdm2 negative feedback loop is recognized as the basis of p53 oscillation, and additional positive feedback loops may make p53 oscillations more robust. On the contrary, it was suggested that the p53-PTEN-Akt-MDM2 positive feedback loop may terminate oscillations by disrupting the p53-MDM2 loop. The strength of DNA damage is repeatedly evaluated; the cell survives after transient p53 pulses, or apoptosis is induced by sustained p53 pulses. This may represent a reliable and flexible mechanism [75].

p53 and cell cycle.

The best characterized antiproliferative effect of p53 is its role in G1 phase arrest of cell cycle. p53 is required for DNA damage-induced G1 arrest primarily through transactivation of p21, a cyclin-dependent kinase inhibitor. When levels increase p21 binds and inactivates cyclin E/Cdk2 or cyclinD/Cdk4 complexes resulting in RB hypophosphorylation and cell cycle arrest; RB is a negative regulator of the transcription factor E2F, which is required for expression of S-phase-specific genes [76]. Anyway, there must be other actors implicated in p53 effects because p21 KO cells are only partially defective in DNA-damage induced growth arrest while p53 deficiency totally abolishes it [77-79].

In addition to this early checkpoint, p53 also regulates the maintenance or sustained G2/M arrest. In this case,
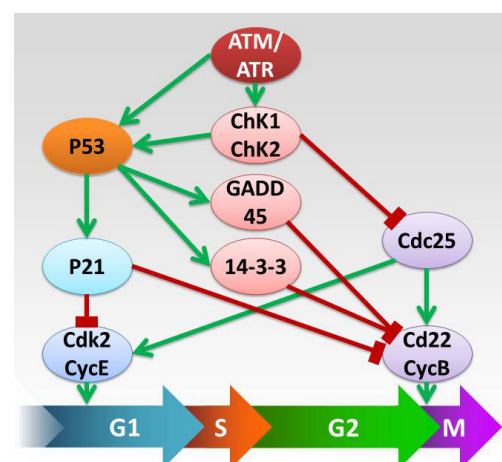
Fig 18. p53 and cell cycle regulation. Cell cycle checkpoint and correlated p53 actions.

rather than mediated by p21, which has little CDK1 inhibitory capacity, other p53 targets may act as effectors that inhibit the activation of Cdc2. Cdc2 is inhibited simultaneously by three transcriptional targets of p53, GADD45, p21 and 14-3-3. Binding of Cdc2 to Cyclin B1 is required for its activity, and repression of the Cyclin B1 gene by p53 also contributes to blocking entry into mitosis. p53 also represses Cdc2 gene, to help ensure that cells do not escape from the initial block [79-81].

p53 and senescence

Cellular senescence is a permanent cell cycle arrest that ocours in response to different stimuli, including telomere dysfunction, oncogene activation, and DNA damage. Senescent cells display several characteristic morphological and biochemical features: they have a much larger flattened cytoplasm that contain many vacuoles and cytoplasmic filaments, a bigger nucleus and nucleoli and are sometimes multinucleated; in some cases, senescent cells display an increase in the number of lysosomes and a prominent golgi. They often become resistant to cell-death signals, like apoptosis, and they acquire widespread changes in gene expression

It has been shown that the p53 levels were increased in senescent cells; overexpression of p53 is sufficient to induce premature senescence in p53-null cells while inactivation or loss of p53 results in an extension of cell lifespan.Moreover it has recently been demonstrated that p53 restoration induces premature senescence and tumor regression [82-84].

Senescence is usually triggered by p53 or by p16/pRB pathways: active p53 induces the expression of p21 that, among other activities, suppresses the phosphorylation and the inactivation of pRB. Anyway, although p21 contributes to the growth arrest of senescent cells, it is unlikely to be solely responsible for the complex changes that characterize senescence. Senescence signals that engage the p16–pRB pathway generally do so by inducing the expression of p16, another CDK inhibitor that prevents pRB phosphorylation and inactivation. Moreover there is reciprocal regulation by these pathways [84-85] .

p53 and mitotic catastrophe

In addition to cell cycle arrest in response to DNA damage, p53 plays a fondamental role in G1 arrest following alterations in spindle pole organization and chromosomes segregation. In this

case p53 activation causes a definitive arrest at a tetraploid G1 state. There is a broad consensus that p53-deficient cells that are in the tetraploid G1 state are not prevented from reentering the cell cycle to reduplicate their DNA unchecked, leading to polyploidy and subsequent chromosomal instability with subsequent propagation of errors of late mitosis and the generation of aneuploidy [86].

Importantly, the loss of p53 can sensitize cells to microtubule poisons such as paclitaxel due to its capacity of inactivating the polyploidy checkpoint. After treatment with spindle inhibitors, cells possessing an intact p53 system undergo G1 arrest and thus are resistant to antimicrotubule agents. Cells deficient for p53 fail to undergo such a G1 arrest and endoreduplicate their DNA, leading to massive cell death by a definite mechanism called mitotic catastrophe [86-88].

Mitotic catastrophe is defined as "a cell death mode occurring either during or shortly after a dysregulated/failed mitosis and can be accompanied by morphological alterations including micronucleation (which often results from chromosomes and/or chromosome fragments that have not been distributed evenly between daughter nuclei) and multinucleation (the presence of two or more nuclei with similar or heterogeneous sizes, deriving from a deficient separation during cytokinesis). However, there is no broad consensus on the use of this term, and mitotic catastrophe can lead either to an apoptotic morphology or to necrosis" [89].

A group of various stimuli and perturbations can trigger mitotic catastrophe. Some inducers of mitotic catastrophe directly affect the integrity of the genetic material (for example, DNA-damaging agents), whereas others interfere with the complex molecular machinery that ensures the correct segregation of chromosomes (for example, microtubular poisons). Finally, some compounds trigger mitotic catastrophe via uncharacterized signalling pathways [90].
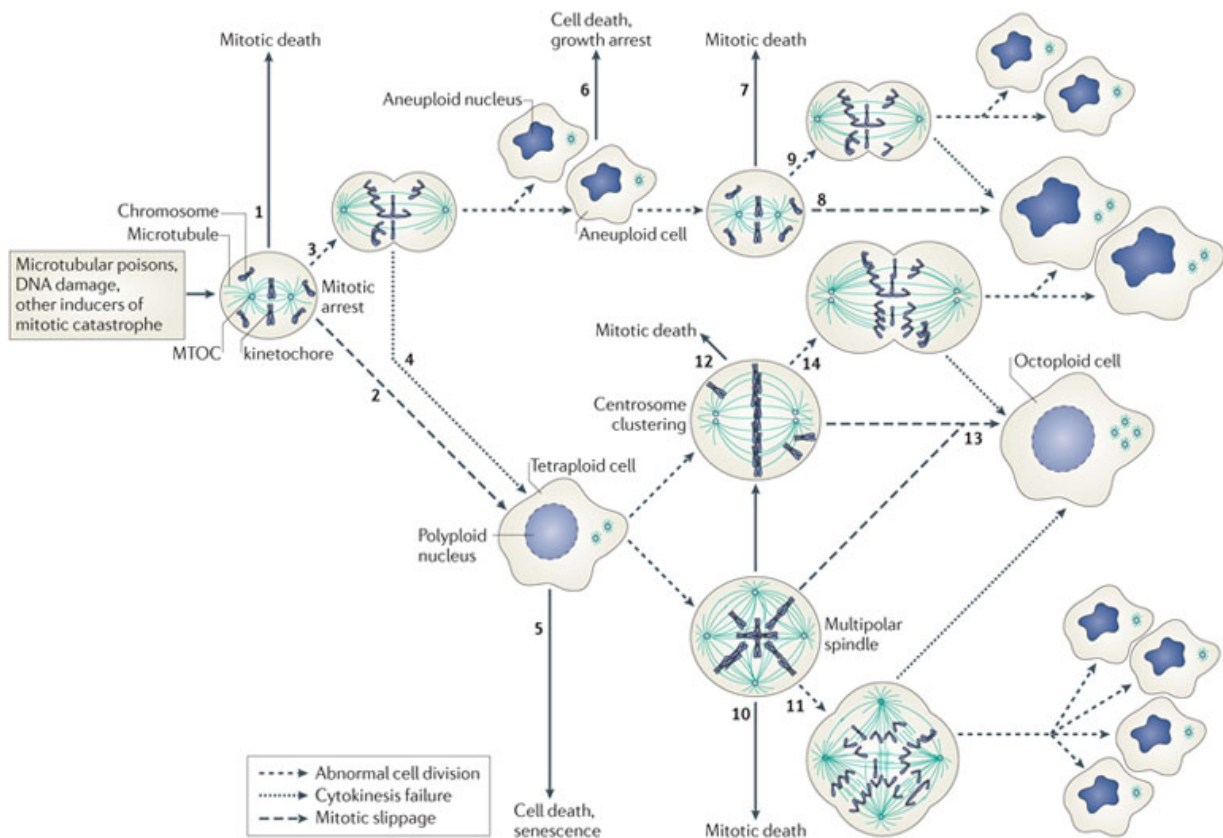
Fig 19. Mitotic catastrophe mechanisms. 1: In response to DNA damage or mitotic altertations cells arrest in mitosis and usually undergo the mitotic death programme. 2-4: mitosis-incompetent cells can escape the mitotic arrest, either by slipping into the interphase or by undergoing one round of aberrant mitosis that often cannot be completed resulting in cytokinesis failureand generation of tetraploid cell. 5: most of tetraploid cells die or become senescent. 6: completion of aberrant division results in aneuploid cells owing to gross chromosomal rearrangements that result in cell death of growth arrest. 7-9: In rare cases these aneuploids survive but undergo the mitotic death programme, mitotic slippage or another round of aberrant mitosis. 10-14: in some instances, tetraploid cells proliferate giving rise to multipolar divisions, succumb to mitotic catastrophe-initiated mitotic death, undergo mitotic slippage or undertake aberrant divisions, leading to the generation of potentially tumorigenic aneuploid daughter cells. Adapted from [90]**.**

p53 and apoptosis

In large part, the potent anti-cancer activity of p53 has been linked to the intrinsic mitochondria-mediated pathway of apoptosis. As a transcription factor, p53 induces several pro-apoptotic Bcl-2 family members including Bax, Puma, Noxa and Bid, and represses the transcription of some anti-apoptotic factors, including Bcl-2, Bcl-xL and survivin. In addition to its complex functions as a nuclear transcription factor, p53 can act in the cytosol and mitochondria to promote apoptosis through transcription-independent mechanisms [91-93].

The hallmark of the transcriptionally independent p53-mediated apoptosis is the stress-induced accumulation of p53 in the cytosol and in the mitochondria that leads to interactions with several members of the Bcl-2 family. Binding of p53 to Bak in the outer mitochondrial membrane

catalyses Bak activation; for this process acetylation of p53 at lysine 120 seems to be important. Moreover, activation of Bax correlates also with cytosolic accumulation of p53; in this case instead of the central DNA-binding domain that binds to Bak, Bcl-2 and Bcl-xL, the N-terminus of p53 and in particular its proline-rich domain is indispensable for direct activation of Bax. Both Bak and Bax activation lead to cytochrome c release [94-95].

In addition p53 is able to interact with Bad, another pro-apoptotic Bcl-2 family member. The formation of a p53–Bad complex leads to cytosolic and mitochondrial accumulation, thereby facilitating its function in directly activating Bax or Bak [96].

Regulation of p53 nuclear export and abundance in the cytosol and mitochondria is the fundamental way to controll its transcription-independent pro-apoptotic activity. As long as p53 is preferentially accumulated in the nucleus, large amounts of protein are required for cytosolic localization. Moreover, the accumulation of large amounts of non-nuclear p53 can also be the result of specific localisation signals, such as posttranslational p53 modifications or the interaction with nuclear export factors. Among the posttranslational modifications of p53, ubiquitylation appears to have a prominent role as mono-ubiquitylation is a signal for nuclear export while only polyubiquitylation targets p53 for proteasomal degradation [93, 97].
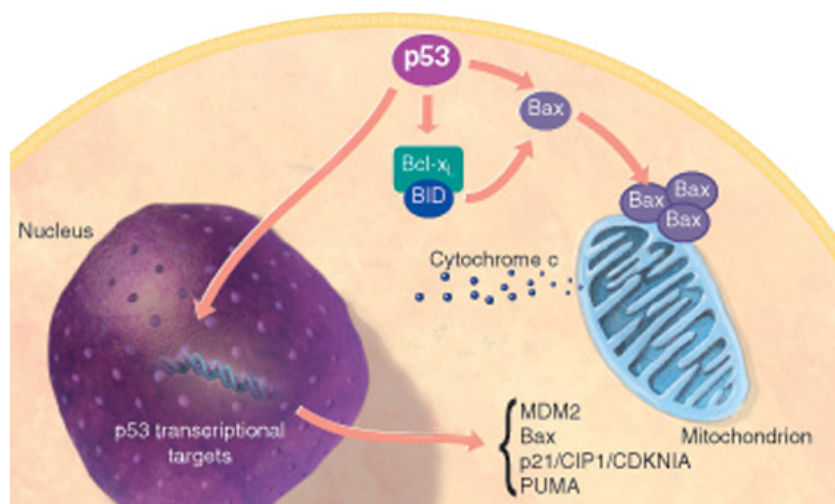
Fig 20. p53 and mitochondrial apoptosis induction. p53-dependent apoptosis can be trascription-dependent through the induction of Bax and PUMA or trascription-independent, including direct effects on Bax and Bcl-x$_L$. While in the first case nuclear translocation and post-traslational modifications are required, in the second one the cytoplasmatic pool of p53 acts direcly through protein-protein interactions. Adapted from [98]

3.3 P53 AND THYROID CANCER

At variance with other human malignancies, p53 point mutations are not frequent in thyroid cancer while functional inactivation by a variety of different mechanisms is apparently very

common; the principal alterations are related to the complex network of p53 family member isoforms and include the expression of proteins with dominant negative function, malfunction or overexpression of regulatory proteins. For these reasons the prevalence of p53 mutations in well-differentiated thyroid carcinoma ranges from 0% to 25% while p53 protein overexpression has been reported as 11% to 59%. p53 indirect inactivation may be an important prerequisite for early phases of thyroid cell transformation while p53 mutations have been implicated as a transitional step between well-differentiated thyroid carcinoma and anaplastic carcinoma, as P53 alterations have been reported in more than 60% of ATCs [99-101]. Moreover p53 inactivation plays a fundamental role in tumor aggressiveness, metastatic behaviour and chemoresistance acquisition; several reports indicate that wild-type p53 gene delivery into anaplastic thyroid cancer cells induces a partial differentiation, with the re-expression of thyroid specific-genes, and makes cells more vulnerable to the effect of chemotherapy. This effect may be increased by the concomitant use of histone deacetylase inhibitors, which stimulate p53 acetylation and functional activation [99, 102-104] .
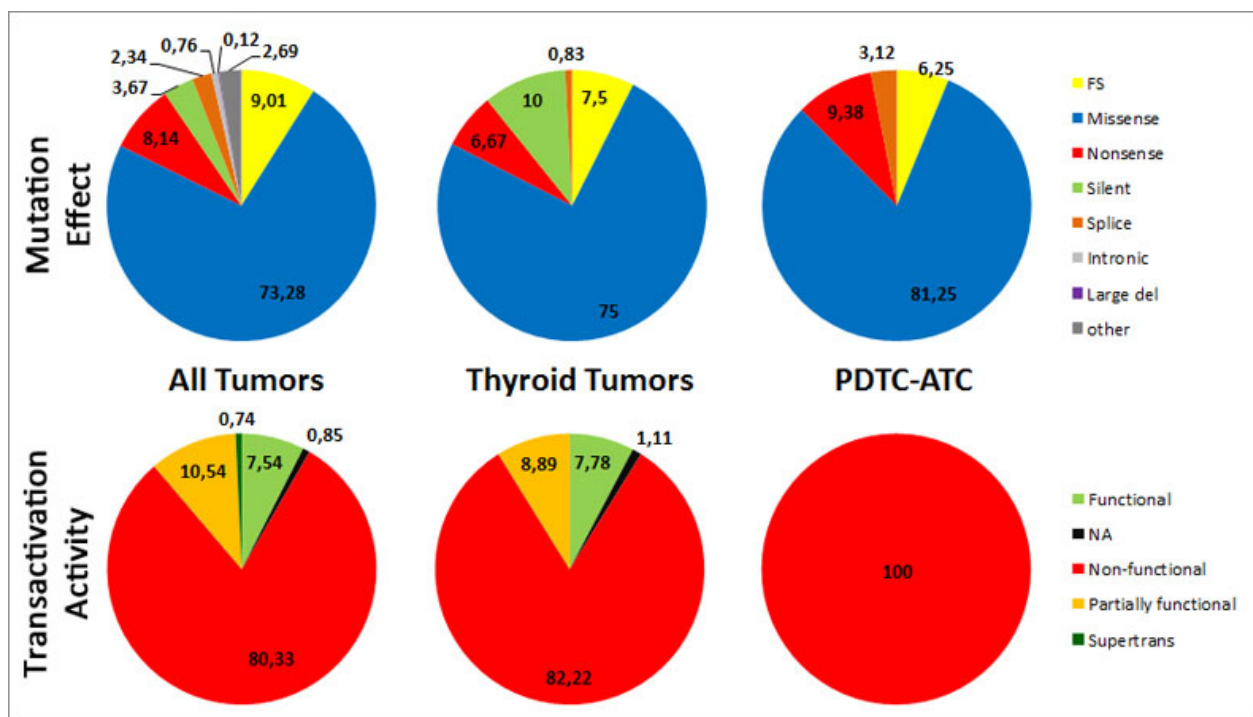
Fig 21. p53 mutation and activity. Graphical elaboration of mutation effect and their residual transactivation activity in total human cancers and in thyroid cancer. As it can be seen in undifferentiated thyroid cancers p53 mutations result in total loss of p53 transactivational activity. Statistical data from [105], database version R17, November 2013 .

4
MICROTUBULES &
CELL DYNAMICS

Microtubules are essential components of the cytoskeleton that play a major role in many cellular functions; in most cells, cytosolic microtubules are involved in intracellular transport, organelle positioning, cell shape and motility. They control differentiative processes involving intracellular rearrangements and changes in morphology. Last but not least, they form two essential structures in dividing cells: the mitotic spindle and the midbody [106-107].

Microtubules are hollow tubular structures with an external diameter of 25 nm, constituted of heterodimers of α and β tubulin; lateral and longitudinal interactions between the tubulin subunits are responsible for maintaining the tubular form. Longitudinal contacts between the ends of adjacent subunits link the subunits head to tail into a linear *protofilament.* Through lateral interactions, protofilaments associate side by side into a sheet or cylinder.

In most cells, they originate in the perinuclear region, at the Microtubule Organizing Center (MTOC) that is formed by two centrioles surrounded by peri-centriolar material containing proteins implicated in microtubule nucleation and organization. Microtubules are thus polarized with a minus-end capped and anchored at the MTOC and a plus-end generally localized at the periphery of the cell. The plus-ends explore the cytoplasm in a very dynamic manner: microtubules undergo phases of growth, pause and shrinkage, separated by rescue (transition from shrinkage to growth phase) or catastrophe (transition from growth phase to shrinkage) [106, 108].

Polymerization and depolymerization of microtubules is driven by the binding, hydrolysis and exchange of a guanine nucleotide on the β-tubulin monomer; GTP hydrolysis is not directly involved in microtubule assembly but is necessary for switching between catastrophe and rescue. Polymerization is typically initiated from a pool of GTP-loaded tubulin subunits. GTP hydrolysis occurs shortly after subunit incorporation and it has been postulated that this process changes the conformation of a protofilament from a slightly curved tubulin-GTP to a more profoundly curved tubulin-GDP structure. This nucleotide dependent conformational model predicts that the curved tubulin-GDP is forced to remain straight when it is part of the microtubule wall. Growing microtubule sheets are thus believed to maintain a 'cap' of tubulin-GTP subunits to stabilize the straight tubulin conformation within the microtubule lattice. Closure of the terminal sheet structure generates a metastable, blunt-ended microtubule intermediate, which might pause, undergo further growth or switch to the depolymerization phase. A shrinking microtubule is characterized by fountain-like arrays of protofilament structures, a conformational change driven by tubulin-GDP that destabilize lateral contacts between adjacent protofilaments. The

polymerization–depolymerization cycle is completed by exchanging GDP of the disassembly products with GTP [109].

Microtubule dynamics are precisely regulated through intrinsic processes such as the presence of a plus-end GTP-cap and through extrinsic processes, mostly due to the interaction with microtubule associated proteins (MAPs).
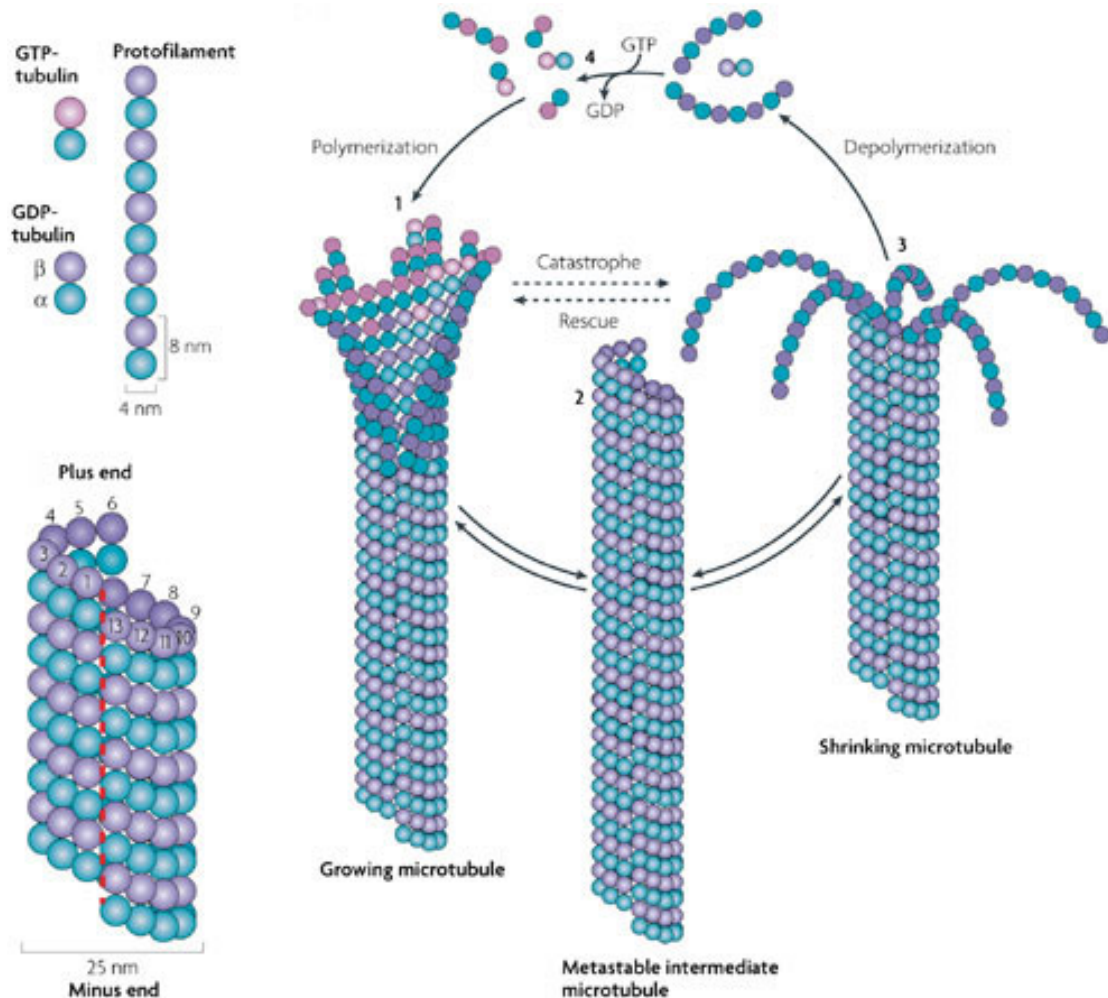
Fig 22. Microtubules structure and dynamic. Polymerization is typically initiated from a pool of GTP-loaded tubulin subunits. Growing microtubule ends fluctuate between slightly bent and straight protofilament sheets and its closure generates a metastable, blunt-ended microtubule intermediate, which might pause, undergo further growth or switch to the depolymerization phase. The polymerization–depolymerization cycle is completed by exchanging GDP of the disassembly products with GTP. Adapted from [109]

4.1 MICROTUBULES ASSOCIATED PROTEINS

Microtubule dynamics and function are modulated by interactions with other proteins, microtubule motor proteins and non-motor microtubule associated proteins (MAPs).

The two major families of microtubule motors are the kinesins and dyneins. Motor proteins

32

generate force upon interaction with microtubules and these forces are used for various intracellular functions, most obviously intracellular transport. Microtubule dependent transport takes place in almost all cell types, serving diverse functions. Moreover, other kinesin motors catalyse the depolymerization of microtubules, thus participating in the complex network of interacting proteins that regulate microtubule dynamics [107, 110-113].

The heterogeneous group of non-motor MAPs comprises not only many proteins that stabilize microtubules but also severing proteins which destabilize the microtubule network [113].
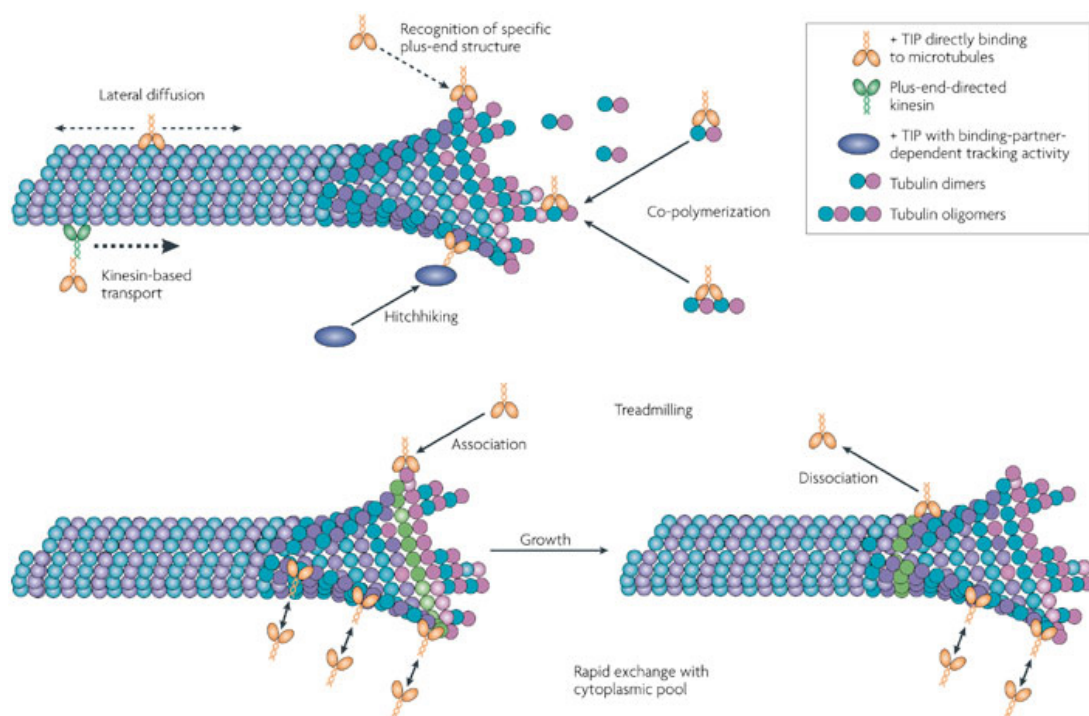
Fig 23:Mechanisms of microtubules plus-end tracking. +TIPs can arrive at the microtubule tips by diffusion in the cytoplasm or along the microtubule lattice. Alternatively, they can also be transported to microtubule plus ends by kinesins. +TIPs that recognize a specific structure at the growing microtubule end (or co-polymerize with tubulin) might be immobilized at the ends until this structure is converted into the regular microtubule lattice. Adapted from [109].

Another important group of MAPs is constituted by plus end-tracking proteins (+TIPs), which help to control microtubule dynamics and interactions with cellular organelles and subcellular domains, thus coordinating complex aspects of cell architecture. Most +TIPs bind to growing microtubule plus ends because of the presence of the GTP-cap and specific sites exposed only on protofilaments [109, 114]. +TIPs can either recognize growing plus ends or co-polymerize with tubulin; individual +TIPs are not able to move on microtubules but are transiently immobilized

at the growing end. Anyway, association with microtubule-binding partners such as kinesins might be sufficient to target some proteins to microtubule ends through 'hitchhiking', a mechanism that is common for many +TIPs. Dissociation of +TIPs from microtubule ends can occur spontaneously or can be driven by structural changes in the microtubule lattice, a mechanism known as treadmilling [109, 115-117].

An important function of +TIPs is to attach and stabilize microtubule ends at the cell cortex, either by linking microtubule ends directly to actin or to cortically bound factors. +TIPs can stabilize microtubules independently of each other, but can also function cooperatively. Because microtubules act as 'rails' for transport, selective microtubule attachment and stabilization, they can help to establish targeted delivery of vesicles and macromolecules to cellular subdomains, such as leading cell edges, intercellular junctions or growing cell ends. In addition, +TIPs can also link microtubule ends to intracellular membranes [109].

4.2 MICROTUBULES MODIFICATIONS

Many tubulin post-translational modifications are known: detyrosination and the related D2 modification, glutamylation, glycylation, acetylation, phosphorylation and palmitoylation. Most of them occur on tubulin subunits after polymerization into microtubules with the exception of phosphorylation on serine residue S172 of b-tubulin by the Cdk1 kinase that occurs on the unpolymerized tubulin dimer and inhibits its incorporation into assembling microtubules. It has long been known that stable microtubules, as compared to dynamic microtubules, accumulate more modifications and these modifications play specific role as differences in tubulin patterns can be seen between stable microtubules [118-120].

Detyrosination involves the removal of C-terminal tyrosine of a-tubulin in microtubule polymers by an unidentified carboxypeptidase wich is related to Nna1/CCP1. The reverse tyrosination reaction occurs on soluble tubulin heterodimers and is catalyzed by tubulin tyrosine ligase (TTL). Detyrosinated a-tubulin may undergo a second proteolysis, Δ2 PTM, that removes the terminal glutamic acid residue. The Δ2 a-tubulin that is released from microtubules during depolymerization cannot revert to an unmodified state, thus limiting the amount of a-tubulin that undergoes recycling [121-124].

The detyrosination/tyrosination cycle differentially recruits two types of microtubule-binding proteins, molecular motors and plus-end tracking proteins (+TIPs). For example motor protein

Kinesin-1 binds preferentially to detyrosinated microtubules rather than tyrosinated microtubules; this could enable Kinesin-1 to preferentially move various cargoes along detyrosinated microtubules [125-127].

Proper functioning of the detyrosination/tyrosination cycle has also been shown to influence tumorigenesis. Multiple studies have shown that TTL is downregulated in animal and human cancers. Low levels of TTL protein and tyrosinated tubulin correlate with increased tumorigenisis, tumor invasiveness, and poor prognosis, suggesting that detyrosinated tubulin provides a growth advantage [128-130].

Glutamylation and glycylation involve the addition of variable numbers of glutamate or glycine residues onto the C-terminal tails (CTTs) of both a- and b-tubulin. Glycylation is mainly limited to tubulin incorporated into axonemes of cilia and flagella whereas glutamylation is prevalent in neuronal cells, centrioles, and the mitotic spindle. Both modifications have been found on the same tubulin CTT and there is cross-talk between the a- and b-tubulin tails regulating the type and level of each modification [119, 131]. Recent work has shown that polymodifications of the tubulin CTTs could mark specific microtubules for severing and thus influence polymer dynamics and density. Mutations of the b-tubulin polymodification sites resulted in an inability of cells to complete cytokinesis in a similar way to loss of the severing proteins [132-133].

The tubulin glutamylases belong to a family of enzymes that contain a tubulin tyrosine ligase-like (TTLL) domain. Eight mammalian TTLL domain-containing proteins are known to be tubulin glutamylases that differ in their specificity for a- or b-tubulin and in preferential chain-initiating or chain-elongating activity [134]. Both glycylation and glutamylation are reversible reactions, however the pathways responsible for the reverse reaction are still not clarified; a recent study identifies the carboxypeptidase CCP5 as the tubulin deglutamylase but it has not yet been reported how deregulation of CCP5 affects microtubules dynamics [135].

Acetylation is unique among the known tubulin modifications in that it occurs on lysine 40 of a-tubulin which is postulated to reside on the luminal face of microtubules. It is unclear how the enzymes that carry out acetylation/deacetylation would have access to this site and how this luminal modification could influence microtubule-based functions that occur on the cytoplasmic face.

The acetylation appears with a delay after microtubule assembly and is seen as a marker of polymer age. MEC-17, a protein related to GCN5 histone acetyltransferases was recently identified as an important a-tubulin acetyltransferase. In animal cells, several acetyltransferases

colocalize with acetylated microtubules and some of them (NAT1, NAT10 and ELP3) regulate the level of a-tubulin acetylation, but it is not known whether any of these enzymes have direct activity on a-tubulin [118, 136]. Deacetylation is catalyzed by HDAC6 and SIRT2 deacetylases, enzymes that are related to histone deacetylases. Knockdown of either HDAC6 or Sirt2 results in hyperacetyled tubulin suggesting that the two enzymes may be interdependent [137-139].
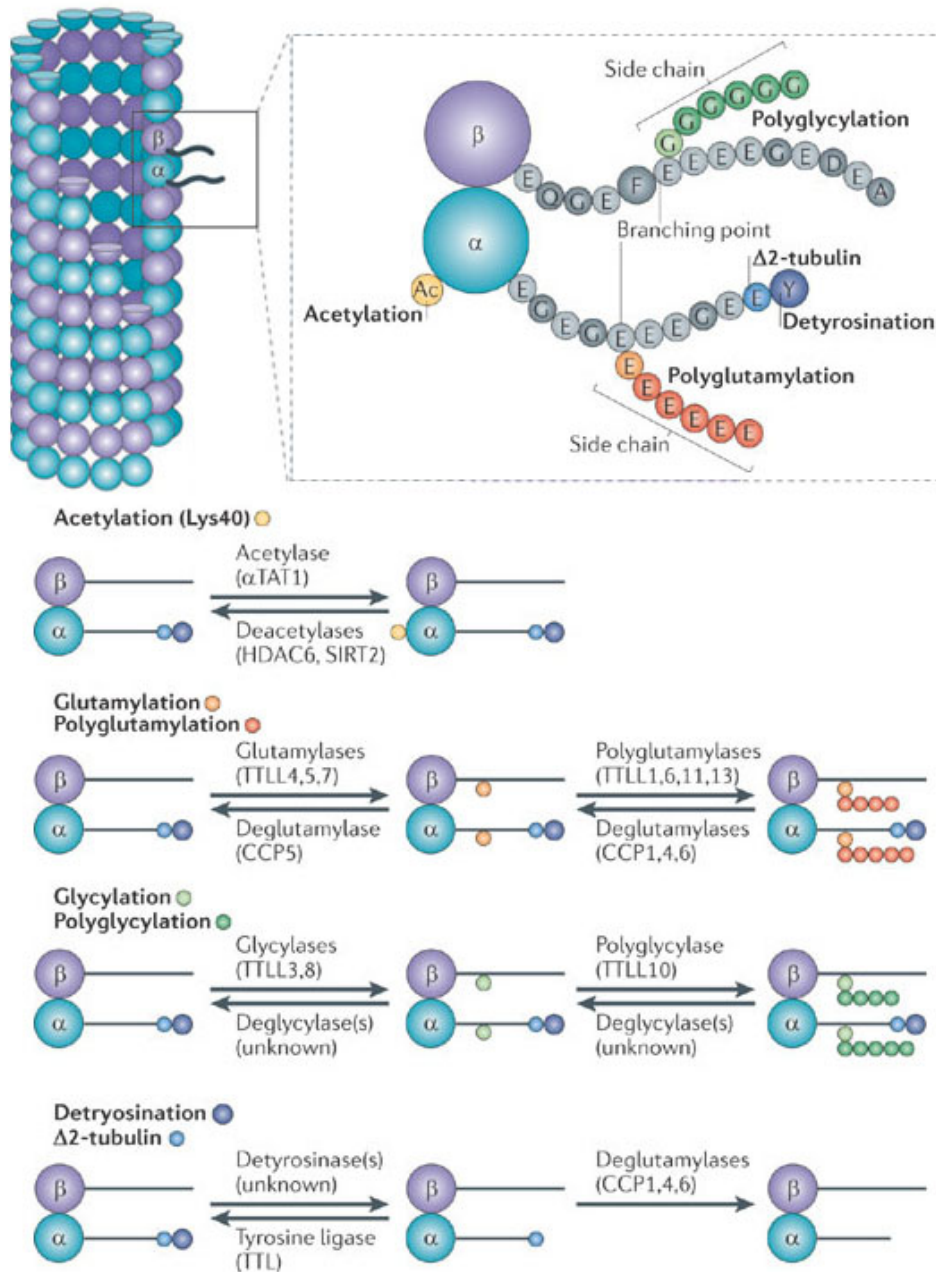
Fig 24. Microtubules post-translational modification and relative enzymes. The carboxy-terminal tails of both tubulins are represented as amino acid sequences. Both α-tubulin and β-tubulin can be modified by polyglutamylation and polyglycylation on different Glu residues within those tails. Together with detyrosination at the C terminus and the follow-up removal of the penultimate Glu residue (which generates Δ2-tubulin), these modifications are specific to the C-terminal tails of tubulin. Acetylation (Ac) of Lys40 is localized at the amino-terminal domain of α-tubulin. Adapted from [107].

Acetylation of a-tubulin on lysine 40 is very common and can be found on stable microtubules in most cell types. Although tubulin acetylation is not necessary for cell and organism survival, recent work has suggested that a-tubulin plays a positive role in motor-based trafficking in mammals [140]. As HDAC6 has recently been shown to deacetylate cytosolic proteins other than tubulin (e.g. Cortactin, HSP90 and b-catenin) and regulates a variety of other cellular events (e.g. aggresome formation, cell motility, ciliary disassembly, and transcriptional corepression), the role of HDAC6/Sirt2 deacetylation of a-tubulin in regulation of microtubule-based functions remain to be clarified.

4.3 MICROTUBULES AND INTRACELLULAR ORGANIZATION

In normal, not-polarized resting cells there is a major asymmetry between the center and the periphery established mainly by the microtubule network. Minus-ends of microtubules are in general located at the cell center, bound to a MTOC while their plus-ends explore the cell periphery. +TIPs bind to the plus-ends of growing microtubules and participate in the regulation of their dynamics at the periphery of the cells. In most animal cells in interphase the major MTOC is constituted by the the centrosome; the centrosomal microtubules spread out in the whole cell through the cytoplasm, playing a role in positioning, organization and maintenance of different organelles. In some cells the nucleus and the Golgi apparatus can be additional sites of microtubule nucleation and influence their own organization with a sub-population of specific microtubules [106].

Nuclear positioning depends mostly on centrosomal microtubules and proteins found at their plus-ends, like dynein and dynactin, and the dynein activator complex; these proteins appear to interact with cortical proteins to generate forces that regulate nuclear positioning. Centrosomal microtubules also interact directly with the nuclear envelop. By the compensation of all these forces and connection astral microtubules are able to maintain the nucleus at the center of the cell; some additional proteins are particularly important in pushing or pulling forces to participate in nuclear positioning: CLASPs, found on microtubules of the leading edge of migrating cells, IQGAP1, an actin-binding protein, and APC involved in interactions between microtubules plus-ends and the cortex. [141-142].

Microtubule dynamics play a central role in the positioning and function of organelles involved in intracellular trafficking: the endoplasmic reticulum (ER), the Golgi apparatus and the endosomes/lysosomes.

ER morphology and movements are essential for its function in protein synthesis and trafficking to the Golgi. In animal cells kinesin-1 seems to be the major motor protein involved in ER positioning and movement. Kinesin-1 is also involved in positioning and motility of ER exit-sites and participates in ER to Golgi trafficking [143]. Moreover STIM1 is a +TIP that is not a cytoplasmic protein but an integral protein of the ER and play a major role in ER remodeling. It also plays a significant role in the regulation of calcium storage as microtubule depolymerization is involved in calcium entry at the ER and STIM1 localization and function are necessary for this process [144]. In most mammalian cells, the Golgi apparatus is shaped like a ribbon closely associated with the centrosome. Its juxta-nuclear localization requires the presence of microtubules; without them the Golgi apparatus is dispersed in the form of mini-stacks formed at ER exit-sites and unable to migrate to the cell center [145]. Microtubule-dependent molecular motors are essential for Golgi organization and in particular the minus end directed motor, cytoplasmic dynein and its regulatory proteins. Plus-end directed motors are also involved in Golgi organization; a fraction of /kinesin-1 for example is localized at the Golgi and its depletion induces the compaction of the Golgi apparatus [146]. Golgi-nucleated microtubules indeed play a key role in Golgi organization. This microtubule sub-population is stable and acetylated; upon exit from mitosis golgi membranes specifically stabilize a microtubule subset thatis involved in the organization of Golgi in the centrosomal area. The important role of Golgi-derived microtubules in the of Golgi apparatus formation and maintenance suggests some organelles are not only passively arranged by elements but also actively participate in cellular and cytoskeleton organization [147-148].
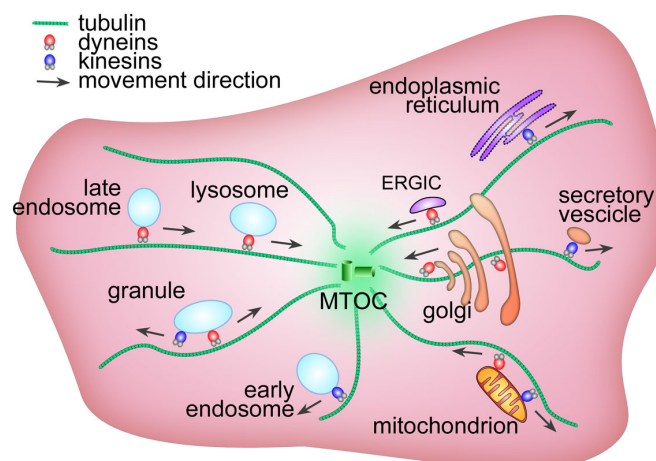
Fig 25. Microtubules transport and organization of cellular organelles. Microtubules constitute the skeleton by which intracellular organelles maintain their position and shape; moreover endosome-lysosome trafficking occours on it. Graphical rielaboration of [108].

Importantly, microtubules are essential for mitochondria positioning and transport. Mitochondria transport has been studied especially in axons, in neuronal cells, but also in non-polarized cells and it has been observed that several motor proteins transport mitochondria as cargos along microtubules. Mitochondrial tubules grow and shrink along with dynamic microtubules, and immobile mitochondria are captured by plus-ends of growing microtubules [149].

4.4 MICROTUBULES AND CELL MIGRATION.

Migration is a dynamic, cyclical process in which a cell extends a protrusion at its front, the leading edge, that attaches to the substratum on which the cell is migrating, followed by a contraction that moves the cell body toward the protrusion, and finally the attachments at the cell rear, the trailing edge, release as the cell continues to move forward.

The main players in this process are actin and myosin, that provide the forces pushing forward the leading edge, endocytic vescicles that allow redistribution of membrane and proteins from the trailing edge to the leading edge and the microtubules that reallocate intracellular structures, regulates vescicles transport and allow specific enzymes to reach action sites [150-152].
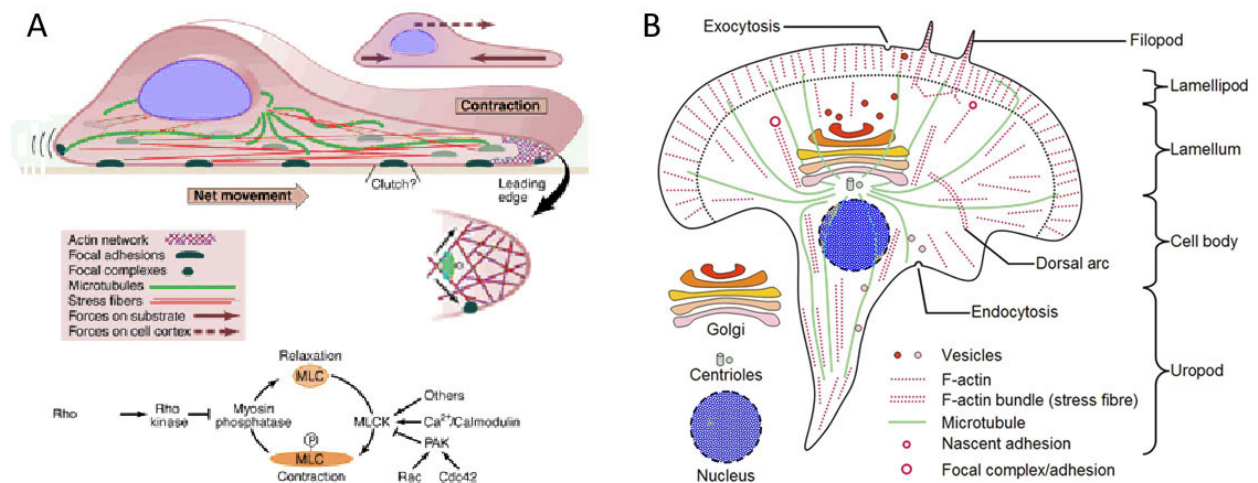
Fig 26. Cell migration. A: in migrating cells the movement is mainly due to pulling and pushing forces generated by actomyosin contraction, an event finely regulated by Rho kinase. B: actin and microtubles reorganization confer peculiar morphology to cellular structures.

During cell migration there is constant formation and sequential disruption of adhesive contacts. At the leading edge of the cell there are two types of protrusive structures called lamellipodia (protrusive sheet-like structures consisting of a cross-linked meshwork of actin-myosin filaments) and filopodia (fingerlike structures consisting of thin parallel bundles of actin

filaments oriented in the direction of protrusion) that form weak sites of attachment called focal complexes [150, 153].

at the leading edge as new adhesions form, they can disassemble (adhesion turnover) or stabilize and grow into more mature, larger ones. The molecular components of stable and nascent adhesions are similar, although there are molecules present only in specific subtypes. The molecular mechanisms underlying the fate of an adhesion are unclear. Rho GTPases are critical effectors in this process. They in turn are controlled by signals emanating from adhesion-related signalling modules, such as a multi-protein complex that includes FAK, Src, paxillin, Crk, CAS, PAK and GIT.

Adhesion that undergo maturation form large focal adhesion complexes which provide robust anchorage just behind the leading edge. Actomyosin filament bundles form and insert into it and movement is possible via the contractile activity of these filaments and the polymerization of actin filaments at the leading edge.

Actomyosin-based contraction is controlled by the small Rho GTPases Cdc42, Rac and RhoA. Regulation by these GTPases is antagonistic. RhoA activates Rho-kinase (also called ROCK), which in turn phosphorylates and inactivates the phosphatase that dephosphorylates MLC, resulting in increased contractility. A similar mechanism has been shown for Cdc42, acting through MRCK. Conversely, Rac activates PAK, which phosphorylates and inactivates MLC kinase, thus leading to decreased contractility and promoting spreading. However, PAK may also phosphorylate MLC directly, which would increase contractility. The predominance of the first or the second mechanism seems to be regulated by spatial considerations or differential regulation of PAK activity. Finally, PAK regulates microtubules through stathmin phosphorylation, which results in decreased microtubule catastrophe [150, 153-154].

Microtubules partecipate in cell migration by allowing transport of specific proteind and of endocytic vescicles at the required sites. A local regulation of +TIPs and small GTPases at the leading edge is necessary for the establishment of cell polarization; the most important ones are Rho, Rac, and Cdc42 that coordinate assembly and disassembly of actin filaments in response to extracellular signals, Rab GTPases that control endocytosis, Src that accumulates at cadherin based cell adhesions where it is responsible for reforming and maintaining the strength and integrity of established cell-cell contacts, FAK that in concert with Src signaling has been shown to be critical for the regulation of adhesion turnover at the leading edge of migrating cells, while Glycogen Synthase Kinase 3-beta (GSK3β), Casein Kinase I (CKI) and the scaffolding proteins

Axin and Adenomatous Polyposis Coli (APC) regulate β-catenin and intercellular adhesion [153].
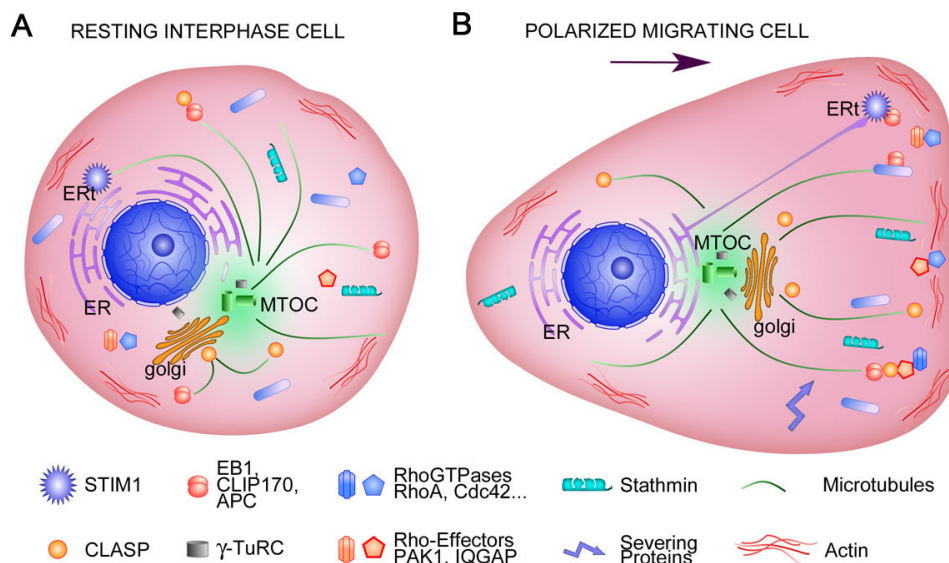
Fig 27. Differences in resting and migrating cells. A: in a non-polarized cell the most important polarity is established by the asymmetry between the center and the periphery of the cell. B: strong cellular polarization, as observed during migration, imposes an additional axis, a front and a rear of the cell being differentiated in addition to the center and periphery. The reorganization of the MTOC and other organelles during polarization allows the formation of the leading edge. Graphical rielaboration of [106].

A very important link between microtubules and cell migration is constituted by the activity of HDAC6: this enzyme regulates multiple important biological processes, such as cell migration, cell spreading, the degradation of misfolded proteins and stress granule formation through complexes with partner proteins. HDAC6-mediated deacetylation regulates microtubules dependent cell motility as its inhibition leads to an increased accumulation focal adhesion sites and prevents migration. In addition to its interaction with tubulin, HDAC6 is translocated to actin-enriched membrane ruffles, where it interacts with the F-actin binding protein cortactin. The inhibition of HDAC6 activity results in cortactin hyperacetylation, prevents its translocation to the cell periphery, blocks any association with F-actin, and impairs cell motility. By altering the ability of cortactin to bind F-actin, HDAC6 also regulates autophagosome-lysosome fusion, another important process that regulates cell migration and in particular rear end detachment. Moreover HDAC6 regulates β-catenin levels through modulation of proteosomal degradation; b-catenin plays a fundamental role in linking cytoskeleton to adherens junctions and its degradation is required for cell migration. Inhibition of HDAC6 causes a substantial increase in

β-catenin levels thus inhibiting migration; of given importance, HDAC6 activity is required for β-catenin nuclear translocation and its inhibition negatively affects not only cell migration but even cell proliferation [155-158] .

4.5 MICROTUBULES AND CELL DIVISION

The mitotic spindle is a bipolar, self-organizing microtubule based machine that accurately segregate sister chromatids into the daughter cells during division. The dynamic properties of microtubules are obviously important for spindle morphogenesis as well as force generation within the spindle. The first sign of microtubule dynamic alterations is in prophase when long interphase microtubules disappear and are replaced by shorter, less stable and more numerous mitotic microtubules that nucleate form the centrosome.
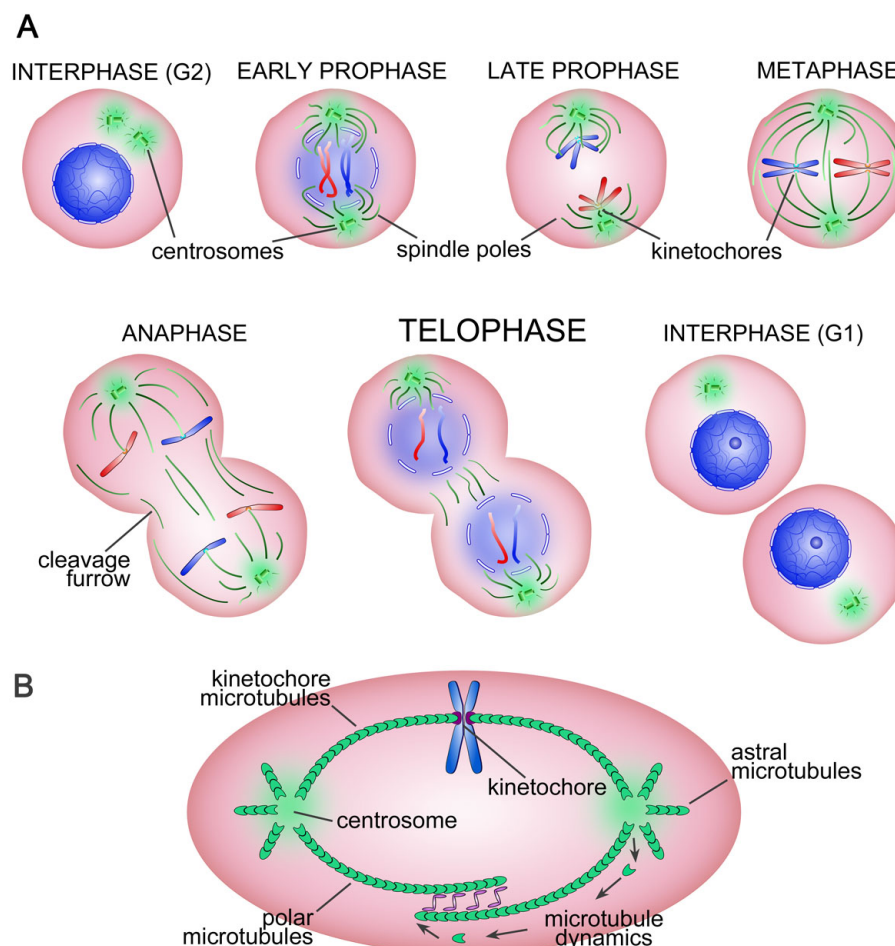
Fig 28. Microtubules dynamics in mitotic cells. A: different phases of mitosis progression with related microtubules organization. B spindle poles microtubule subclasses at metaphase. Graphical rielaboration of [108, 159]

Position, organization and functionality define three distinct subclasses of microtubules in the mature mitotic spindle: the astral ones, the interpolar ones and the kinetochore ones (K-fibers). Astral microtubules originate from the two centrosomes and extend all the way to the cell cortex. They have a major role in centrosome separation during prophase and in spindle positioning; they are involved as well in activating the assembly of actin and myosin ring that is fundamental for cytokinesis [108, 160].

The interpolar microtubules are the most dynamic and abundant class and comprise the main body of the mature spindle. They don't interact with chromosomes but emanate from the centrosome and extend towards the center of the spindle, where they interact in an antiparallel fashion with interpolar microtubules emanating from the opposite spindle pole. The most important function of these fibers is the establishment and maintenance of spindle bipolarity [108, 161].

K-fibers are bundles of 20–40 parallel MTs whose main function is to attach the chromosomes to the two spindle poles and to segregate the sister chromatids into the daughter cells. The mechanism driving the assembly of the K-fibers is still not fully understood. The attachment to the kinetochore occurs progressively as the cell moves from prometaphase to anaphase, in a process called K-fiber maturation. Erroneous K-fiber–kinetochore attachments are released for error correction through a mechanism involving the targeting and regulation of various kinetochore factors by the kinase Aurora B. It has been shown that the loss of tubulin subunits at the K-fiber minus-end occurs without spindle pole detachment and drives the polewards tubulin flux. This mechanism is sufficient for generating pulling forces at the kinetochores that stretch the centromeres in metaphase. In anaphase, dramatic changes in K-fiber dynamics promote their shortening and chromosome segregation [161-163].

During mitosis microtubule can originate through three different pathways, centrosomal, chromosomal and microtubule-dependent, all of them cooperating to form the spindle. The centrosome asters define the position of the two spindle poles and the axis of cell division; the chromosomal microtubules facilitate the capture of the kinetochores and the formation of the K-fibers; the microtubules amplification contributes to the strengthening of the whole structure. The combination of the three pathways could therefore allow the timely assembly of the bipolar spindle and allow mitosis to progress successfully [161].

Mitosis initiation and progression is regulated by a complex machinery, with different activities being switched on and off at precise times and locations throughout the cell. One essential player

is the chromosomal passenger complex (CPC), which comprises Aurora-B protein kinase, the inner centromere protein INCENP, survivin and borealin. CPC localization is highly dynamicis and regulates at the same time chromosomal arrangements and spindle pole organization by correcting nonbipolar microtubule-kinetochore interactions. In prophase, the CPC is found on chromosome arms where it phosphorylates histone H3 on Ser10 and Ser28, an early event required for chromosome condensation. During this phase it accumulates at centromeres where the maturation of kinetochores begins and continues through prometaphase. The CPC is required for the formation of a bipolar spindle and its stability from prophase/prometaphase to anaphase. In metaphase, it localizes at centromeres, where it has a central role in centromeric cohesion and the regulation of kinetochore–microtubule attachments. It controls the correct alignment of chromosomes on the spindle equator and the spindle checkpoint. In anaphase, the CPC translocates to the spindle midzone and appears at the cortex; it is involved in the formation of the central spindle. In telophase, the CPC concentrates at the cleavage furrow and, subsequently, at the midbody, where it is required for completion of cytokinesis [164-165].
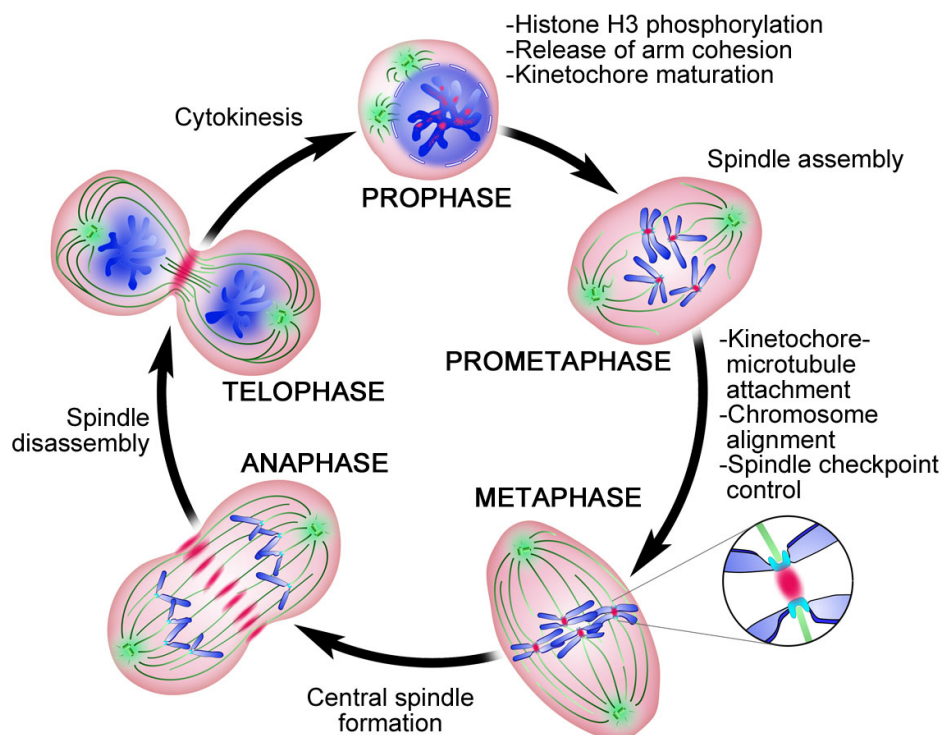
Fig 29. Microtubules organization and CPC localization through mitosis. CPC is fundamental in organizing mitotic progression through different phases. CPC localization is represented in red and fundamental actions are described. Microtubule rearrangements are represented in green.

4.6 MICROTUBULES AND CANCER THERAPY

Microtubules play an important part in an array of cellular functions including mitosis, movement of organelles, vesicles and proteins, development and maintenance of cell shape and growth. The complex dynamics of microtubules are highly regulated and sensitive to manipulation. If bipolar spindle dynamics are compromised, mitotic block or slowing occurs at the metaphase-anaphase transition, eventually leading to apoptosis. Agents that disrupt microtubule dynamics play key roles in both curative and palliative cytotoxic chemotherapeutic regimens [166-167].

Drugs that interferes with microtubular structure and function are classically divided into stabilizers and destabilizersMicrotubule destabilizers consist predominantly of drugs that act at the Vinca alkaloid and colchicine-binding sites. The oldest class of cytotoxic agents that interfere with microtubules are the Vinca alkaloids; these agents are active in a variety of malignancies including lymphomas, non-small cell lung cancer (NSCLC), and breast cancer. It is thought that the Vinca alkaloids interact with the central portion of the b-tubulin subunit peventing polymerization. Colchicine acts at a separate site on b-tubulin named the colchicine-binding site [168].

Until recently, the only clinically important microtubule stabilizers were the taxanes, such as paclitaxel and docetaxel. Taxanes are widely used cytotoxic agents that are active in a range of solid tumor malignancies such as breast cancer, NSCLC, ovarian cancer, gastroesophageal cancer, germ cell tumors, as well as cancers of the head and neck. They are routinely used in the neoadjuvant, adjuvant, and metastatic setting alone and in combination with drugs with different mechanisms of action and nonoverlapping toxicity profiles. The taxanes bind to tubulin, stabilize the microtubule, and inhibit its disassembly leading ultimately to cell death by apoptosis [168-169]. The clinical use of the taxanes is limited by tumor resistance, risk of hypersensitivity reactions and toxicity. Acquired and intrinsic resistance of tumor cells to taxanes remains a significant clinical problem. It occurs through a variety of mechanisms, most important one being the expression of multidrug resistance proteins such as P-glycoprotein, which belongs to a family of ATP-binding cassette transporters and which is the product of the multidrug resistance-1 gene. Resistance to the taxanes can also occur due to interruption of the interaction between the drug and the target protein, b-tubulin: tumor cells can overexpress the bIII isoform of tubulin leading to demonstrable clinical resistance; intrinsic and acquired mutations in the tubulin protein can interfere with the normal binding of taxanes to the target protein; altered expression

of microtubule-associated proteins can also prevent taxane binding [167].

Epothilones are macrolide antibiotics that cause microtubular stabilization and cellular arrest in a similar way to the taxanes. They bind to the tubulin-binding pocket in a specific and independent manner, suggesting that rather than a common pharmacophore for taxanes and epothilones, tubulin has a promiscuous binding pocket, allowing different molecules to interact according to their unique structures [170].

Laulimalide is a structurally complex substance derived from marine sponges that also maintains antimitotic activity against paclitaxel-resistant cells. The interaction of laulimalide and microtubules is complex, but there is evidence for a distinct laulimalidebinding site on a-tubulin. Xenograft studies in mice have shown that the drug has a narrow therapeutic index and marked toxicity without evidence of efficacy, probably limiting its further development [171-172].
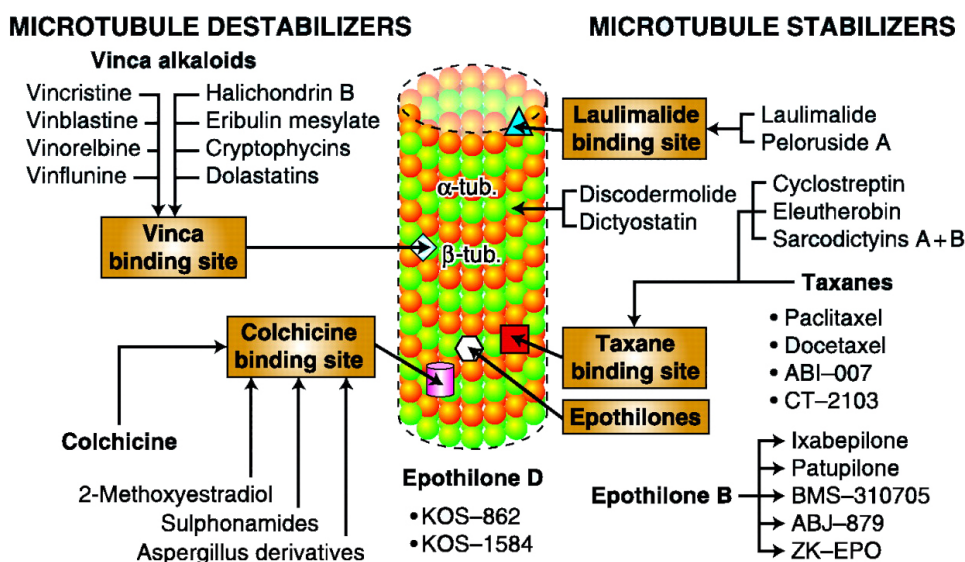
Fig 30. microtubules stabilizers and destabilizers. Adapted from [167].

MATHERIALS & METHODS

CHEMICALS

SP600125 (1,9-Pyrazoloanthrone), MTT (3-(4,5-Dimethyl-2-thiazolyl)-2,5-diphenyl-2H-tetrazolium bromide), Monoclonal anti-β-Catenin antibody 6F9, Monoclonal Anti-α-Tubulin, clone DM1A, Monoclonal Anti-Acetylated Tubulin Clone 6-11B-1, L-Glutamine Solution 200 mM, Sodium Pyruvate Solution 100mM, Dulbecco's PBS, PBS tablets, Trypsin EDTA Solution, Penicillin/Streptomicyn Solution, Foetal Bovine serum, were purchased from Sigma-Aldrich.

p53 antibody, caspase3 antibody, Phospho-p53 (Ser46) Antibody, p53 (1C12) Mouse mAb, p27 Kip1 (D69C12)XP Rabbit mAb, p21 Waf1/Cip1 (DCS60) Mouse mAb, p21 Waf1/Cip1 (12D1) Rabbit mAb, Acetyl-p53 (Lys382) Antbody, Phospho-p53 (Ser15) Antibody, HDAC (D2E5) Rabbit mAb, PARP Antibody were purchased from Cell Signaling Technologies.

Purified Mouse Anti-Actin Ab-5 was purchased from BD Biosciences.

Goat anti Rabbit IgG, (H+L) HRP conjugate, Goat anti-Mouse IgG Antibody, Peroxidase Conjugated, H+L Ischemin (MS120), pifithrin-μ (CAS 64984-31-2) were purchased from Merk Millipore.

Wheat Germ Agglutinin 594 conjugate, LysoTracker Red DND-99, ProLong Gold Antifade Reagent with DAPI, Alexa Fluor 488 F(ab')2 Fragment of Goat Anti-Rabbit IgG (H+L) Antibody, Alexa Fluor 488 F(ab')2 Fragment of Goat Anti-Rabbit IgG (H+L) Antibody, Alexa Fluor® 555 F(ab')2 Fragment of Goat Anti-Rabbit IgG (H+L), Goat serum New Zealand, DMEM GlutaMAX™ Supplement , DMEM/F-12 GlutaMAX™ Supplement, Ham's F-12 Nutrient Mix, GlutaMAX™ Supplement, Ham's F-12K (Kaighn's) Medium were purchased from Life Technologies.

RPMI 1640 medium was purchased from EuroClone.

cOmplete, Mini Protease Inhibitor Cocktail Tablets were purchased from Roche.

NE-PER Nuclear and Cytoplasmic Extraction Reagents, TUBB1 antibody, Phospho-Histone H3 pSer10 Antibody, Restore Western Blot Stripping reagent were purchased from Thermo Scientific.

HDAC Activity/Inhibition Direct Assay Kit (Colorimetric) was purchased from Epigentek.

MycoAlert Mycoplasma Detection Kit was purchased from Lonza.

Caspase-Glo 3/7 Assaywas purchased from Promega.

Proteome Profiler Human Phospho-Kinase Array was purchased from R&D Systems.

CELL CULTURE

All thyroid cancer cell lines were stored in liquid nitrogen**.** For defrosting, cells were placed in 37°C water bath, gently shaken for 1 minute and then immediately seeded in pre-warmed culture media. The day after, media was changed and cells cultured for at least 10 days before experiments being performed.

All cells were grown as monolayers in 100 mm plastic culture dishes and kept in a humidified incubator at 37°C under 5 % CO_2, with media change every 3-4 days. Cells were passaged when reaching 70-80 % confluency.

All cell lines had been identified of thyroid cancer derivation [173].

All cell lines were routinely screened for mycoplasma contamination with MycoAlert Mycoplasma Detection Kit (Lonza).

DTC	**FTC-133**	Description	FTC-133 was obtained from a FTC lymph node metastasis of a 42-year-old male. Grown as monolayer. The morphology differs from flat polygonal to spindle formed cells. They retained differentiated thyrocyte function and thyrocyte responsiveness to thyrotropin and local active growth factors. [174-176]
		Colture Media	DMEM : Ham's F12 supplemented with 10% FBS, 2mM L-Glutamine;
		Genetics	PTEN -/R130*, p53 R273H
	TPC-1	Description	Obtained from a papillary thyroid carcinoma of a female patients. Retains thyroid differentiation markers. Grown as monolayer organized in multi-cellular, trabecula-like structures. [177-182]
		Colture Media	RPMI supplemented with 10% FBS, 1 mM sodium pyruvate, 2mM L-Glutamine.
		Genetics	RET/PTC1, t (1;10;21)
PDTC	**HTC/C3**	Description	Human thyroid carcinoma established from cancer cells disseminated in the pleural fluid of a 44-year-old japanese woman with undifferentiated giant cell carcinoma of the thyroid. Epithelial-like cells growing as monolayer. [183]
		Colture Media	DMEM supplemented with 10% FBS, 2mM L-Glutamine.
		Genetics	BRAF V600E/WT, p53 P152L, DUSP26 amplification
	SW579	Description	Squamous cell thyroid carcinoma established from 59 years old caucasian male in 1973. Epithelial cells growing as monolayer. [176, 184-186]
		Colture Media	Ham's F12 supplemented with 10% FBS, 2mM L-Glutamine.
		Genetics	P53 I255S
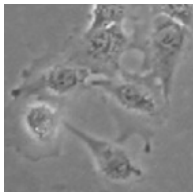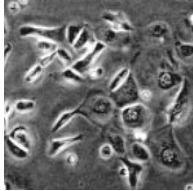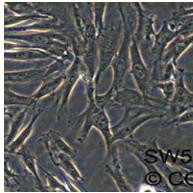
ATC	**SW1736**	Description	Anaplastic thyroid carcinoma originally developed by Leibowitz and McCombs III at the Scott and White Memorial Hospital (Temple, TX) in 1977. Their epithelial origin was confirmed by demonstration of cytokeratin expression. Grown as monolayer. [187-189]
		Colture Media	DMEM supplemented with 10% FBS, 2mM L-Glutamine.
		Genetics	BRAF V600E/WT, p53 -/-
	Hth74	Description	Human anaplastic thyroid carcinoma cell line was isolated from thyroid carcinoma tissue of a 73-year-old woman. HTh74 cells were shown to express some thyroid specific genes like functional TSH receptor protein, and mRNA for thyroglobulin, albeit both at very low levels.Epithelial-like, grown as monolayer. [176, 189-190]
		Colture Media	DMEM supplemented with 10% FBS, 2mM L-Glutamine.
		Genetics	P53 K286E, Akt pathway hyperactivation
MTC	**TT**	Description	The TT cell line was established from a 77 year old female with thyroid medullary carcinoma. Epithelial-like, grown as monolayer; TT cells continuously produce high levels of calcitonin and CEA. Chromosomal analysis of the cell line reveal an aneuploid human karyotype with several marker chromosomes. Harbour a MEN2A-type mutation. [191-193]
		Colture Media	Ham's F12K supplememted with 10% FBS
		Genetics	RET C634W
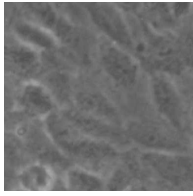
Table 6. Cell lines used in this study and their main characteristics.

MTT PROLIFERATION ASSAY

Cells were seeded at the optimal density in 96-well plates with the exception of the outer wells; after 24 hours cells were treated with SP600125 diluited in the appropriate colture media (100μL/well) at concentrations in the range 0-50 μM and incubated for the given time (0-96h).

On the day of the assay MTT (Sigma) solution (5 mg/ml in PBS) was equilibrated at room temperature and 10μL were added to each well to a final concentration of 0.5 mg/ml; from this moment exposure to direct light was avoided.

The plates were incubated at 37˚C and 5 % CO_2 for 2 hours for all cells except TT which required 4 hours, colture media was then gently removed and formazan crystals solubilized in 200μL of EtOH:DMSO 1:1 solution. After 5 minutes solubilization on a plate shaker assorbance was red at 540nm using ELx800 Absorbance Microplate Reader (BioTek).

CELLULAR FRACTIONING

The cellular fractioning was performed with NE-PER Nuclear and Cytopalsmic Extraction Reagents (Thermo Scientific) kit.

Cells were seeded at the optimal density in 6 cm petri dishes and after 24 hours treated with DMSO or SP600125 10 μM. Cells were harvested with trypsin-EDTA, pelleted and resuspended in PBS. 2.000.000 cells were tranferred to a new tube, pelleted and PBS was completely removed. Samples were resuspended in 200 μl of ice cold CER I buffer, vortexed on the highest setting for 30 seconds and incubated on ice for 10 minutes. CER II buffer was added, followed by 10 minutes vortexing twice, separated by 1 minute incubation on ice. Samples were centrifuge at 14500g for 5 minutes and the surnatant containing cytoplasmic extract immediately transferred to a new tube. Pellets were suspended in ice cold NER buffer and vortexed for 15 seconds every 10 minutes for a total of 40 minutes, followed by centrifugation at 14500g for 10 minutes. Surnatant containing the nuclear fraction was transferred to a new tube and the pellet discharged.

Cytoplasmic and nuclear extracts were sonicated and analyzed by electrophoresis and western blotting on 4-12% acrilammide gels. For assess of correct cellular fraction separation GAPDH was used as cytoplasmic marker while PARP was used as nuclear marker.

CO-IMMUNOPRECIPITATION ASSAY

Co-immunoprecipitation (Co-IP) is a popular technique to identify physiologically relevant protein-protein interactions by using target protein-specific antibodies to indirectly capture proteins that are bound to a specific target protein.

Cells were seeded at the optimal density in 10 cm petri dishes and after 24 hours treated with DMSO or 10 μM SP600125.

Cells were washed twice with warm PBS and then lysed with 500μl of hypotonic buffer (150 mM NaCl, 1 mM EDTA, 0.5% NP40, 20 mM Tris-HCl (pH 7.5) plus freshly added protease inhibitors cocktail); cells were collected in tubes and incubated for 15 min on ice in agitation. Samples were then centrifuged 14000g for 10 minutes and surnatant immediately transferred to new tubes.

Protein G-sepharose (Protein G Sepharose 4 Fast Flow, GE Healthcare) was washed twice with PBS and 100 μl of Protein G-sepharose:PBS 1:1 solution was added to each sample followed by 1h incubation at 4°C in agitation. After centrifugation at 14000g for 10 minutes surnatant was transferred to new tubes and total protein amount quantified with DC Protein Assay (BIORAD); all samples were diluited in PBS to obtain final protein concentration of 1 μg/ml (total extract fraction).

2 μl of primary antibody against acetyl-α-tubulin was added to 500 μl of each sample followed by over night incubation at 4°C in agitation.

On the following day 100 μl of Protein G-sepharose:PBS 1:1 solution was added to each sample followed by 2h incubation at 4°C in agitation. After centrifugation at 14000g for 10 minutes the surnatant was transferred to new tubes (surnatant fraction); the pellet containing immunoprecipitated proteins was washed twice with PBS, resuspended in 50 μl of lysis buffer and boiled for 5 minutes (immunoprecipitated fraction); after centrifugation at 14000g for 10 minutes the surnatant was transferred to new tubes and the whole sample was analyzed by electrophoresis and western blotting.

TUBULIN POLYMERYZATION ASSAY

An *in situ* cellular assay was used, in which the tubulin monomer (soluble) and polymer (unsoluble) forms were separated by centrifugation in hypotonic buffer and relative amounts analyzed by electrophoresis and Western blotting [194-195].

Cells were seeded at the optimal density in 6 cm petri dishes and after 24 hours treated with DMSO or 10 μM SP600125.

All buffers were mainteined at 37°C to avoid temperature-dependent variations in tubulin polymerization.

Cells were washed twice with warm PBS and then lysed with 100μl of hypotonic buffer (1 mM MgCl2, 2 mM EGTA, 0.5% NP40, 20 mM Tris-HCl (pH 6.8) plus freshly added 2 mM PMSF and protease inhibitor cocktail) for 10 minutes at 37°C. Cells were collected in tubes and the particulate fraction was separated from the soluble cytosolic fraction by centrifugation at 14000g for 10 minutes. Surnatant containing the monomeric tubulin was immediately collected and transferred to a new tube while the pellet containing the polymeric form was resuspended in equal amount of hypotonic buffer.

All samples were sonicated and analyzed by electrophoresis and western blotting on 10% acrilammide gels.

PROTEIN EXTRACTION AND WESTERN BLOTTING

Samples preparation

Cells were seeded at the optimal density in 6 cm petri dishes and after 24 hours treated with DMSO or 10 μM SP600125.

For phospho-protein evaluation cells were washed with PBS and then lysed with 100 μl of Laemmli buffer (62.5 mM Tris-HCl pH 6.8, 5% SDS) supplemented with freshly added protease inhibitors (cOmplete Mini, Roche) and phosphatase inhibitors (Phosphatase Inhibitor Cocktail 2, Sigma) pre-warmed in boiling water [196]. Samples were collected in pre-chilled tubes, boiled for 3 minutes and sonicated.

For all the other samples, cells were washed with PBS and lysed with ice-cold RIPA buffer (50 mM Tris-HCl pH 7.5, 150 mM NaCl, 0.1% SDS, 1% NP40, 1% Sodium deoxycholate, 2 mM EDTA) supplemented with freshly added protease inhibitors (cOmplete Mini, Roche) and phosphatase inhibitors (Phosphatase Inhibitor Cocktail 2, Sigma), collected in pre-chilled tubes and sonicated [197-198]. For apoptosis evaluation cell medium was collected to new tubes, cells harvested with trypsyn and added to their own medium. After pelleting cells were resuspended in supplemented RIPA buffer, collected in pre-chilled tubes and sonicated.

Protein amount was quantified with bicinchoninic acid method (BCA Protein Assay Reagent, thermo Scientific) [199] and for each sample the same protein amount was prepared with 10X Denaturing Sample Buffer (500mM Tris-HCl pH 6.8, 10% SDS, 60% Glycerol, 10% β-mercaptoethanol, 0.04% bromophenole blue), boiled for 5 minutes and analyzed by electrophoresis.

Electrophoresis

All samples with the exception of tubulin polymerization assay and Co-Immunoprecipitation ones were resolved with Novex NuPAGE® SDS-PAGE Gel System on NuPAGE® Novex 4-12% Bis-Tris Gels in MOPS Running Buffer. Tubulin Assay and Co-Immunoprecipitation samples were resolved on 10% acrylamide gels in Running Buffer (250 mM Tris, 1.92 M Glycine, 10% SDS).

Protein transfer was performed with iBlot Blotting System (Life Technologies) on iBlot Transfer

Stack, Nitrocellulose, followed by Ponceau Staining as control.

Immunoblotting

Nitrocellulose membranes were incubated for 1 hour in 5% milk in TBS-T (30 mM Tris-HCl pH 7.5, 150 mM NaCl, 0.1% Tween-20) in agitation, washed three times with TBS-T and incubated over night at 4°C with primary antibody following manufactor instruction. The following day membranes were washed three times with TBS-T and incubated for 1 hour in secondary antibody solution (anti rabbbit or anti-mouse HRP-conjugated Ab (Millipore), 1:5000 in 5% milk in TBS-T).

Detection

After three times washing with TBS-T, a chemiluminescence-based immunodetection was performed with Novex ECL Chemiluminescent Substrate Reagent Kit; Amersham Hyperfilm ECL (GE Healthcare) were exposed for different times in a dark room and manually developed (Kodak Dental Readymatic Developer and Fixer). Images were quantified with ImageJ software.

Antibody	productor	code	Concentration	Solution (TBS-T)
actin	BD	612657	1:5000	5% milk
Acetyl-p53 Lys382	Cell Signaling	#2525	1:1000	5% BSA
Acetyl-tubulin Lys40	Sigma	T6793	1:1000	2.5% milk
β-catenin	Sigma	C7207	1:1000	5% BSA
Caspase3	Cell Signaling	#9662	1:800	2.5% milk
GAPDH	Santa Cruz	sc-25778	1:2000	5% milk
HDAC6	Cell Signaling	#7558	1:1000	5% BSA
p21	Cell Signaling	#2947	1:1000	5% BSA
p27	Cell Signaling	#3686	1:1000	5% BSA
p38	Cell Signaling	#9212	1:1000	5% BSA
p53	Cell Signaling	#9282	1:1000	5% milk
PARP	Cell Signaling	#9542	1:1000	5% milk
Phospho-Histone H3 Ser10	Thermo Scientific	PA5-17869	1:1000	5% BSA
Phospho-p38 Thr180/Tyr182	Cell Signaling	#9212	1:1000	5% milk
Phospho-p53 Ser15	Cell Signaling	#9284	1:1000	5% BSA
Phospho-p53 ser46	Cell Signaling	#2521	1:1000	5% BSA
tubulin	Sigma	T9026	1:2000	2.5% milk

Table 7. Antibodies and settings used in western blot assays.

IMMUNOFLUORESCENCE AND CONFOCAL IMAGING

Cells were seeded at the optimal density on 22x22 mm glass slides and after 24 hours treated with DMSO, 10 μM and 20 μM SP600125.

For cell membrane visualization living cells were incubated with 5 μg/ml Wheat Germ Agglutinin Alexa-Fluor 594 Conjugate (Life Technologies) in PBS for 10 minute at 37°C in 5% CO2 prior to samples fixation.

For lysosome visualization living cells were incubated with 1μM LysoTracker® Red DND-99 (Life Technologies) in appropriate colture medium for 2 hours at 37°C in 5% CO2 prior to samples fixation.

Samples were washed three times with pre-warmed PBS and fixated by incubation for 10 minutes in pre-warmed 4% PFA in PBS except for membrane and lysosme visualization where it was used a 2% PFA solution. After washing with PBS cells were pearmibilized with 0.2% Triton-X in PBS for 10 minutes and then incubated for 1 hour RT with 5% goat serum in PBS. After washing, cells were incubated over night at 4°C with primary antibody solution. On the following day cells were washed three times in PBS, secondary antibody solution (anti-rabbit Alexa-Fluor 564 conjugate or anti-mouse Alexa-Fluor 488 conjugate, Life Technologies, 1:500) was added, and 1 hour incubation was performed in the dark. After PBS washing samples were mounted on microscope slides with 15 μl of ProLong Gold Antifade Reagent with DAPI (Life technologies)

Images were acquired with Nikon EclipseTi-E inverted microscope with IMA10X Argon-ion laser System by Melles Griot; all images were acquired with CFI Plan Apo VC 60X Oil (Nikon) objective except those for mitotic index that were acquired with CFI Plan Apo VC 20X (Nikon) objective. p53, Acetyl-tubulin and WGA stained cells were acquired with ulterior 1.3x digital zoom. Mitotic morphology cells were acquired with ulterior 5x digital zoom. Migrating cells details were acquired with ulterior 4x digital zoom. For microtubules, mitosis and migration imaging whole cells were acquired with Z-series acquisition, 0.15 μm step and 3D structure reconstucted with NIS-Elements AR software.

MATHERIALS & METHODS

Antibodies & Dyes	productor	code	Concentration	Solution (PBS)
Acetyl-tubulin	Sigma	T6793	1:500	5% goat serum
β-catenin	Sigma	C7207	1:200	5% goat serum
Lysotracker	Life Technologies	L-7528	1μM	DMEM or RPMI
p53 1C12	Cell Signaling	#2524	1:200	5% goat serum
Phospho-Histone H3 Ser10	Thermo Scientific	PA5-17869	1:250	5% goat serum
Phospho-p53 Ser15	Cell Signaling	#9284	1:250	5% goat serum
tubulin	Sigma	T9026	1:500	5% goat serum
Wheat Germ Agglutinin	Life Technologies	W11262	5.0 μg/mL	PBS

Table 8. Antibodies and settings used in immunofluorescence experiments.

CASPASE ACTIVITY ASSAY

Caspase activity was measured with Caspase-Glo 3/7 Assay (Promega). Cells were seeded at the optimal density in 96-well white and transparent plates with the exception of the outer wells; after 24 hours they were treated with DMSO or 10 μM SP600125 for 0-72h.

On the day of the assay reagents were bring to room temperature and to each well of the white plastic plate 100μl of reconstituted Caspase-Glo Reagent was added. After 30 seconds shake, plates were incubated in the dark at room temperature for 1 hours. Fluorescence was measured using a Fluoroskan Ascent FL Microplate Reader (Thermo Scientific) luminometer.

At the same time MTT assay was performed on the transparent plates to determine cell viability and variations in cell number.

PHOSPHO-KINASE ANTIBODY ARRAY

The assay was performed using manufacture instructions.

Cells were seeded at the optimal density in 10 cm petri dishes and after 24 hours treated with DMSO or 10 μM SP600125; after 60h samples were extracted in 400μl of Lysis Buffer 6.

After 30 minutes incubationon ice on a rocking platform samples were centrifuged at 14000g for 5 minutes, the surnatant transferred to new tube and total protein amount quantified.

A and B membranes were blocked in 1ml of Array Buffer 1 for 1 hour at room temperature. Blocking buffer was discharged and 300 μg of proteins eluted in array buffer 1 to a total amount of 2 ml were added to each membrane. Membranes were then incubated at 4°C overnight on a orbital shaker.

The following day membranes were washed in 20 ml of washing buffer and each one was incubated in 1 ml of reconstituted detection cocktail for 2 hours at room temperature on a orbital shaker. After washing each membrane was incubated with 1 ml of streptavidin-HRP conjugated for 30 minutes room temperature, washed and developed with 500 μl of ChemiReagent mix.

Analysis was performed with ImageJ software.

WOUND HEALING ASSAY

Cells were seeded at the optimal density in 6-well multiwell and after 24 hours treated with DMSO or 10 μM SP600125; after 72h cells were scraped with a p200 tip, washed with PBS and returned to control or treated medium. Images were acquired at 0, 12 and 16h with Kodak EasyShare C195 camera on Olympus CK2 microscope with A10PL 10X objective.

Wound dimensions were quantified with ImageJ software.

HDACs ASSAY

The assay was performed with Epigenase HDAC Activity/Inhibition Direct Assay Kit (colorimetric) with minimal modifications to manufacter's instruction.

Cells were seeded at the optimal density in 10 cm petri dishes and after 24 hours treated with DMSO or 10 μM SP600125. On the day of the assay cell fractioning was performed with NE-PER Nuclear and Cytopalsmic Extraction Reagents as described, using doubled number of cells to obtain high concentrated samples. HDAC activity was tested in both nuclear and cytoplasmic fractions, control samples with 5 μM TSA were used as inhibition control. Samples (15μg for cytosol and 10μg for nuclear extracts) and standard curve (range 0.1-4ng/μl) were added to plate wells, sealed with adhesive film and incubated for two hours at 37°C in the dark. After washing 50 μl of HO4 solution were added to each well and then incubated for 1 hour room temperature in the dark. After washing 50 μl of HO5 solution was added and incubated for 30 minutes at room temperature in the dark. After washing 100 μl of Developing Solution were added and incubated at room temperature for 20 minutes in the dark; a blue color developed in presence of HDACs activity. 100 μl of Stop Solution were added and absorbance readed at 450 nm with reference background at 655nm.

On the same samples a western blot was performed to assess the amount of HDAC6 in the different samples.

PATHWAYS ANALYSIS

STRING (Search Tool for the Retrieval of Interacting Genes/Proteins)

STRING [49, 200] is an on-line database, a meta resource that aggregates most of the available information on protein-protein associations, scores and wheights it, and augmants it with predicted interactions as well as with the results of automatic literature-mining searches.

The basic interaction unit in STRING is the "functional association" , which is defined as the specific and meaningful interaction between two protein that jointly contribute to the same functional process.

The STRING website aims to provide easy and intuitive interfaces for searching and browsing the protein interaction data, as well as for inspecting the underlying evidence. Users can query for a single protein of interest,or for a set of proteins, using a variety of different identifier name spaces.

The resulting network can then be inspected, rearranged interactively or clustered at variable stringency. Each protein node in the network shows a preview to 3D structural information, if available, and can be clicked to reveal a pop-up window with more information about the protein (including its annotation, SMART domain-structure, structure homology models from SWISS-MODEL Repository etc).

Each edge in the network denotes a known or predicted interaction, and leads to a pop-up window providing details on the underlying evidence and the interaction confidence scores.
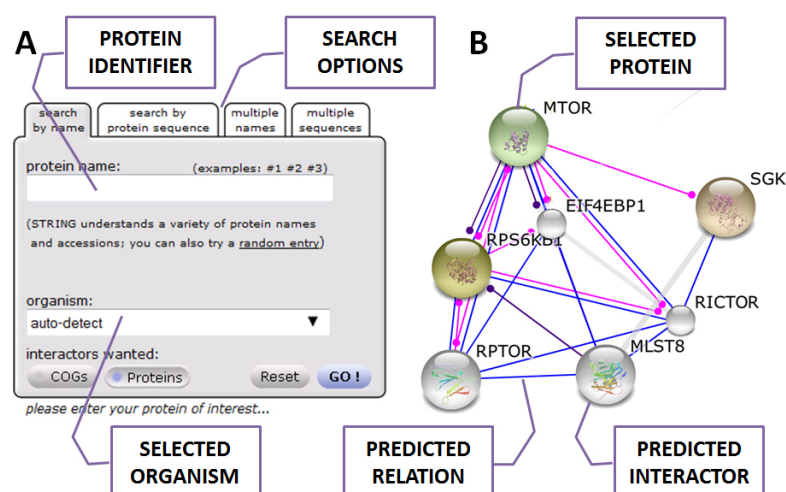
Fig 31: STRING user's interface. A: protein selection tool; B: resulting network.

An interactive view allows for rearrangement and ad-hoc clustering of nodes; three modes provides different views on the network:

- confidence view: single edges connect the items with thickness proportional to the confidence;

- actions view: each edge represents a given type of action, like activation, inhibiton or binding;

- evidence view: each edge represents a given type of evidence, like text mining or experimental evidence.

STITCH (Search Tool for Interacting Chemicals)

STITCH [201-203] is a interactive database about chemicals-proteins interaction knowledge. It enables the user to search by compound name displaying a network view of most probable interactions; for proteins and chemicals the structure annotations and links to source databases are shown while for edges available scores are shown. More than 300000 chemicals interactions are available, with more than 110000 high-confidence interactions and more than 250000 high-confidence edges for interactions between chemicals and human proteins. To provide crucial context for the aggregated protein-chemicals interactions, protein-protein interactions from STRING database are incorporated into a seamless network view.

An interactive view allows for rearrangement and ad-hoc clustering of nodes; three modes provides different views on the network:

- confidence view: single edges connect the items with thickness proportional to the confidence;

- actions view: each edge represents a given type of action, like activation, inhibiton or binding;

- evidence view: each edge represents a given type of evidence, like text mining or experimental evidence.

Analysis parameters

SP600125 interactions have been indagated with STITCH 3 while protein-protein interactions have been indagated with STRING v9.1.

For both analysis the following settings were used:

- co-occourrence, co-expression, experiments and databases were selected as active predicting methods;

- confidence score was setted as > 0.700 (high);

- node enrichment +10 nodes

- custom limit of no more than 20 interactors shown;

- network clustering with MCL algorithm;

DATA ELABORATION AND STATISTICAL ANALYSIS

All western blot and cell migration quantifications were made with ImageJ Software, version 1.47

All confocal microscopy based quantifications were made with Nikon NIS-Elements Software, followed by ImageJ analysis when required.

All statistical analysis were performed with GraphPad Prism Software, version 5.04 on a minimum of four replicates. Values are expressed as mean standard error. One-way or two-way ANOVA followed by appropriated post-hoc test were used to evaluate differences between means.

On the whole document significativity levels were reported as follows:

*   p<0,05

**   p<0,01

***   p<0,001

RESULTS

1 EFFECTS ON CELL PROLIFERATION

1.1 SP600125 AFFECTS CELL PROLIFERATION.

Since it has recently been demonstrated that SP600125 is able to inhibit the proliferation of p53 null cells [57], for first it was tested on six thyroid cancer derived cell lines with different p53 status: three cell lines harboring p53 point mutations (HTC/C3, Hth74 and SW579), one with a pseudo-null status (SW1736) and two p53 wild type ones (TPC1 and TT). Cells were exposed to different concentrations (0-50 μM) for different periods of time (0-96h) and viability asessed with MTT assay.
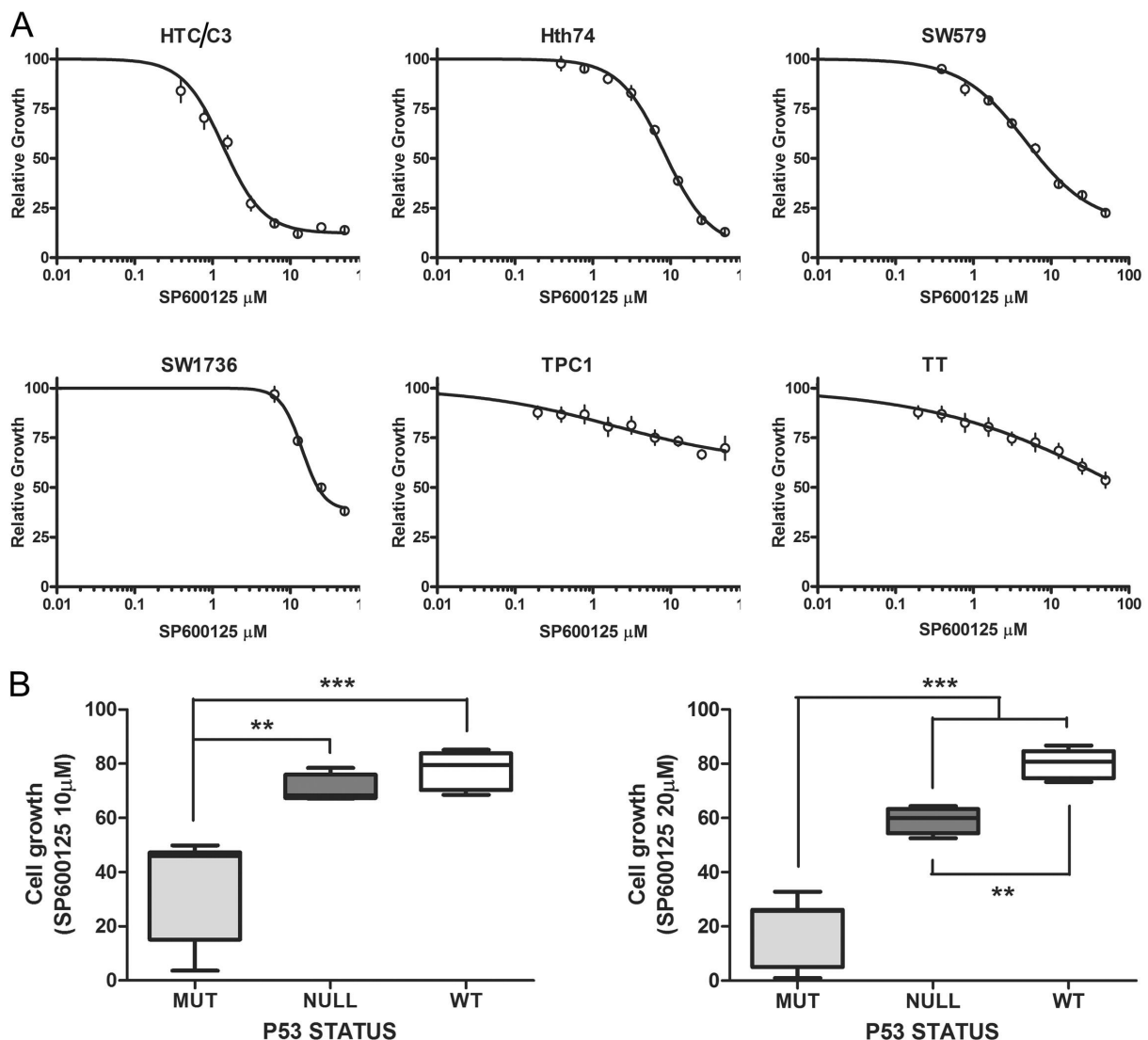
Fig 1. **Effects on cell proliferation.** Cells were incubated for 96h with the indicated concentrations of SP600125 and then viability was assessed with MTT assay; DMSO was used as control. **A**: dose dependent growth inhibition (% control); **B**: differences in cells growth inhibition correlated with p53 status. MUT p53 metated cells, NULL p53 null cells, WT p53 wild type cells.

The results shown that SP600125 was able to reduce cell growth with various efficacy in a time and concentration dependent way (Fig 1A). Moreover, if proliferation data are grouped by p53 status, it can be noticed that there are significant differences in growth inhibition (Fig 1B) and that these differences are exacerbated with an increase in dose and time of incubation: while at 10 μM only p53 mutated cell lines exhibited significant growth inhibition compared to wild type, at 20 μM significant effects were obtained also on p53 null cells. From the obtained data it can be inferred that SP600125 acts preferentially on cell lines with altered p53, with much more efficacy on point mutations vs. null status. On the basis of obtained results, the concentrations of 10 μM and 20 μM were chosen for further experiments.

2 EFFECTS ON P53

2.1 SP600125 INFLUENCES P53 LOCALIZATION

As long as SP600125 action was confirmed be influenced by p53 status, to clarify p53 involvement further experiments were performed. Fist of all, as p53 nuclear translocation plays an important role inits activation, subcellular localization was analyzed by confocal microscopy analysis and cellular fractioning experiments.
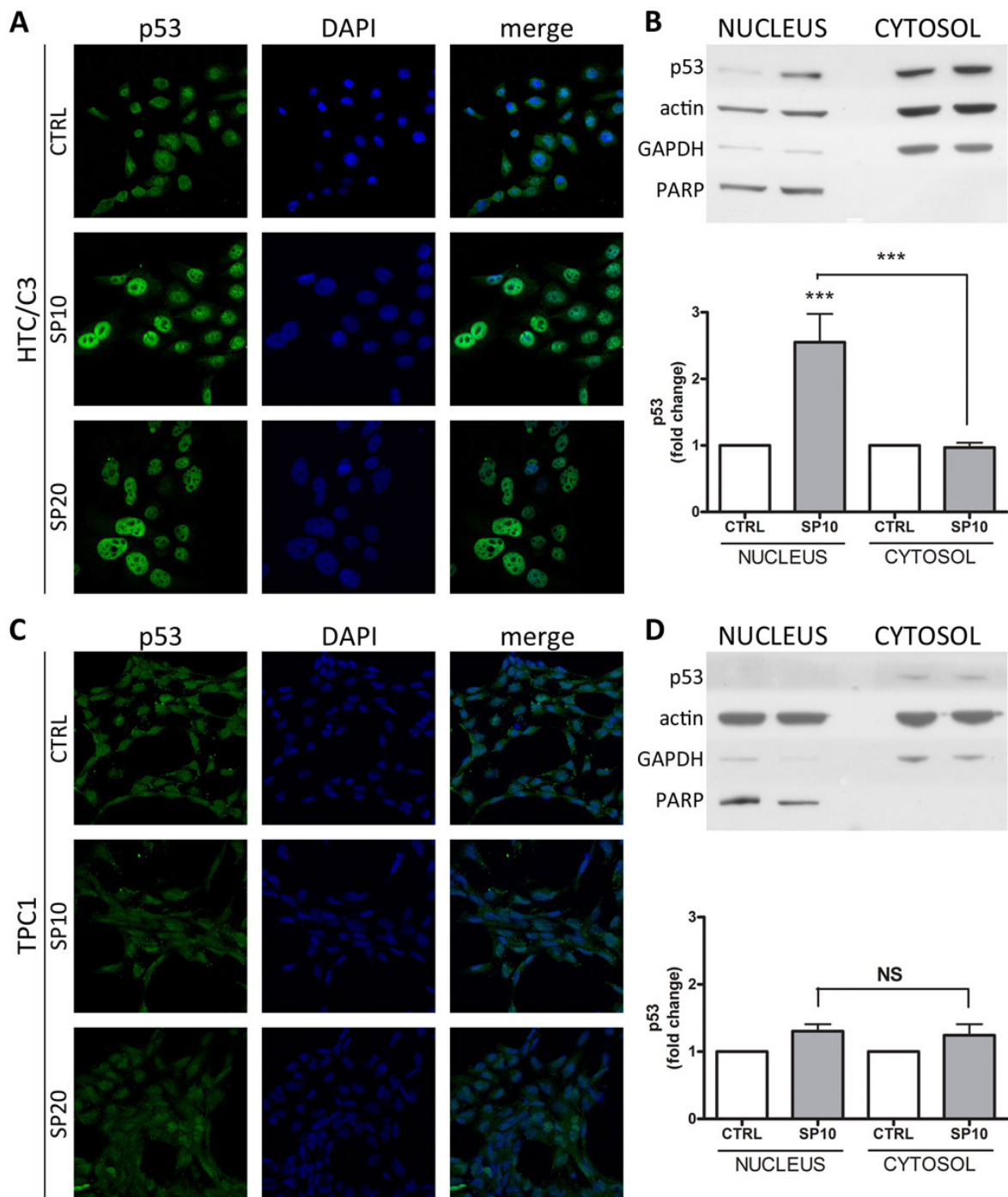
◄**Fig 2. Effects on p53 subcellular localization.** Cells were incubated with SP600125 or DMSO for 72h and then immunofluorescence (A,C) or cellular fractioning and western blotting (B,D) were performed. PARP and GAPDH were used as nuclear and cytosolic markers, respectively. **A, B**: SP600125 treatment induced p53 nuclear translocation in HTC/C3 cells; **C,D**: SP600125 had no effects on the wild type p53 in TPC1 cells.

Interestingly SP600125 caused a significant variation of p53 localization in HTC/C3 cells: after 72h of exposure an intense nuclear staining was detected in HTC/C3 cell line (Fig 2 A) and this data was confirmed by cellular fractioning showing a marked increase in the nuclear fraction of p53 (Fig 2 A). Conversely no variations were detected in p53 WT TPC1 cells (Fig 2 C,D) and no signal was detected in p53 pseudo-null SW1736 (data not shown).

Moreover, as p53 is transported to the nucleus through microtubules, a co-immunoprecipitation assay was performed. After tubulin precipitation the different fractions were hibridized with anti-p53 antibody. As it can be seen p53-tubulin binding reached a peak around 48 hours and as counterpart its levels diminished in the surnatant fraction while no changes were detected on total protein extracts (Fig 3). This data are in complete agreement with the ones previously shown as p53 binds and it's transported on tubulin in the first 48h of treatment while its levels decreases in both the immunoprecipitated and the surnatant because by that time the majority is localized in the nucleus.
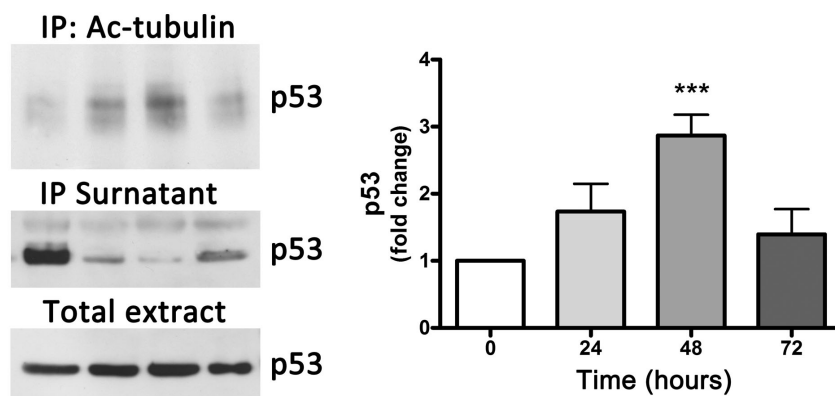
Fig 3. p53 bound tubulin at early time points. Cells were incubated with DMSO or SP600125 for the indicated times and then immunoprecipitation was performed. The total protein extract, the immunoprecipitated and the surnatant fraction were resolved on polyacrilammide gels and p53 hybridization was performed. Shown are representative images and quantification of p53-tubulin bound fraction.

2.2 SP600125 CAUSES P53 PHOSPHORYLATION AND P21 INDUCTION

As p53 nuclear translocation is one of the earliest step in the process of its activation, other modification involved in this process were investigated.

A

B
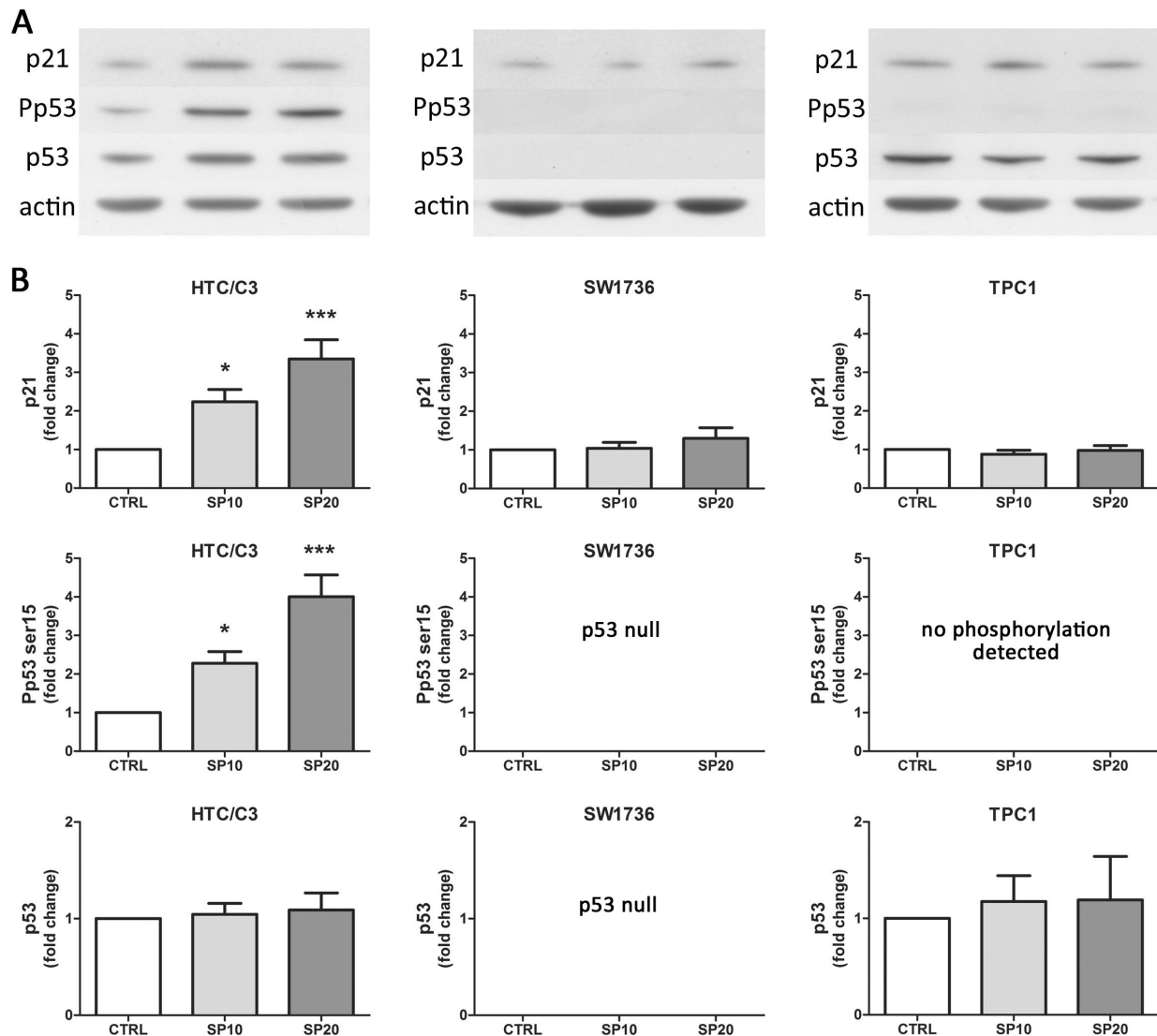
Fig 4. SP600125 effects on p53 pathway. Cells were incubated with SP600125 or DMSO for 72h and then protein were estracted. **A:** representative western blot images of mutated, null and WT p53 celll ines; **B**: relative western blot quantification.

It can be seen that an increase of p53 phosphorylation on serine 15 was detected in the p53 mutated cell line (Fig 4), a post-translational modification known to mask a nuclear export signal and therefore enhancing p53 retaining within the nucleus, increasing interactions with CPB/p300, inducing other post-translational modifications that stabilize the protein and increasing its half-life and transactivational power. No other p53 phosphorylated residues were

detected (data not shown).

Concomitant to this modification an increase in p21 levels, a well-known effect of p53 activation was detected (Fig 4).

Moreover, as p53 activation is involved in apoptosis, the activation of this pathway was investigated through evaluation of caspase 3 cleavage and activity but the results showed only slight variations after 48h of incubation (data not shown), thus indicating that the apoptotic process is not involved in SP600125 mechanism of action.

2.3 P53 IS PARTIALLY RESPONSIBLE OF SP600125 ANTIPROLIFERATIVE EFFECTS.

As long as it has been known that the three p53 mutations affecting our cell lines are supposed to impair p53 activity, further experiments were performed to elucidate if p53 phosphorylation and p21 induction were related and involved in SP600125 mechanism of action. The two main p53-activities, transactivation and apoptosis induction were investigated with the use of two different p53 inhibitors: ischemin and pithfirin-μ, the first being an inhibitor of p53 transactivational activity and the latter an inhibitor of p53 pro-apoptotic activity through mitochondrial pathway.
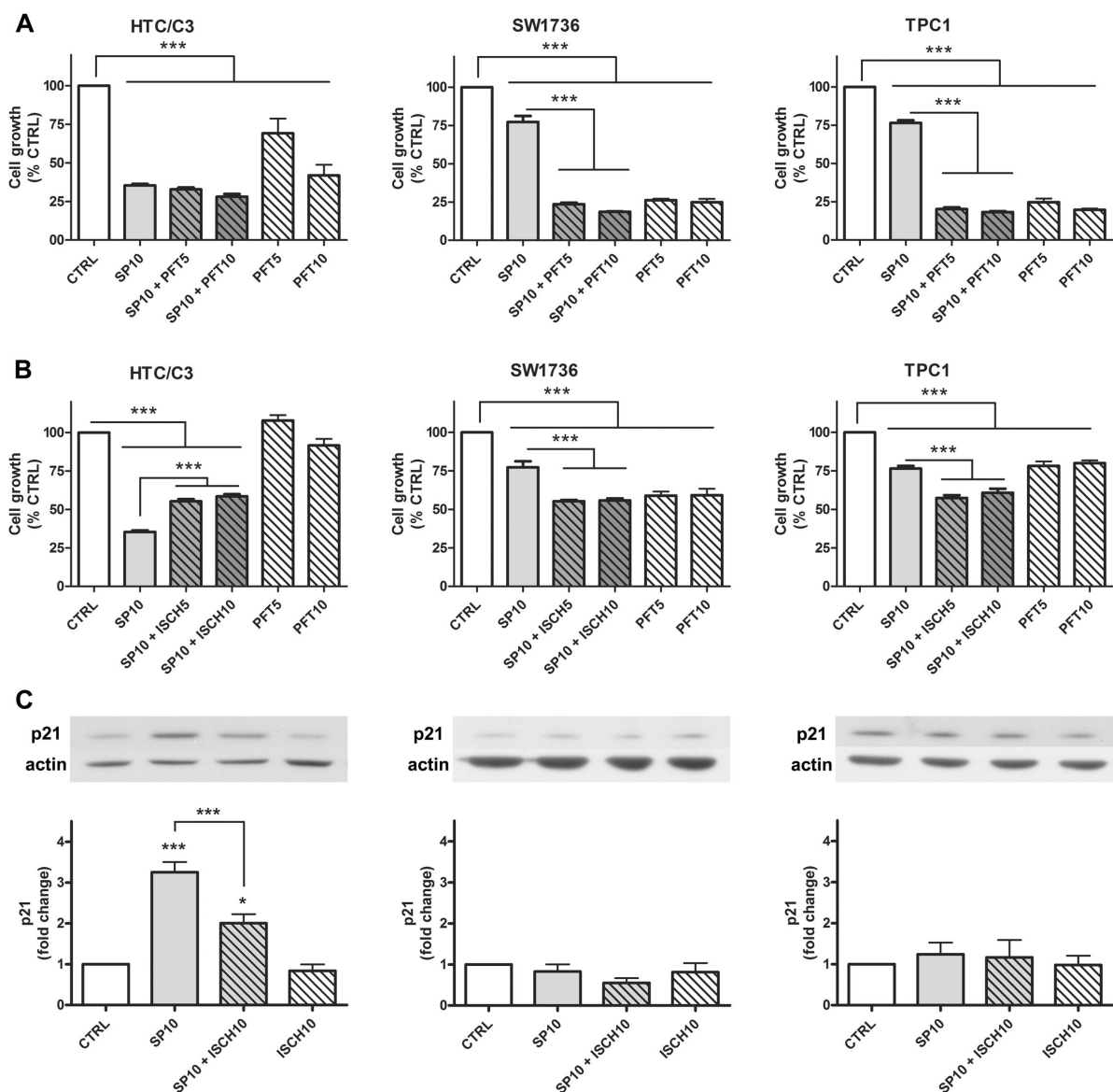
Fig 5. p53 transactivational activity inhibition partially revert SP600125 effects. Cells were incubated for 72h with DMSO, SP600125, pifithrin-μ and ischemin at the indicated concentration. **A**: pre-incubation with pifithrin-μ didn't affected SP600125 growth inhibition but show a slight synergysm; **B**: pre-incubation with ischemin partially reverted SP600125 growth inhibition in HTC/C3 cells; **C**: pre-incubation with ischemin partially reverted p21 induction in HTC/C3 cells but had no effects on SW1736 and TPC1. CTRL control, SP10 SP600125 10μM, PFT5 pifithrin-μ 5μM, PFT10 pifithrin-μ 10μM, ISCH5 ischemin 5μM, ISCH10 ischemin 10μM.

After pre-incubation with each of the p53 inhibitors, effects on cell proliferation and p21 levels were analyzed.First of all, as no results indication pro-apoptotic activity were detected, pre-incubation with pithfirin-µ had no effects but a slight synergism on SP600125 growth inhibition (Fig 5A). Differently, pre-incubation with ischemin was able to significantly, although partially, revert SP600125 antiproliferative effects in HTC/C3 cell line, while it had no effects on SW1736 and TPC1 cells (Fig 5B). Accordingly to these results, pre-incubation with ischemin induced a significant decrease in p21 induction only in HTC/C3 cells (Fig 5C), thus demonstrating a direct involvement of p53 and p21 in SP600125 antiproliferative effects.

3 EFFECTS ON CELL MORPHOLOGY

3.1 SP600125 INDUCES ALTERATIONS IN CELLULAR AND NUCLEAR MORPHOLOGY

Previous results indicated that SP600125 causes alterations in p53 and p21, a pathway that usually regulates cell replication and senescence. For this reason further analysis were performed in this direction.
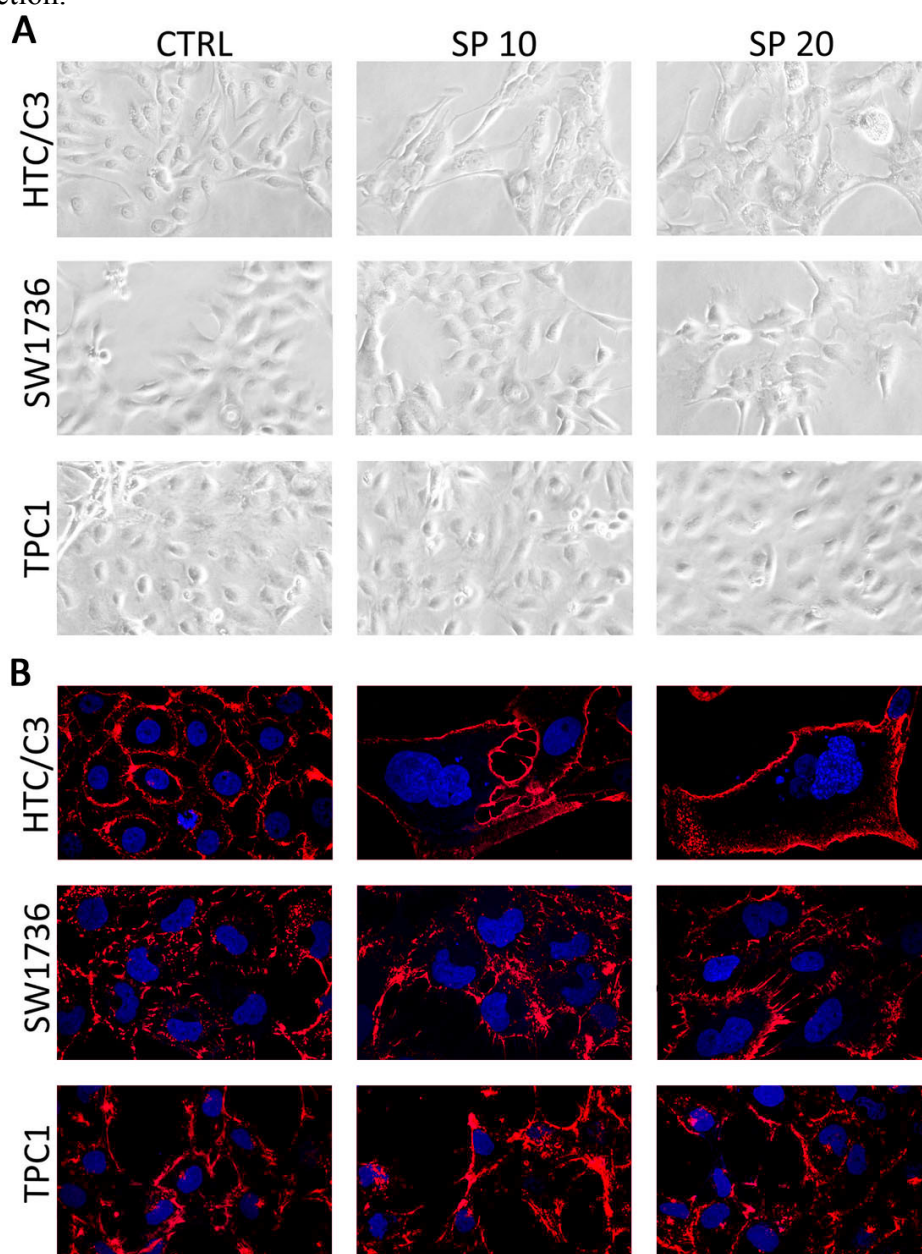
Fig 6. Effects on cellular morphology. Cells were incubated with SP600125 or DMSO for 72h and then images were acquired at light microscope or confocal after WGA and DAPI staining. **A**: SP600125 treatment induced variations in cellular morphology and content; **B**: SP600125 treatment induces nuclear and cellular dimension alterations.

First of all cell dimensions and morphology were characterized; the microscopical anlysis revealed that in affected cells there is a significant alteration in cellular morphology. At light microscope HTC/C3 cells appeared flattened, bigger, with increased amount of cytoplasmic vacuoles and more disomogeneous cytoplasmic content (Fig 6A). These alterations were accompanied by changes in nuclear morphology: in treated cells different abnormalities were present, including giant, polylobated or multiple nuclei as well as micronuclei and cytoplasmic budding of chromatin fragments, increased nucleoli size and number, chromatin alterations with presence of disomogenities and heterochromatin condensation foci (Fig 6B). Only slight variations were detected in SW1736 cells and no alterations were found in TPC1 cells.

Following confocal analysis, cellular and nuclear dimensions were quantified, proving a significative increase in HTC/C3 cells and, to a lesser extent, in SW1736 (Fig 7).
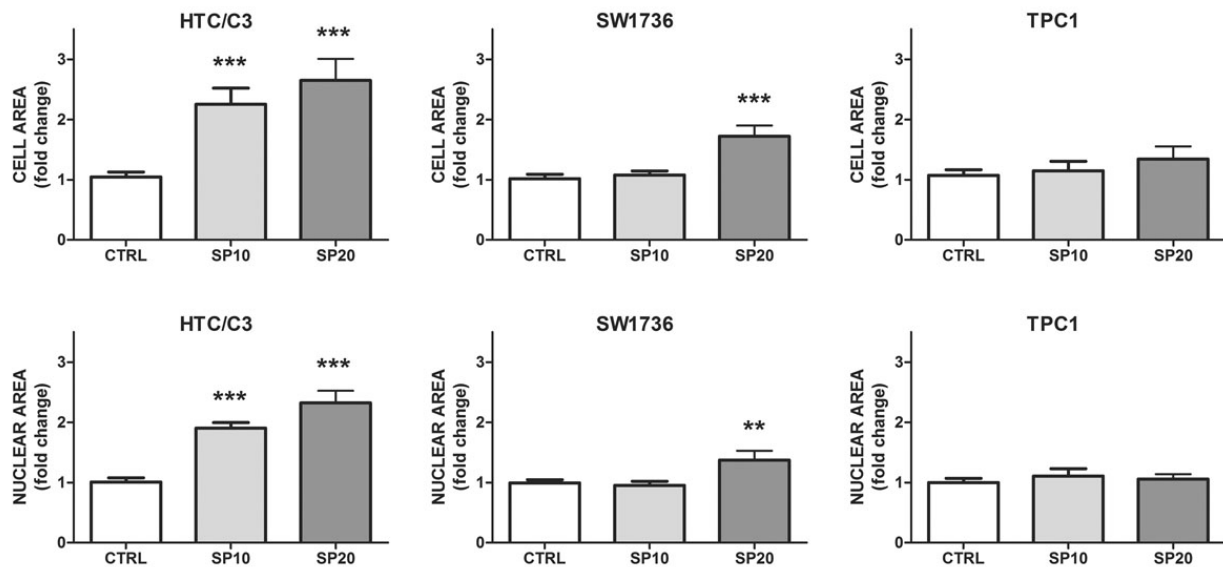
Fig 7. Effects on cellular and nuclear dimensions. Cells were incubated with SP600125 or DMSO for 72h and then immunofluorescence was performed. Tubulin and WGA staining were used for cellular area quantification while DAPI was used for nuclear staining and quantification.

3.2 SP600125 INDUCES ALTERATIONS IN LYSOSOME MORPHOLOGY AND LOCALIZATION

Confocal microscopy demonstrated an alteration in dimensions and subcellular localization of lysosomes. In HTC/C3 treated cells lysosomes appeared to be widespread in the cytosol, bigger and with more complex shape (Fig 8).
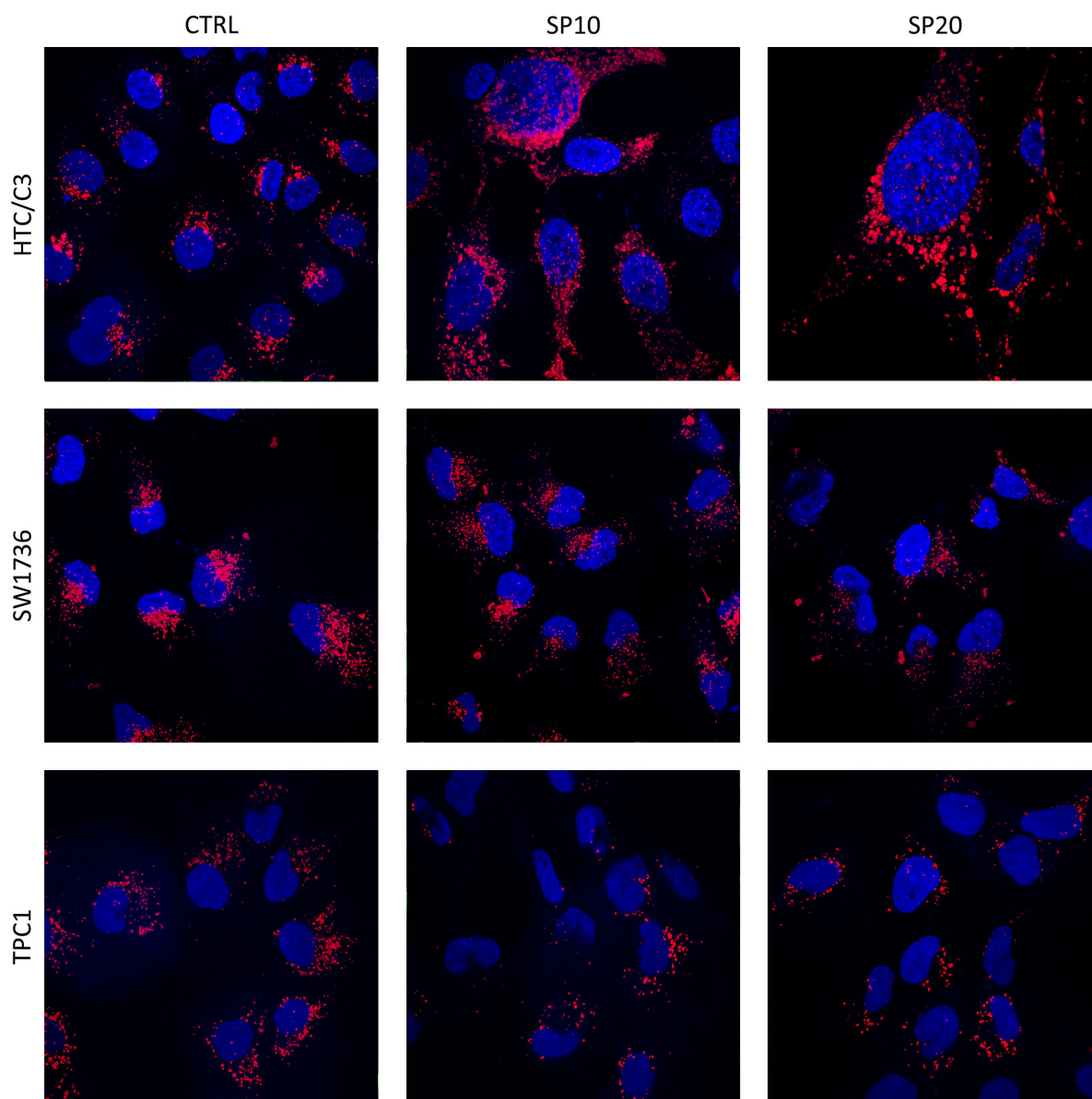
Fig 8. Variations in lysosome morphology. Cells were incubated with SP600125 or DMSO for 96h and then lysosomes and nucleus were stained.

All these morphological alterations of cells, nuclei and lysosomes are higly specific of cellular senescence and in agreement with p21 levels increase following SP600125 treatment.

4 EFFECTS ON MITOSIS PROGRESSION

4.1 SP600125 REDUCES THE MITOTIC INDEX OF P53 MUTATED CELLS

Given the previous results demonstrating an involvement of p21 and presence of nuclear

alterations, the effects on mitosis were investigated. First of all the percentage of mitotic cells

was quantified through staining with an antibody directed against Histone H3 phosphorylation at

serine 10. The results showed that in HTC/C3 cell lines there is a significant decrease in

phospho-histone H3 levels as well as in cells undergoing mitosis while in TPC1 only slight

variations were detected; SW1736 showed an intemerdiated effect. Another difference existed

between HTC/C3 and SW1736 cells: when looking at mitotic and pre-mitotic fractions it can be

noticed that in HTC/C3 the bigger reduction is in the mitotic one while in SW1736 the ratio is

conserved (Fig 9).
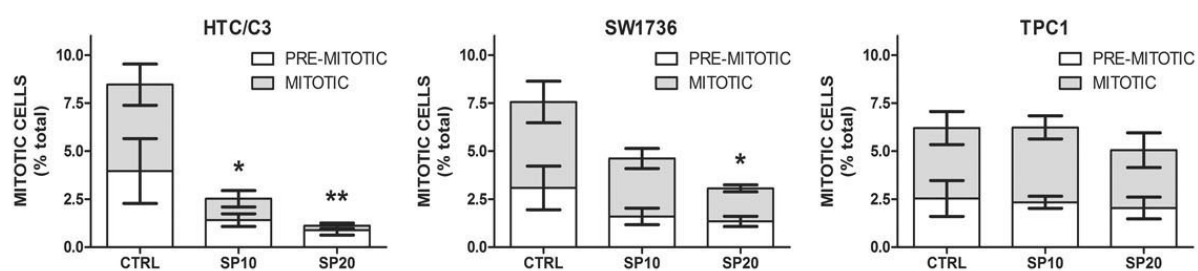
Fig 9. Mitotic index. Cells were exposed to SP600125 or DMSO for 96h and then cells stained with Phospho Histone H3 and tubulin. Mitotic Index was quantified as percentage of pre-mitotic or mitotic cells on total cells number per optic fields at 20x objective.

4.2 SP600125 INDUCES ABERRANT MITOSIS IN P53 MUTATED CELLS

As second step mitosis morphology was investigated by confocal microscopy.

The results showed that in HTC/C3 there was an increase in the percentage of abnormal mitotic figures with an increase in chromosome number, multiple spindle formation, impairment of chromosome alignment and segregation (Fig 10B).

Systematic analysis of mitosis revealed a significant increase in the number of abnormal and multipolar figures in HTC/C3 cells while only slight alterations were found in SW1736 and no alterations were found in TPC1 (Fig 10A).
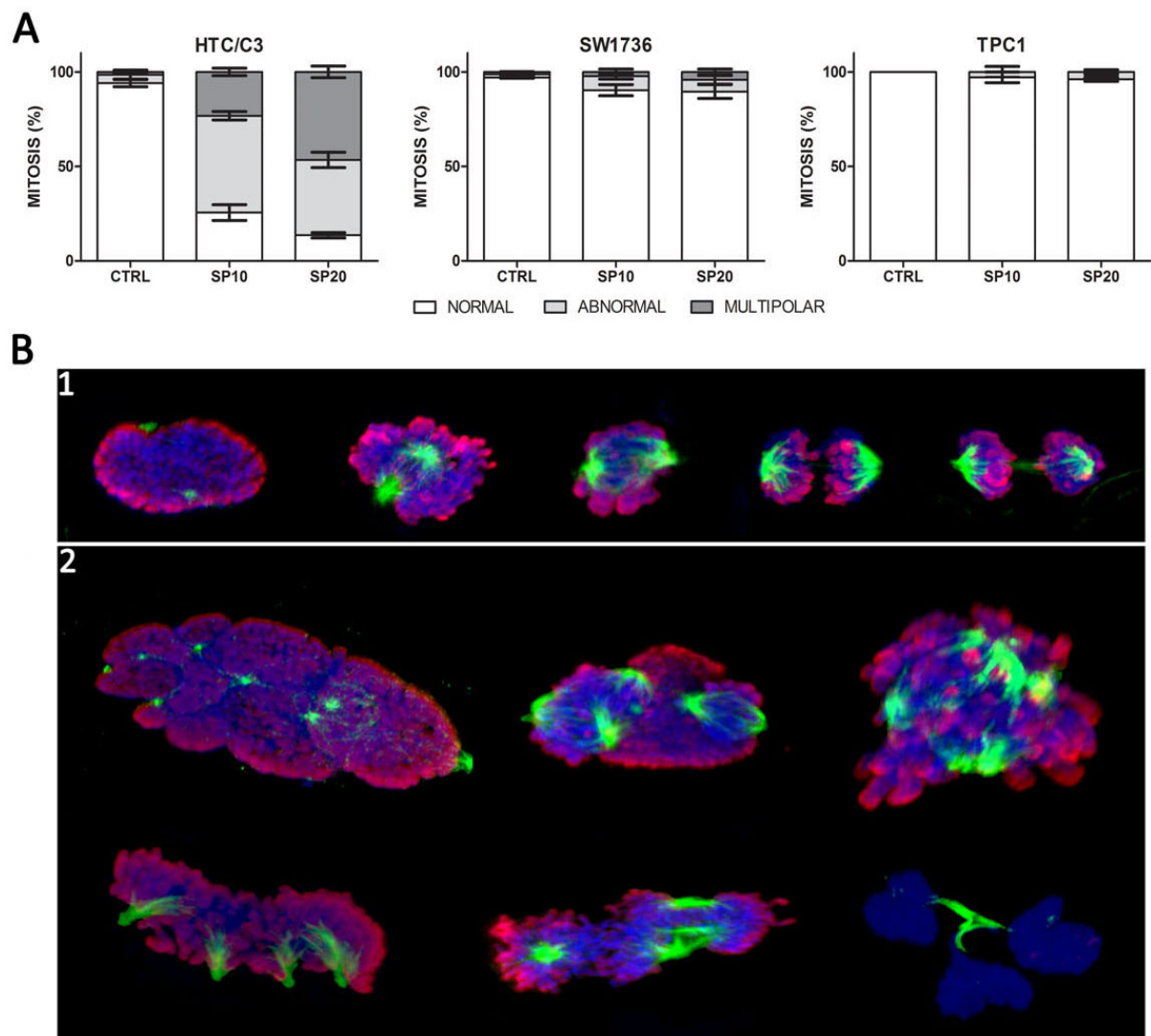
Fig 10. Mitosis morphology. Cells were exposed to SP600125 or DMSO for 96h and then cells stained with Phospho Histone H3 (Red), DAPI (Blue) and tubulin (Green). All images were acquired with 60x immersion objective with ulterior 2.5 zoom.

These mitotic abnormalities are the possible cause of the nuclear alterations previously described as multipolar mitosis are known to generate poliploid cells with giant lobated nuclei or to generate micronuclei as result of unbalanced chromosome segregation.

5 EFFECTS ON MICROTUBULES

5.1 SP600125 INDUCES MICROTUBULES ALTERATIONS

Although very interesting, p21 involvement was only partially responsible of SP600125 effects and other mechanisms are required. As long as one of the main actor in mitosis progression is the mitotic spindle, requiring intact microtubules dynamics and p53 mutations are known to confer high susceptibility to microtubule poisons, further experiments were performed in this direction. First of all it was investigated if SP600125 was able to induce alterations in tubulin polymerization.
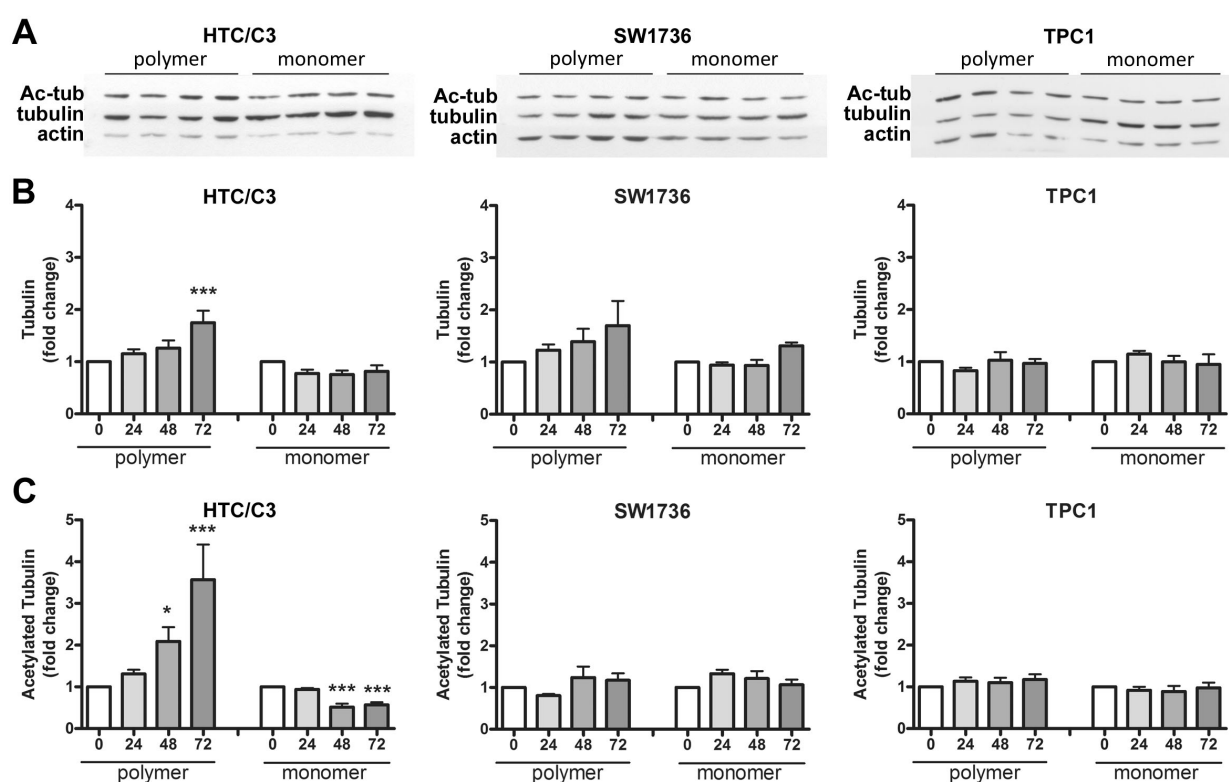
Fig 11. Effects on microtubules. Cells were incubated with SP600125 10μM for the indicated period of time and a tubulin fractioning assay was performed. A: representative images of tubulin polymerization and acetylation variations; B: variations in tubulin polymeric and monomeric fractions inrealtion to total tubulinamount; C: variations in different tubulin fractions acetylation.

A tubulin fractionation assay was performed and results analyzed by western blotting; it can be noticed that SP600125 induced a significant increase in the fraction of polimerized tubulin compared to the monomer form in cell lines with p53 impairment, with higher effects after 72h (Fig 11B). Moreover in p53 mutated cells this alteration was accompanied by a strong increment

in the acetylation of the polymer form, a marker of microtubule stability (Fig 11C).
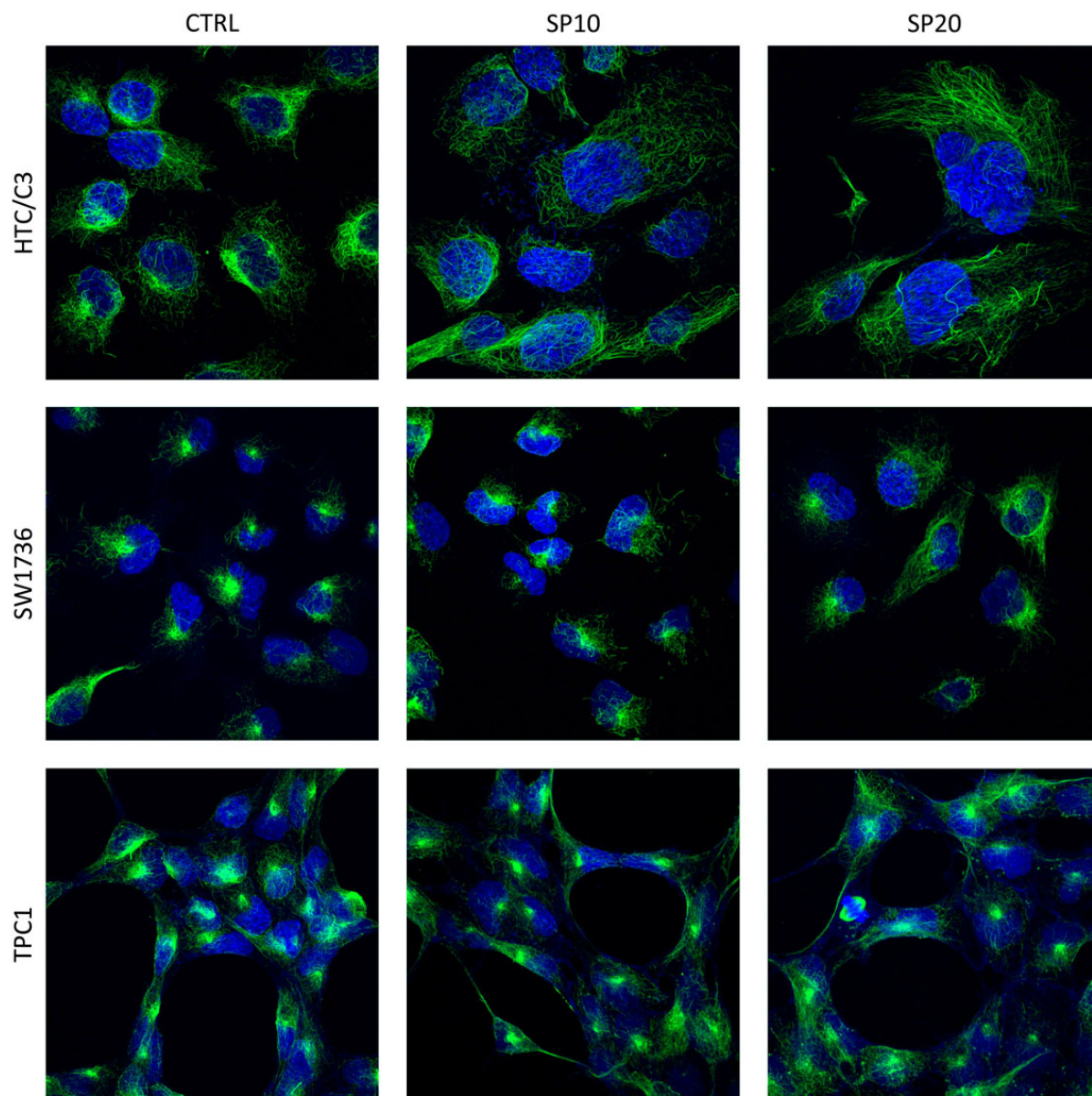
Fig 12. Effects on acetylated tubulin morphology. Cells were incubated for 96h with DMSO or SP600125 for the indicated concentrations and then immunofluorescence performed. SP10 SP600125 10μM, SP20 SP600125 20μM.

Furthermore confocal microscopy analysis of tubulin acetylation showed not only a general increase but a complete upheaval of microtubule architecture in HTC/C3 cells: while in untreated cells it was clearly recognizable the typical polarization of acetylated fibers emerging from the MTOC, in treated cells they appeared thicker, widespread through the cytosol without an organizing center and completely unrelated to the nucleus; only slight effects could be noticed in p53 null SW1736 cells while no effects were detected on wild-type TPC1 (Fig 12).

6 EFFECTS ON CELL MOTILITY

6.1 SP600125 AFFECTS CELL MIGRATION

As long as intact microtubular dynamic is required for cell migration, a wound healing assay was performed to highlight if this skill was compromised. As it can be seen 16h post wound TPC1 completely recovered while in HTC/C3 no progression was detected, demostrating a severe impairment of cell mobility; SW1736 showed an intermediated phenotype (Fig 13).
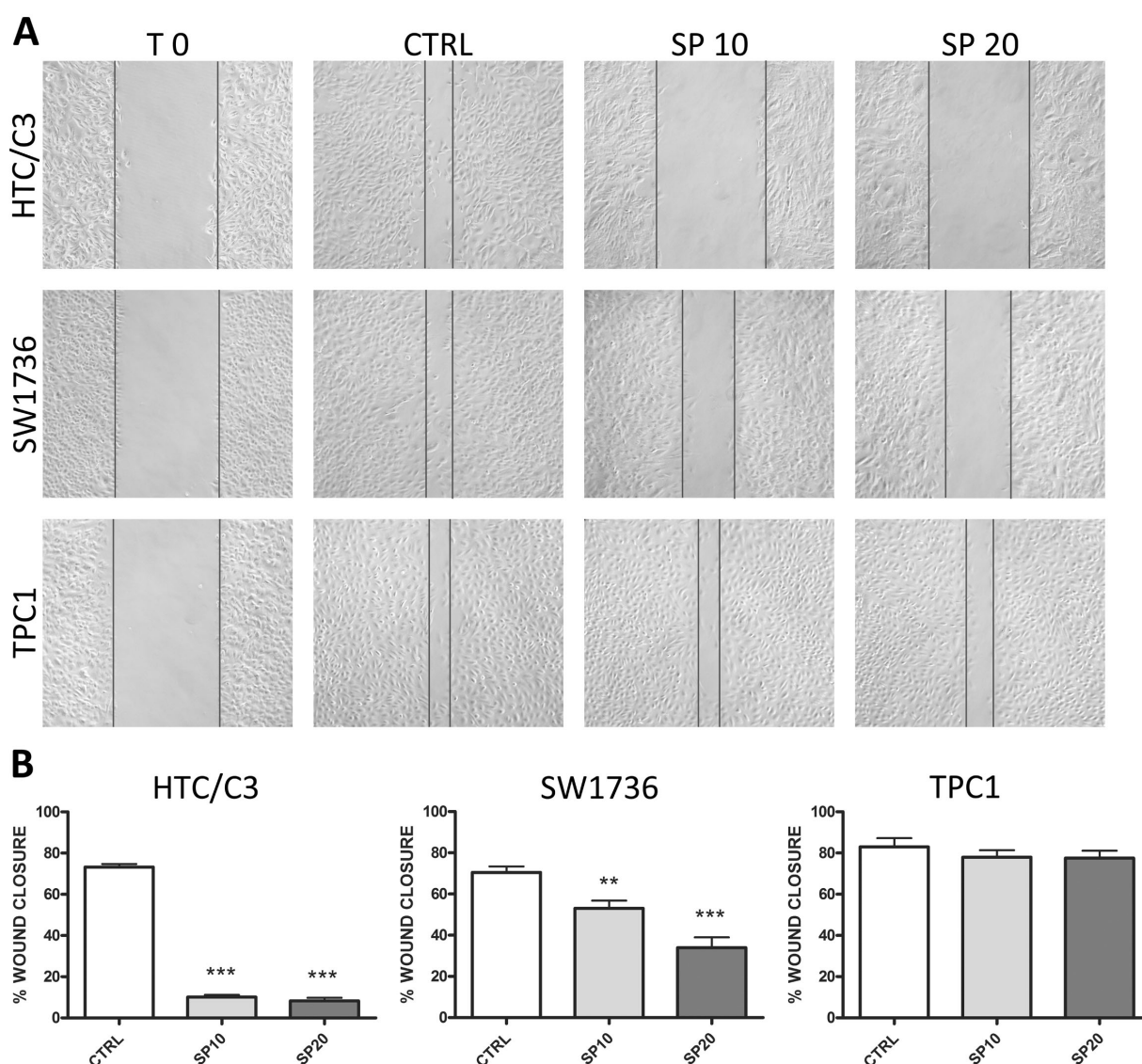
Fig 13. Effects on cell motility. Cells were incubated for 72h with DMSO or SP600125 at the indicated concentrations, scraped with a p200 tip and images acquired at 0 and 16h. **A**: representative images acquired at 0h (To) and 16h (CTRL, SP10 and SP20); **B** quantitative analysis of wound repair. SP10 SP600125 10μM, SP20 SP600125 20μM.

RESULTS

6.2 SP600125 CAUSES ALTERATION IN PROTEINS INVOLVED IN CELL MIGRATION

To further characterize the effects of SP600125, different proteins were analyzed in HTC/C3 cells using Human Phospho-Kinase Antibody Array by R&D System.

The results showed that there were different levels of involvement in SP600125 action.

First of all three different group could be noticed: the first one (Fig 14A) included proteins undergoing only slight variations, the second one (Fig 14B) included proteins with mean increase after SP600125 exposure and the third one (Fig 14C) included proteins with more than a two-fold increase after SP600125 exposure. Of noticeable interest, the proteins detected in the third group are, from the lower to the highest one, FAK, GSK3β, STAT5b, Lck, Fgr, and β-catenin; all of them are involved in cellular adhesion and migration.
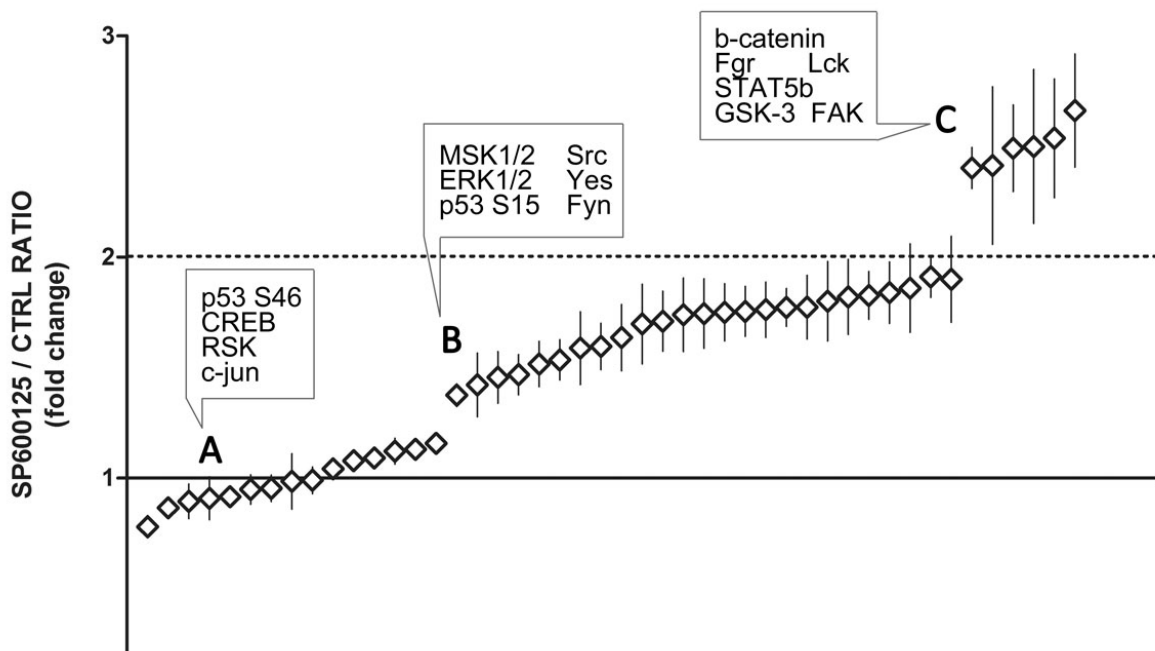
Fig 14. Plotting of SP600125/CTRL phosphorilation ratio. Cells were incubated with 10μM SP600125 or DMSO for 60h and then the assay was performed. A, B, C represents different subgroups corresponding to different fold changes in kinases phosphorylation; most interesting proteins are reported above each group.

Being β-catenin the most affected, further experiments were performed.

Morphological analysis of migrating HTC/C3 cells demonstrated striking β-catenin localization differences following SP600125 treatment. In control cells β-catenin staining clearly marked the leading edge of migrating cells highlighting typical structures such as lamellipodia and filopodia

86

while in treated cells not only β-catenin was missing from cell front but instead it strongly stained intercellular junctions, indicating absence of single cell migration and permanence of adhesion (Fig 15).
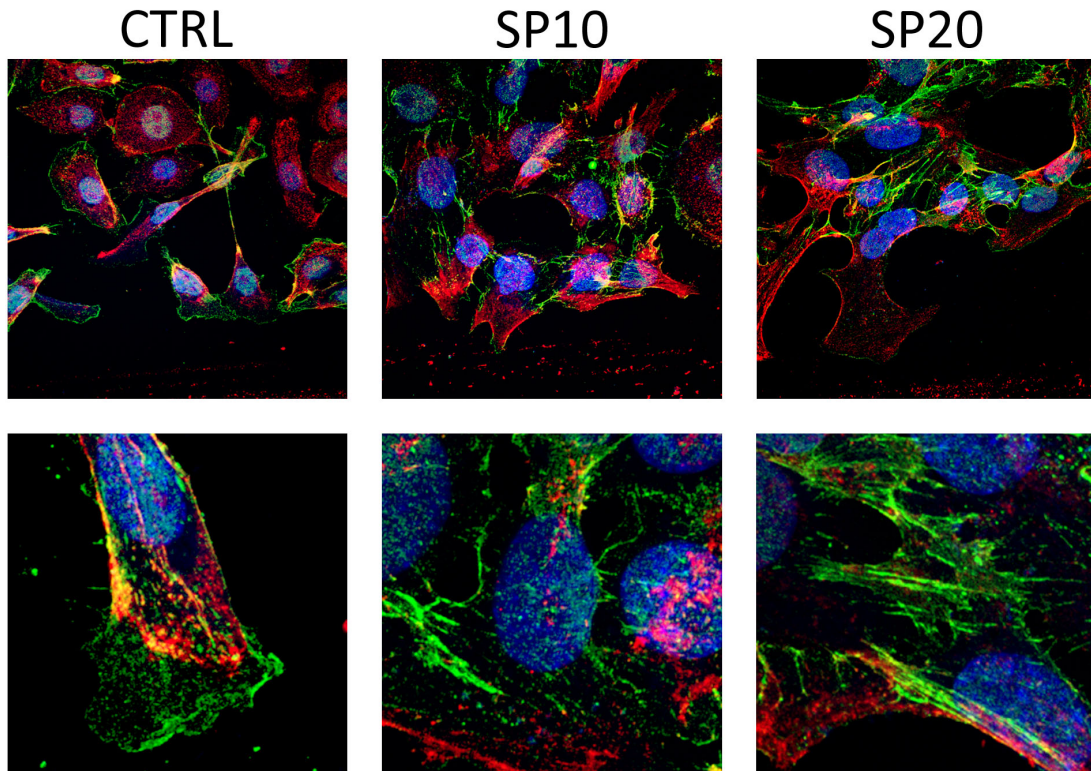
Fig 15. β-catenin localization in migrating cells. Cells were exposed to SP600125 or DMSO for 72h, scraped with a p200 tip and after 16h stained with WGA and then immunofluorescence was performed. Images show different cellular morphology at the wound edge, with 4x magnification in the lower raw.

6.3 SP600125 AFFECTS HDACs ACTIVITY

HDAC6 is an histone deacetylase responsible of the regulation of tubulin acetylation and b-catenin degradation; for this reason its activity was investigated to elucidate wether this enzyme was involved in SP600125 mechanism of action. Unluckily there was no availability of direct assays for HDAC6 activity in cellular extracts. Therefore a general HDACs activity assay was performed on concentrated cytoplasmic extracts, as HDAC6 and HDAC10 accounts for the major part of cytoplasmic HDACs activity.
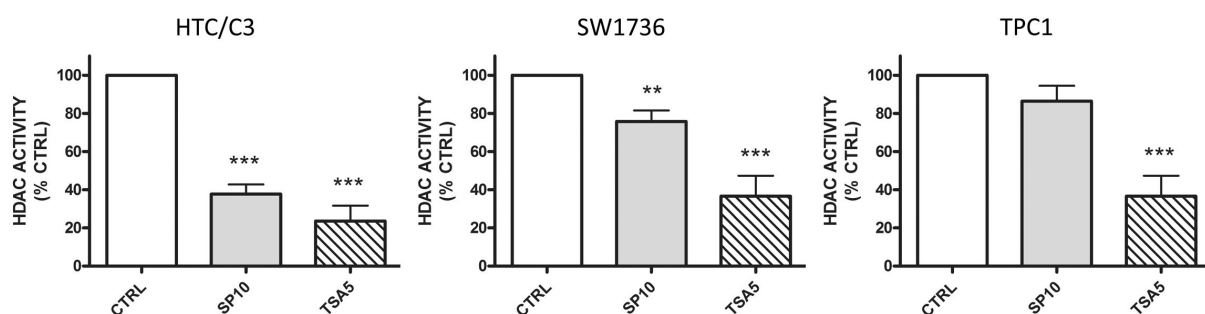
Fig 16. Effects on cytoplasmatic HDACs activity. Cells were incubated for 72h with DMSO, SP600125 10µM or TSA 5µM and a colorimetric assay was performed on cytoplasmic extracts. SP10 SP600125 10µM, TSA5 Trichostatin A 5µM.

The results showed that after SP600125 exposure there was a significant decrease in HDACs activity in HTC/C3 cells and, with lower intensity, in SW1736. Only a slight decrease was detected in TPC1 cells (Fig 16). All the cells promptly responded to exposure to Trichostatin A, a well known HDACs inhibitor.

88

DISCUSSION

SP500125 is a multi-kinase inhibitor that has recently been shown to be a promising, selective anticancer drug [57, 204-205]. In the last five years it has been proved able to induce endoreduplization and subsequent polyploidization in treated cells but there are contrasting results about its intracellular actions and there is no certainty on the specific mechanism of action. Depending on cell type, concentration and time of incubation opposite results have been obtained [52, 56, 206-208].

Most of the studies postulated that SP600125 effects are a direct results of JNKs inhibition, anyway no specific connection was ascertained [52, 205-206]. Besides the effects on JNKs, the only known direct interaction that has been charachterized is with MPS1, a fundamental protein in mitotic spindle assembly checkpoint [55]; anyway even in this case there are contrasting results as SP600125 has been proved to have no effects on MPS1 in immortalized human BJ-Tert fibroblasts [54].

In 2012, in a small molecule screening, SP600125 resulted the more effective in inhibiting p53 deficient cancer cells growth [57]; even in this case there are previously contrasting results showing no differences between p53 wild type and null cells [207, 209-210]. On this subject it has to be highlighted that all studies were conducted comparing the same cell line in different conditions, by silencing wt p53 or by transfecting it into null cells thus creating artificial imbalances in cell growth.

With this premises the aim of the current study was to characterize SP600125 mechanism of action. For this purpose six thyroid cancer derived cell lines with different p53 status were used. Of noticeable interest for the first time SP600125 effects were investigated on three different p53 status spontaneously occourred, revealing new and promising effects like the ability to partially restore p53 function. In addition SP600125 action was investigated with a wider perspective revealing at the same time the less known effects on microtubule and cell migration as well as the interconnections between these pathways.

First of all, we analyzed the effects on p53 protein. The results demonstrated that SP600125 is able to induce p53 nuclear translocation and subsequent phosphorylation at serine 15 in p53 mutated cells (Fig 2,4); no previous data exist about this modification while there is consensus about the lack of action on p53 transcriptional activity in p53 wt cells [207, 210]. Moreover this p53 phosphorylation is at least partially responsible of p21 induction (Fig 5). The effects of SP600125 on p21 levels have been well described, anyway there are discordant hypothesis about

the underlying mechanism depending on cell type and treatment concentration [208, 210]. The group of Moon recently proposed that high doses of SP600125 are able to induce p21 through Akt and ERKs; in this work the two pathways were partially responsible of p21 alterations and no intermediate effector between SP600125 and Akt or ERK was found [52]. Being SP600125 a multi-kinase inhibitor it can be hypothesized a simultaneous action on different pathways resulting in p21 induction.

As no alterations of p53 phosphorylation were previously reported, different assumptions can be made to explain this effect.

The first hypothesis involve a direct interaction between SP600125 and p53. An increasing amount of small molecules that are able to restore transcriptional activity of mutated p53 has been described, including PRIMA-1, MIRA-1, NSC319726, WR1065 [211-214]. Treatment with these compounds often result in p53 phosphorylation at serine 15 and p21 induction, a similar effect to SP600125 one [212, 215]. It must be remembered that cancer cells harbouring p53 mutations usually have oncogenic lesions or damage signals capable of potently activating p53 and thus its restoration causes much more dramatic effects than simple p53 activation in normal wt cells; this fact can explain why of the three p53 status examined, mutated cells resulted the most affected by SP600125 treatment [216-218]. Moreover cell lines used in the current study harbour different p53 mutations that affect the β-sandwich structure of the protein and β-sandwich mutants are the most promising target for rescue by small compounds, as stabilizing the affected protein in the wt conformation is often sufficient to restore its activity [219-221].

The second hypothesis involves microtubule alterations as a possible cause of p53 activation. Up to date there are no significant studies on SP600125 effect on microtubules with the exception of a study reporting that high doses (200μM) of SP600125 are able to induce spontaneous tubulin polymerization in an in vitro assay [208]. Accordingly to these results, our study shown an increase of microtubule stability starting after 24h of incubation while most dramatic changes are detected after 72-96h (Fig 11, 12). In accordance with this data coimmunoprecipitation assay shown that p53-tubulin binding reach a peak between 24 and 48 hours of incubation (Fig 3), exactly when microtubule dynamics are already affected but tubulin still maintain the nuclear-periphery polarization. In literature there is abundant evidence that alterations of microtubules dynamics lead to p53 pathway activation but various mechanism have been postulated. The historical theory is that alterations of microtubule dynamics brings to aberration in spindle pole

formation and in chromosome disjunction, with consequent formation of poliploid cells and micronuclei, both of them being able of activate p53 [87, 222-224]. This process anyway is not able to explain the activation of mutated p53 and should be considered not as the principal cause but as the final effect of SP600125 induced alterations, as p53 inactivation is known to confer hypersensibility to microtubule interacting drugs. Recent studies suggest that suppression of microtubule dynamics in interphase cells leads to a more stable tubulin network, allowing efficient molecular transport and thus enhancing p53 nuclear translocation [225-226]. It was also demonstrated that microtubule alterations and DNA damage induce p53 phosphorylation at different residues, being serine 15 and threonine 18 the most frequent in the first case and serine 20 and serine 46 in the second one [226-228].

The third hypothesis involves the previous ones as well as cell migration: it has been demonstrated that alterations of microtubule dynamics in interphase cells induces an increase in number and size of focal adhesions; this process is accompanied by activation of FAK and MAPKs that in the end trigger p53 activation [229-231]. In this case we have to remember that SP600125 inhibited cell motility through the involvement of microtubule, β-catenin, GSK3 and FAK pathways (Fig 13,14,15) and that previous activation of ERK pathways was hypothesized as SP600125 mechanism of action on p53 [52].

Given the importance of SP600125 effects on microtubules and cell adhesion we will proceed to examine these results in detail.

The results shown that SP600125 is able to alter microtubule dynamics as shown by increase in acetylation levels and changes in morphology. In treated cells there was first an increase in the intensity of acetylated tubulin signal and after 48h a complete subversion of microtubule architecture (Fig 11,12). As it can be seen from the scheme microtubule are usually directed from a perinuclear MTOC constituted by centrioles toward the cell

Schematic rapresentation of microtubule alterations in control (up) and treated (down) cells. Microtubules are represented in green, nuclei in blue.
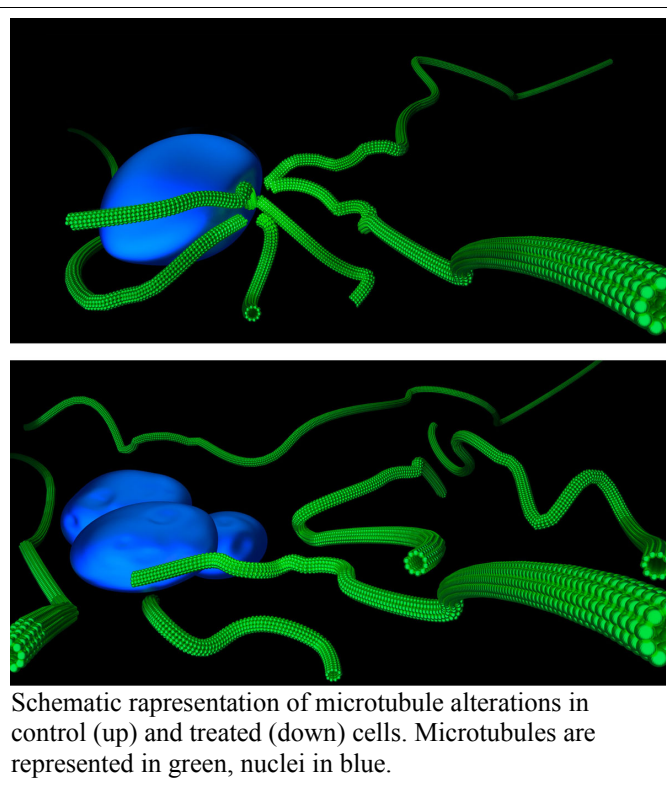
periphery while in treated cell they appear to be widespread through the cytoplasm without any apparent polarization. Moreover treated cells microtubules have the typical features of microtubule bundles, structures formed by more microtubule packed together by specific proteins like CLASP and cis1p [232-233]. The formation of disorganized bundles is a well known effect of microtubule stabilizing agents like taxanes and epothilones and depends upon direct drug-tubulin interactions [234-237].

Although microtubule alterations are considered indipendent from p53 or at least acting upstream, the dramatic morphological changes in tubulin architecture were found only in the p53 mutated cell lines, with very slight effect on the p53 null one; this is probably due to p53 reactivation that seems to play a fundamental role in SP600125 actions on microtubule.

Even if it is not possible to determine which one of these two events trigger the other one and abundant contrasting literature exist on this point, it is a fact that both of them equally contribute in generating abnormal mitosis and subsequent cell death by mitotic catastrophe (Fig 9, 10). On one side p21 induction has been demonstrated responsible of SP600125 induced endoreduplication [56, 208, 210] creating polyploid cells, on the other side microtubule dynamics alterations, together with the already described MPS1 inhibition, are responsible of chromosomal segregation alterations, multipolar mitosis formation and impaired cytodieresis [54, 166, 223]. Following microtubule poison treatments most of cells undergo one or two round of abortive mitosis, become unable to progress further and finally die. The polyploid ones that manage to survive have been reported to became prematurely senescent [238-240].

In agreement with what has been reported, after incubation with SP600125 the characteristic morphology of senescent cells could be detected: cells appear flattened, bigger, with increased amount of vacuoles and more disomogeneous cytoplasmic content; nuclei were giant, polylobated or multiple and micronuclei, cytoplasmic budding of chromatin fragments, increased nucleoli size and number, chromatin alterations with presence of disomogenities and heterochromatin condensation foci were detected (Fig 6, 7).

Schematic rapresentation of major SP600125 induced alterations in p53 mutated cells through time (hours).

If we analyze all the effect described in a time
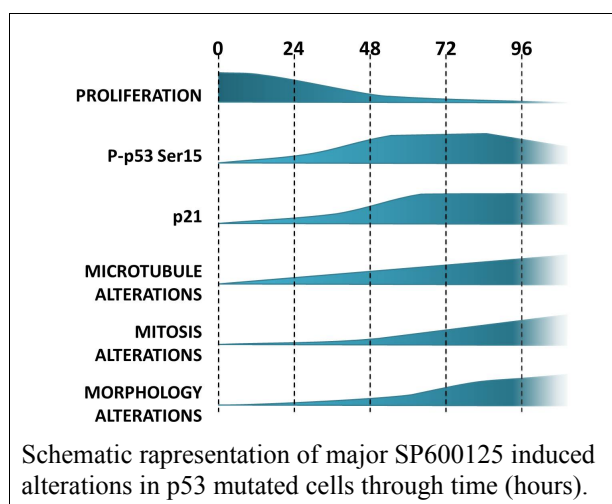
dependent manner is clearly visible that when p53, p21 and tubulin acetylation levels increase there is a sudden decrease in cell proliferation; moreover mitosis and morphology alterations appear with a slight delay, being a consequence of the other variations.

Anyway is still impossible to detect a possible link between p53 and tubulin alterations.

Apart of all these result a complete new effect of SP600125 have been demonstrated that is inhibition of cell migration by microtubule, β-catenin and HDAC6 modulation.

First of all inhibition of microtubule dynamics is known to affect cell migration as different microtubule poisons abrogate cell motility when used at low non-cytotoxic concentrations [241-243]. Various mechanisms have been proposed, including the impairment of the MTOC reorientation toward the leading edge, the inhibition of Rho GTPases and effectors by altering microtubule polymerization-depolymerization cycle, the inhibition of intracellular protein and vescicles trafficking and consequent lamellipodia formation, the alteration of microtubule integrin clustering together with HSP90 degradation [244-247].

Of all this alterations, results shown that in SP600125 affected cells there is a total absence of MTOC organization and a significant alteration of late endosomes/lysosomes morphology and localization (Fig 8). Consequent morphologycal analysis of wound edge cells revealed that, while control cells migrate toward the free space with the classical morphology, treated cells

extend stuctures similar to lamellipodia toward the wound but remain stuck to each other (Fig 15). The inability of detaching from other cells is confirmed by the intense β-catenin staining at intracellular adherens junctions. Moreover a protein phosphorylation array analysis revealed the involvement of different kinases that are fundamental in cell adhesion and migration like FAK, GSK3, Lck and to a lesser extent Src, Fyn And Yes (Fig 14).

Schematic rapesentation of control (left) ant treated (right) cells at the end of a wound. Arrow indicates migration direction, green represents β-catenin, red cell membrane and adhesions, blue nuclei.
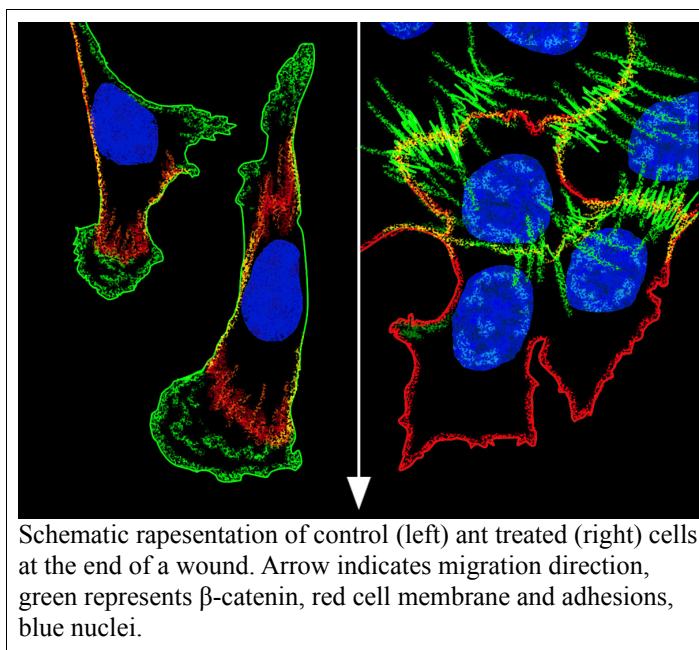
Very interestingly both tubulin and β-catenin are regulated through acetylation levels by HDAC6 and the activity of this enzyme appears to be reduced in a way that is direct proportional

to cell proliferation inhibition.

On the relation between HDAC6 activity and p53 reciprocal influence there is plenty of literature but contrasting hypotesis are reported. Of given importance HDACs inhibitor are a new promising anticancer drugs that are currently undergoing many clinical trials and one of them is already approved for T-cell lymphoma [248-249]. Indeed recent studies provided evidence that HDAC6 inhibitor act preferentially on p53 mutated cell lines because they are able to destabilize the mutated protein by alteration of its interaction with HSP90 and, at the same time, they are able to stabilize wt p53 through increased acetylation [250]. Effects on HDACs provide another interesting interconnection between p53, microtubule and β-catenin alterations that can be found in SP600125 affected cells.

Moreover a direct action of SP600125 in HDAC6 and migration regulation can be hypothesized. In a wide range kinase inhibitor specificity screening study, SP600125 was identified as being able to inhibit ROCK2 activity [48]. This kinase is involved in regulation of RhoA as well as actin and intermediate filaments dynamics and recent studies unveiled a specific pathway linking it to microtubule and β-catenin [157, 251]. ROCK2 is able to phosphorylate TPPP1 inducing its detachment from HDAC6; free cytoplasmic HDAC6 is fully functional and acts on microtubules and β-catenin. In our working hypothesis SP600125 inhibits ROCK kinase activity thus preventing TPPP1 release of HDAC6 and explaining why a decrease in the deacetylase activity was detected without any changes in total protein amount. Inhibition of HDAC6 causes subsequent hyperacetylation of tubulin, leading to alterations in microtubule dynamics, and of β-catenin, leading to ubiquitination sites masking and preventing its proteasomal degradation; moreover β-catenin acetylation inhibits its cleavage locking it to cell membrane and inhibiting its nuclear translocation thus inhibiting another proliferation pathway often hyperactivated in human cancers [251-252].

In conclusion the current study confirmed previously reported data about SP600125 induction of endoreduplication and unveiled completely new features that can be explained by its multikinase inhibition activity. First of all SP600125 action is directed preferentially against p53 mutated cell lines without any relevant effect on p53 wild type cells; as second thing it seems able to restore p53 activity in mutated cell lines; third it affects HDAC6 activity providing new powerful anticancer effects: it alters microtubule dynamics and β-catenin localization thus impairing cell migration.

Schematic representation of different pathways involved in SP600125 action. Previous studies demonstrated the effects on MPS1, ERK and p21 inducing endoreduplication while the current study demonstrated involvement of p53 and MSK1/2 phosphoylation, HDAC inhibition, microtubule and β-catenin involvement in mitosis progression, senescence induction and motility inhibition. Continuous lines represent demonstrated interactions while interrupted lines represent hypotesized ones.

From these results SP600125 is proved to be active both on cell replication and cell diffusion, owing the potential to be a promising therapy for p53 mutated cancers as limiting drug for cells growth and metastases spreading.

BIBLIOGRAPHY

bibliography

1.   Jemal, A., et al., *Global cancer statistics.* CA Cancer J Clin, 2011. **61**(2): p. 69-90.

2.   Wartofsky, L., *Increasing world incidence of thyroid cancer: increased detection or higher radiation exposure?* Hormones (Athens), 2010. **9**(2): p. 103-8.

3.   Howlader N, N.A., Krapcho M, Garshell J, Neyman N, Altekruse SF, Kosary CL, Yu M, Ruhl J, Tatalovich Z, Cho H, Mariotto A, Lewis DR, Chen HS, Feuer EJ, Cronin KA, *Statistics Review, 1975-2010, National Cancer Institute. Bethesda, MD, http://seer.cancer.gov/csr/1975_2010/, based on November 2012 SEER data submission, posted to the SEER web site, 2013.* . 2012. **.**(.): p. .

4.   Siegel, R., et al., *Cancer Statistics, 2014.* CA Cancer J Clin, 2014.

5.   Ferlay, J., et al., *Cancer incidence and mortality patterns in Europe: estimates for 40 countries in 2012.* Eur J Cancer, 2013. **49**(6): p. 1374-403.

6.   S.L. Whelan, D.M.P., and E. Masuyer, *Patterns of cancer in five continents.* Cancer incidence in five continents, ed. I.s.p. n.102. Vol. 5,1990.

7.   Cramer, J.D., et al., *Analysis of the rising incidence of thyroid cancer using the Surveillance, Epidemiology and End Results national cancer data registry.* Surgery, 2010. **148**(6): p. 1147-52; discussion 1152-3.

8.   Davies, L. and H.G. Welch, *Increasing incidence of thyroid cancer in the United States, 1973-2002.* JAMA, 2006. **295**(18): p. 2164-7.

9.   DeLellis, R.A., *Pathology and genetics of tumours of endocrine organs.* World Health Organization classification of tumours. 2004: Lyon : IARC Press, 2004.

10.   Xing, M., *Molecular pathogenesis and mechanisms of thyroid cancer.* Nat Rev Cancer, 2013. **13**(3): p. 184-99.

11.   Sastre-Perona, A. and P. Santisteban, *Role of the wnt pathway in thyroid cancer.* Front

Endocrinol (Lausanne), 2012. **3**: p. 31.

12.   Nikiforov, Y.E. and M.N. Nikiforova, *Molecular genetics and diagnosis of thyroid cancer.* Nat Rev Endocrinol, 2011. **7**(10): p. 569-80.

13.   Xing, M., *BRAF mutation in thyroid cancer.* Endocr Relat Cancer, 2005. **12**(2): p. 245-62.

14.   Xing, M., et al., *BRAF mutation predicts a poorer clinical prognosis for papillary thyroid cancer.* J Clin Endocrinol Metab, 2005. **90**(12): p. 6373-9.

15.   Tufano, R.P., et al., *BRAF mutation in papillary thyroid cancer and its value in tailoring initial treatment: a systematic review and meta-analysis.* Medicine (Baltimore), 2012. **91**(5): p. 274-86.

16.   Caronia, L.M., J.E. Phay, and M.H. Shah, *Role of BRAF in thyroid oncogenesis.* Clin Cancer Res, 2011. **17**(24): p. 7511-7.

17.   Liu, Z., et al., *Highly prevalent genetic alterations in receptor tyrosine kinases and phosphatidylinositol 3-kinase/akt and mitogen-activated protein kinase pathways in anaplastic and follicular thyroid cancers.* J Clin Endocrinol Metab, 2008. **93**(8): p. 3106-16.

18.   Marotta, V., et al., *RET/PTC rearrangement in benign and malignant thyroid diseases: a clinical standpoint.* Eur J Endocrinol, 2011. **165**(4): p. 499-507.

19.   Capdevila, J., et al., *New approaches in the management of radioiodine-refractory thyroid cancer: the molecular targeted therapy era.* Discov Med, 2010. **9**(45): p. 153-62.

20.   Lerch, C. and B. Richter, *Pharmacotherapy options for advanced thyroid cancer: a systematic review.* Drugs, 2012. **72**(1): p. 67-85.

21.   Deshpande, H.A., S. Roman, and J.A. Sosa, *New targeted therapies and other advances in the management of anaplastic thyroid cancer.* Curr Opin Oncol, 2013. **25**(1): p. 44-9.

22.   Granata, R., L. Locati, and L. Licitra, *Therapeutic strategies in the management of patients with metastatic anaplastic thyroid cancer: review of the current literature.* Curr Opin Oncol, 2013. **25**(3): p. 224-8.

23.   Sherman, S.I., *Cytotoxic chemotherapy for differentiated thyroid carcinoma.* Clin Oncol (R Coll Radiol), 2010. **22**(6): p. 464-8.

24.   Harada, T., et al., *Bleomycin treatment for cancer of the thyroid.* Am J Surg, 1971. **122**(1): p. 53-7.

25.   Matuszczyk, A., et al., *Chemotherapy with doxorubicin in progressive medullary and thyroid carcinoma of the follicular epithelium.* Horm Metab Res, 2008. **40**(3): p. 210-3.

26.   Wunderlich, A., et al., *Combined inhibition of cellular pathways as a future therapeutic option in fatal anaplastic thyroid cancer.* Endocrine, 2012. **42**(3): p. 637-46.

27.   Weinstein, I.B. and A. Joe, *Oncogene addiction.* Cancer Res, 2008. **68**(9): p. 3077-80; discussion 3080.

28.   Brilli, L. and F. Pacini, *Targeted therapy in refractory thyroid cancer: current achievements and limitations.* Future Oncol, 2011. **7**(5): p. 657-68.

29.   Regalbuto, C., et al., *Update on thyroid cancer treatment.* Future Oncol, 2012. **8**(10): p. 1331-48.

30.   Steeghs, N., J.W. Nortier, and H. Gelderblom, *Small molecule tyrosine kinase inhibitors in the treatment of solid tumors: an update of recent developments.* Ann Surg Oncol, 2007. **14**(2): p. 942-53.

31.   Coelho, S.M., D.P. Carvalho, and M. Vaisman, *New perspectives on the treatment of differentiated thyroid cancer.* Arq Bras Endocrinol Metabol, 2007. **51**(4): p. 612-24.

32.   Tamm, I., B. Dorken, and G. Hartmann, *Antisense therapy in oncology: new hope for an old idea?* Lancet, 2001. **358**(9280): p. 489-97.

33.   Showalter, H.D., et al., *5-[(Aminoalkyl)amino]-substituted anthra[1,9-cd]pyrazol-6(2H)-ones as novel anticancer agents. Synthesis and biological evaluation.* J Med Chem, 1984. **27**(3): p. 253-5.

34.   Zee-Cheng, R.K., et al., *Structural modification study of mitoxantrone (DHAQ). Chloro-substituted mono- and bis[(aminoalkyl)amino]anthraquinones.* J Med Chem, 1987. **30**(9): p. 1682-6.

35.   Martelli, S., et al., *Synthesis and antineoplastic evaluation of 1,4-bis(aminoalkanamido)-9,10-anthracenediones.* J Med Chem, 1988. **31**(10): p. 1956-9.

36.   Dzieduszycka, M., et al., *Synthesis, peroxidating ability, and antineoplastic evaluation of 1-[(aminoalkyl)amino]-4-hydroxy-10-imino-9-anthracenones.* J Med Chem, 1991. **34**(2):

p. 541-6.

37. Hantel, A., et al., *Phase I study and pharmacodynamics of piroxantrone (NSC 349174), a new anthrapyrazole.* Cancer Res, 1990. **50**(11): p. 3284-8.

38. Zalupski, M.M., et al., *Phase II trial of piroxantrone for advanced or metastatic soft tissue sarcomas. A Southwest Oncology Group study.* Invest New Drugs, 1993. **11**(4): p. 337-41.

39. Sosman, J.A., et al., *A phase II trial of piroxantrone in disseminated malignant melanoma. A Southwest Oncology Group study.* Invest New Drugs, 1995. **13**(1): p. 83-7.

40. Bennett, B.L., et al., *SP600125, an anthrapyrazolone inhibitor of Jun N-terminal kinase.* Proc Natl Acad Sci U S A, 2001. **98**(24): p. 13681-6.

41. Ishii, M., et al., *Inhibition of c-Jun NH2-terminal kinase activity improves ischemia/reperfusion injury in rat lungs.* J Immunol, 2004. **172**(4): p. 2569-77.

42. Guan, Q.H., et al., *The neuroprotective action of SP600125, a new inhibitor of JNK, on transient brain ischemia/reperfusion-induced neuronal death in rat hippocampal CA1 via nuclear and non-nuclear pathways.* Brain Res, 2005. **1035**(1): p. 51-9.

43. Wang, Y., et al., *SP600125, a selective JNK inhibitor, protects ischemic renal injury via suppressing the extrinsic pathways of apoptosis.* Life Sci, 2007. **80**(22): p. 2067-75.

44. Wolf, P.S., et al., *Stress-activated protein kinase inhibition to ameliorate lung ischemia reperfusion injury.* J Thorac Cardiovasc Surg, 2008. **135**(3): p. 656-65.

45. Chen, X., et al., *The c-Jun N-terminal kinase inhibitor SP600125 is neuroprotective in amygdala kindled rats.* Brain Res, 2010. **1357**: p. 104-14.

46. Xu, Y.F., et al., *Protective effects of SP600125 on renal ischemia-reperfusion injury in rats.* J Surg Res, 2011. **169**(1): p. e77-84.

47. Qiu, X.X., et al., *[Protective effects and mechanism of SP600125 on lung ischemia/reperfusion injury in rats].* Zhongguo Ying Yong Sheng Li Xue Za Zhi, 2012. **28**(3): p. 255-8.

48. Bain, J., et al., *The specificities of protein kinase inhibitors: an update.* Biochem J, 2003. **371**(Pt 1): p. 199-204.

49.   Franceschini, A., et al., *STRING v9.1: protein-protein interaction networks, with increased coverage and integration.* Nucleic Acids Res, 2013. **41**(Database issue): p. D808-15.

50.   Nakaya, K., et al., *A JNK inhibitor SP600125 induces defective cytokinesis and enlargement in P19 embryonal carcinoma cells.* Cell Biochem Funct, 2009. **27**(7): p. 468-72.

51.   Wang, M., et al., *JNK is constitutively active in mantle cell lymphoma: cell cycle deregulation and polyploidy by JNK inhibitor SP600125.* J Pathol, 2009. **218**(1): p. 95-103.

52.   Moon, D.O., Y.H. Choi, and G.Y. Kim, *Role of p21 in SP600125-induced cell cycle arrest, endoreduplication, and apoptosis.* Cell Mol Life Sci, 2011. **68**(19): p. 3249-60.

53.   Li, J.Y., et al., *SP600125, a JNK inhibitor, suppresses growth of JNK-inactive glioblastoma cells through cell-cycle G2/M phase arrest.* Pharmazie, 2012. **67**(11): p. 942-6.

54.   Schmidt, M., et al., *Ablation of the spindle assembly checkpoint by a compound targeting Mps1.* EMBO Rep, 2005. **6**(9): p. 866-72.

55.   Chu, M.L., et al., *Crystal structure of the catalytic domain of the mitotic checkpoint kinase Mps1 in complex with SP600125.* J Biol Chem, 2008. **283**(31): p. 21495-500.

56.   Kim, J.A., et al., *SP600125 suppresses Cdk1 and induces endoreplication directly from G2 phase, independent of JNK inhibition.* Oncogene, 2010. **29**(11): p. 1702-16.

57.   Jemaa, M., et al., *Selective killing of p53-deficient cancer cells by SP600125.* EMBO Mol Med, 2012. **4**(6): p. 500-14.

58.   Kastan, M.B. and J. Bartek, *Cell-cycle checkpoints and cancer.* Nature, 2004. **432**(7015): p. 316-23.

59.   Bieging, K.T. and L.D. Attardi, *Deconstructing p53 transcriptional networks in tumor suppression.* Trends Cell Biol, 2012. **22**(2): p. 97-106.

60.   Brady, C.A. and L.D. Attardi, *p53 at a glance.* J Cell Sci, 2010. **123**(Pt 15): p. 2527-32.

61.   Lamb, P. and L. Crawford, *Characterization of the human p53 gene.* Mol Cell Biol, 1986. **6**(5): p. 1379-85.

62.   Isobe, M., et al., *Localization of gene for human p53 tumour antigen to band 17p13.* Nature, 1986. **320**(6057): p. 84-5.

63.   Joerger, A.C. and A.R. Fersht, *The tumor suppressor p53: from structures to drug discovery.* Cold Spring Harb Perspect Biol, 2010. **2**(6): p. a000919.

64.   Bode, A.M. and Z. Dong, *Post-translational modification of p53 in tumorigenesis.* Nat Rev Cancer, 2004. **4**(10): p. 793-805.

65.   Waterman, M.J., et al., *ATM-dependent activation of p53 involves dephosphorylation and association with 14-3-3 proteins.* Nat Genet, 1998. **19**(2): p. 175-8.

66.   Buschmann, T., et al., *p53 phosphorylation and association with murine double minute 2, c-Jun NH2-terminal kinase, p14ARF, and p300/CBP during the cell cycle and after exposure to ultraviolet irradiation.* Cancer Res, 2000. **60**(4): p. 896-900.

67.   Barlev, N.A., et al., *Acetylation of p53 activates transcription through recruitment of coactivators/histone acetyltransferases.* Mol Cell, 2001. **8**(6): p. 1243-54.

68.   Gu, W. and R.G. Roeder, *Activation of p53 sequence-specific DNA binding by acetylation of the p53 C-terminal domain.* Cell, 1997. **90**(4): p. 595-606.

69.   Anderson, A., *Handbook of Cell Signaling.* 2009: Cold Spring Harbor Perspectives in Biology.

70.   Fuchs, S.Y., et al., *JNK targets p53 ubiquitination and degradation in nonstressed cells.* Genes Dev, 1998. **12**(17): p. 2658-63.

71.   Fuchs, S.Y., et al., *MEKK1/JNK signaling stabilizes and activates p53.* Proc Natl Acad Sci U S A, 1998. **95**(18): p. 10541-6.

72.   Leng, R.P., et al., *Pirh2, a p53-induced ubiquitin-protein ligase, promotes p53 degradation.* Cell, 2003. **112**(6): p. 779-91.

73.   Dornan, D., et al., *The ubiquitin ligase COP1 is a critical negative regulator of p53.* Nature, 2004. **429**(6987): p. 86-92.

74.   Li, H.H., et al., *Phosphorylation on Thr-55 by TAF1 mediates degradation of p53: a role for TAF1 in cell G1 progression.* Mol Cell, 2004. **13**(6): p. 867-78.

75.   Zhang, X.P., F. Liu, and W. Wang, *Two-phase dynamics of p53 in the DNA damage*

response. Proc Natl Acad Sci U S A, 2011. **108**(22): p. 8990-5.

76.   Kuerbitz, S.J., et al., *Wild-type p53 is a cell cycle checkpoint determinant following irradiation.* Proc Natl Acad Sci U S A, 1992. **89**(16): p. 7491-5.

77.   Brugarolas, J., et al., *Radiation-induced cell cycle arrest compromised by p21 deficiency.* Nature, 1995. **377**(6549): p. 552-7.

78.   Deng, C., et al., *Mice lacking p21CIP1/WAF1 undergo normal development, but are defective in G1 checkpoint control.* Cell, 1995. **82**(4): p. 675-84.

79.   Wang, S., et al., *Molecular imaging of p53 signal pathway in lung cancer cell cycle arrest induced by cisplatin.* Mol Carcinog, 2012.

80.   Zhan, Q., et al., *Tumor suppressor p53 can participate in transcriptional induction of the GADD45 promoter in the absence of direct DNA binding.* Mol Cell Biol, 1998. **18**(5): p. 2768-78.

81.   Hermeking, H., et al., *14-3-3 sigma is a p53-regulated inhibitor of G2/M progression.* Mol Cell, 1997. **1**(1): p. 3-11.

82.   A. Augert, D.B., *Immunosenescence and Senescence Immunosurveillance: One of the Possible Links Explaining the Cancer Incidence in Ageing Population*, in *Senescence and Senescence-Related Disorders*, Intech, Editor. 2013, Zhiwei Wang and Hiroyuki Inuzuka.

83.   Haferkamp, T.B.S., *Molecular Mechanisms of Cellular Senescence*, in *Senescence and Senescence-Related Disorders*, Intech, Editor. 2013, Zhiwei Wang and Hiroyuki Inuzuka.

84.   Ben-Porath, I. and R.A. Weinberg, *The signals and pathways activating cellular senescence.* Int J Biochem Cell Biol, 2005. **37**(5): p. 961-76.

85.   Rufini, A., et al., *Senescence and aging: the critical roles of p53.* Oncogene, 2013. **32**(43): p. 5129-43.

86.   Castedo, M., et al., *Cell death by mitotic catastrophe: a molecular definition.* Oncogene, 2004. **23**(16): p. 2825-37.

87.   Lanni, J.S. and T. Jacks, *Characterization of the p53-dependent postmitotic checkpoint following spindle disruption.* Mol Cell Biol, 1998. **18**(2): p. 1055-64.

88.   Hawkins, D.S., G.W. Demers, and D.A. Galloway, *Inactivation of p53 enhances*

sensitivity to multiple chemotherapeutic agents. Cancer Res, 1996. **56**(4): p. 892-8.

89.   Kroemer, G., et al., *Classification of cell death: recommendations of the Nomenclature Committee on Cell Death 2009.* Cell Death Differ, 2009. **16**(1): p. 3-11.

90.   Vitale, I., et al., *Mitotic catastrophe: a mechanism for avoiding genomic instability.* Nat Rev Mol Cell Biol, 2011. **12**(6): p. 385-92.

91.   Vousden, K.H. and C. Prives, *Blinded by the Light: The Growing Complexity of p53.* Cell, 2009. **137**(3): p. 413-31.

92.   Laptenko, O. and C. Prives, *Transcriptional regulation by p53: one protein, many possibilities.* Cell Death Differ, 2006. **13**(6): p. 951-61.

93.   Speidel, D., *Transcription-independent p53 apoptosis: an alternative route to death.* Trends Cell Biol, 2010. **20**(1): p. 14-24.

94.   Mihara, M., et al., *p53 has a direct apoptogenic role at the mitochondria.* Mol Cell, 2003. **11**(3): p. 577-90.

95.   Sykes, S.M., et al., *Acetylation of the DNA binding domain regulates transcription-independent apoptosis by p53.* J Biol Chem, 2009. **284**(30): p. 20197-205.

96.   Jiang, P., et al., *The Bad guy cooperates with good cop p53: Bad is transcriptionally up-regulated by p53 and forms a Bad/p53 complex at the mitochondria to induce apoptosis.* Mol Cell Biol, 2006. **26**(23): p. 9071-82.

97.   Li, M., et al., *Mono- versus polyubiquitination: differential control of p53 fate by Mdm2.* Science, 2003. **302**(5652): p. 1972-5.

98.   R&D-Systems. 2013; Available from: http://www.rndsystems.com/cb_detail_objectname_SP04_p53.aspx.

99.   Malaguarnera, R., et al., *p53 family proteins in thyroid cancer.* Endocr Relat Cancer, 2007. **14**(1): p. 43-60.

100.   Morita, N., Y. Ikeda, and H. Takami, *Clinical significance of p53 protein expression in papillary thyroid carcinoma.* World J Surg, 2008. **32**(12): p. 2617-22.

101.   Pollina, L., et al., *bcl-2, p53 and proliferating cell nuclear antigen expression is related to the degree of differentiation in thyroid carcinomas.* Br J Cancer, 1996. **73**(2): p. 139-

43.

102.   Lowe, S.W., et al., *p53 status and the efficacy of cancer therapy in vivo.* Science, 1994. **266**(5186): p. 807-10.

103.   Blagosklonny, M.V., et al., *Effects of p53-expressing adenovirus on the chemosensitivity and differentiation of anaplastic thyroid cancer cells.* J Clin Endocrinol Metab, 1998. **83**(7): p. 2516-22.

104.   Imanishi, R., et al., *A histone deacetylase inhibitor enhances killing of undifferentiated thyroid carcinoma cells by p53 gene therapy.* J Clin Endocrinol Metab, 2002. **87**(10): p. 4821-4.

105.   Petitjean, A., et al., *Impact of mutant p53 functional properties on TP53 mutation patterns and tumor phenotype: lessons from recent developments in the IARC TP53 database.* Hum Mutat, 2007. **28**(6): p. 622-9.

106.   de Forges, H., A. Bouissou, and F. Perez, *Interplay between microtubule dynamics and intracellular organization.* Int J Biochem Cell Biol, 2012. **44**(2): p. 266-74.

107.   Janke, C. and J.C. Bulinski, *Post-translational regulation of the microtubule cytoskeleton: mechanisms and functions.* Nat Rev Mol Cell Biol, 2011. **12**(12): p. 773-86.

108.   Harvey Lodish; Arnold Berk, C.A.K., Monty Krieger, Anthony Bretscher, Hidde Ploegh, Angelika Amon, Matthew P. Scott, *Cell Organization and Movement II: Microtubules and Intermediate Filaments*, in *Molecular Cell Biology.*, W.H.F.a. Company., Editor. 2012, W. H. Freeman and Company.: new York.

109.   Akhmanova, A. and M.O. Steinmetz, *Tracking the ends: a dynamic protein network controls the fate of microtubule tips.* Nat Rev Mol Cell Biol, 2008. **9**(4): p. 309-22.

110.   Vallee, R.B., et al., *Dynein: An ancient motor protein involved in multiple modes of transport.* J Neurobiol, 2004. **58**(2): p. 189-200.

111.   Verhey, K.J. and J.W. Hammond, *Traffic control: regulation of kinesin motors.* Nat Rev Mol Cell Biol, 2009. **10**(11): p. 765-77.

112.   Howard, J. and A.A. Hyman, *Microtubule polymerases and depolymerases.* Curr Opin Cell Biol, 2007. **19**(1): p. 31-5.

113.   Roll-Mecak, A. and F.J. McNally, *Microtubule-severing enzymes.* Curr Opin Cell Biol,

2010. **22**(1): p. 96-103.

114. Schuyler, S.C. and D. Pellman, *Microtubule "plus-end-tracking proteins": The end is just the beginning.* Cell, 2001. **105**(4): p. 421-4.

115. Arnal, I., et al., *CLIP-170/tubulin-curved oligomers coassemble at microtubule ends and promote rescues.* Curr Biol, 2004. **14**(23): p. 2086-95.

116. Perez, F., et al., *CLIP-170 highlights growing microtubule ends in vivo.* Cell, 1999. **96**(4): p. 517-27.

117. Bieling, P., et al., *Reconstitution of a microtubule plus-end tracking system in vitro.* Nature, 2007. **450**(7172): p. 1100-5.

118. Wloga, D. and J. Gaertig, *Post-translational modifications of microtubules.* J Cell Sci, 2010. **123**(Pt 20): p. 3447-55.

119. Hammond, J.W., D. Cai, and K.J. Verhey, *Tubulin modifications and their cellular functions.* Curr Opin Cell Biol, 2008. **20**(1): p. 71-6.

120. Fourest-Lieuvin, A., et al., *Microtubule regulation in mitosis: tubulin phosphorylation by the cyclin-dependent kinase Cdk1.* Mol Biol Cell, 2006. **17**(3): p. 1041-50.

121. Verhey, K.J. and J. Gaertig, *The tubulin code.* Cell Cycle, 2007. **6**(17): p. 2152-60.

122. Westermann, S. and K. Weber, *Post-translational modifications regulate microtubule function.* Nat Rev Mol Cell Biol, 2003. **4**(12): p. 938-47.

123. Rodriguez de la Vega, M., et al., *Nna1-like proteins are active metallocarboxypeptidases of a new and diverse M14 subfamily.* FASEB J, 2007. **21**(3): p. 851-65.

124. Lafanechere, L. and D. Job, *The third tubulin pool.* Neurochem Res, 2000. **25**(1): p. 11-8.

125. Liao, G. and G.G. Gundersen, *Kinesin is a candidate for cross-bridging microtubules and intermediate filaments. Selective binding of kinesin to detyrosinated tubulin and vimentin.* J Biol Chem, 1998. **273**(16): p. 9797-803.

126. Kreitzer, G., G. Liao, and G.G. Gundersen, *Detyrosination of tubulin regulates the interaction of intermediate filaments with microtubules in vivo via a kinesin-dependent mechanism.* Mol Biol Cell, 1999. **10**(4): p. 1105-18.

127. Lin, S.X., G.G. Gundersen, and F.R. Maxfield, *Export from pericentriolar endocytic*

recycling compartment to cell surface depends on stable, detyrosinated (glu) microtubules and kinesin. Mol Biol Cell, 2002. **13**(1): p. 96-109.

128. Lafanechere, L., et al., *Suppression of tubulin tyrosine ligase during tumor growth.* J Cell Sci, 1998. **111 (Pt 2)**: p. 171-81.

129. Soucek, K., et al., *Normal and prostate cancer cells display distinct molecular profiles of alpha-tubulin posttranslational modifications.* Prostate, 2006. **66**(9): p. 954-65.

130. Mialhe, A., et al., *Tubulin detyrosination is a frequent occurrence in breast cancers of poor prognosis.* Cancer Res, 2001. **61**(13): p. 5024-7.

131. Redeker, V., et al., *Mutations of tubulin glycylation sites reveal cross-talk between the C termini of alpha- and beta-tubulin and affect the ciliary matrix in Tetrahymena.* J Biol Chem, 2005. **280**(1): p. 596-606.

132. Thazhath, R., C. Liu, and J. Gaertig, *Polyglycylation domain of beta-tubulin maintains axonemal architecture and affects cytokinesis in Tetrahymena.* Nat Cell Biol, 2002. **4**(3): p. 256-9.

133. Campbell, P.K., et al., *Mutation of a novel gene results in abnormal development of spermatid flagella, loss of intermale aggression and reduced body fat in mice.* Genetics, 2002. **162**(1): p. 307-20.

134. Janke, C., et al., *Tubulin polyglutamylase enzymes are members of the TTL domain protein family.* Science, 2005. **308**(5729): p. 1758-62.

135. Kimura, Y., et al., *Identification of tubulin deglutamylase among Caenorhabditis elegans and mammalian cytosolic carboxypeptidases (CCPs).* J Biol Chem, 2010. **285**(30): p. 22936-41.

136. Akella, J.S., et al., *MEC-17 is an alpha-tubulin acetyltransferase.* Nature, 2010. **467**(7312): p. 218-22.

137. Hubbert, C., et al., *HDAC6 is a microtubule-associated deacetylase.* Nature, 2002. **417**(6887): p. 455-8.

138. Matsuyama, A., et al., *In vivo destabilization of dynamic microtubules by HDAC6-mediated deacetylation.* EMBO J, 2002. **21**(24): p. 6820-31.

139. North, B.J., et al., *The human Sir2 ortholog, SIRT2, is an NAD+-dependent tubulin*

deacetylase. Mol Cell, 2003. **11**(2): p. 437-44.

140.   Bulinski, J.C., *Microtubule modification: acetylation speeds anterograde traffic flow.* Curr Biol, 2007. **17**(1): p. R18-20.

141.   Mellad, J.A., D.T. Warren, and C.M. Shanahan, *Nesprins LINC the nucleus and cytoskeleton.* Curr Opin Cell Biol, 2011. **23**(1): p. 47-54.

142.   Razafsky, D. and D. Hodzic, *Bringing KASH under the SUN: the many faces of nucleo-cytoskeletal connections.* J Cell Biol, 2009. **186**(4): p. 461-72.

143.   Wozniak, M.J., et al., *Role of kinesin-1 and cytoplasmic dynein in endoplasmic reticulum movement in VERO cells.* J Cell Sci, 2009. **122**(Pt 12): p. 1979-89.

144.   Smyth, J.T., et al., *Role of the microtubule cytoskeleton in the function of the store-operated Ca2+ channel activator STIM1.* J Cell Sci, 2007. **120**(Pt 21): p. 3762-71.

145.   Cole, N.B., et al., *Golgi dispersal during microtubule disruption: regeneration of Golgi stacks at peripheral endoplasmic reticulum exit sites.* Mol Biol Cell, 1996. **7**(4): p. 631-50.

146.   Allan, V.J., H.M. Thompson, and M.A. McNiven, *Motoring around the Golgi.* Nat Cell Biol, 2002. **4**(10): p. E236-42.

147.   Rios, R.M., et al., *GMAP-210 recruits gamma-tubulin complexes to cis-Golgi membranes and is required for Golgi ribbon formation.* Cell, 2004. **118**(3): p. 323-35.

148.   Efimov, A., et al., *Asymmetric CLASP-dependent nucleation of noncentrosomal microtubules at the trans-Golgi network.* Dev Cell, 2007. **12**(6): p. 917-30.

149.   Yaffe, M.P., N. Stuurman, and R.D. Vale, *Mitochondrial positioning in fission yeast is driven by association with dynamic microtubules and mitotic spindle poles.* Proc Natl Acad Sci U S A, 2003. **100**(20): p. 11424-8.

150.   Vicente-Manzanares, M., D.J. Webb, and A.R. Horwitz, *Cell migration at a glance.* J Cell Sci, 2005. **118**(Pt 21): p. 4917-9.

151.   Pollard, T.D. and G.G. Borisy, *Cellular motility driven by assembly and disassembly of actin filaments.* Cell, 2003. **112**(4): p. 453-65.

152.   Doherty, G.J. and H.T. McMahon, *Mediation, modulation, and consequences of*

membrane-cytoskeleton interactions. Annu Rev Biophys, 2008. **37**: p. 65-95.

153.   Amin, N. and E. Vincan, *The Wnt signaling pathways and cell adhesion.* Front Biosci (Landmark Ed), 2012. **17**: p. 784-804.

154.   Jaffe, A.B. and A. Hall, *Rho GTPases: biochemistry and biology.* Annu Rev Cell Dev Biol, 2005. **21**: p. 247-69.

155.   Li, Y., D. Shin, and S.H. Kwon, *Histone deacetylase 6 plays a role as a distinct regulator of diverse cellular processes.* FEBS J, 2013. **280**(3): p. 775-93.

156.   Valenzuela-Fernandez, A., et al., *HDAC6: a key regulator of cytoskeleton, cell migration and cell-cell interactions.* Trends Cell Biol, 2008. **18**(6): p. 291-7.

157.   Schofield, A.V., C. Gamell, and O. Bernard, *Tubulin polymerization promoting protein 1 (TPPP1) increases beta-catenin expression through inhibition of HDAC6 activity in U2OS osteosarcoma cells.* Biochem Biophys Res Commun, 2013. **436**(4): p. 571-7.

158.   Muller, T., et al., *Regulation of epithelial cell migration and tumor formation by beta-catenin signaling.* Exp Cell Res, 2002. **280**(1): p. 119-33.

159.   J. Hardin, G.P.B., L. J. Kleinsmith *Becker's World of the Cell: International Edition*. 8 ed. 2011: Pearson Higher Ed.

160.   Rosenblatt, J., *Spindle assembly: asters part their separate ways.* Nat Cell Biol, 2005. **7**(3): p. 219-22.

161.   Meunier, S. and I. Vernos, *Microtubule assembly during mitosis - from distinct origins to distinct functions?* J Cell Sci, 2012. **125**(Pt 12): p. 2805-14.

162.   Joglekar, A.P., K.S. Bloom, and E.D. Salmon, *Mechanisms of force generation by end-on kinetochore-microtubule attachments.* Curr Opin Cell Biol, 2010. **22**(1): p. 57-67.

163.   Salmon, E.D., et al., *Merotelic kinetochores in mammalian tissue cells.* Philos Trans R Soc Lond B Biol Sci, 2005. **360**(1455): p. 553-68.

164.   Ruchaud, S., M. Carmena, and W.C. Earnshaw, *Chromosomal passengers: conducting cell division.* Nat Rev Mol Cell Biol, 2007. **8**(10): p. 798-812.

165.   Vader, G., et al., *The chromosomal passenger complex controls spindle checkpoint function independent from its role in correcting microtubule kinetochore interactions.*

Mol Biol Cell, 2007. **18**(11): p. 4553-64.

166.   Harrison, M.R., K.D. Holen, and G. Liu, *Beyond taxanes: a review of novel agents that target mitotic tubulin and microtubules, kinases, and kinesins.* Clin Adv Hematol Oncol, 2009. **7**(1): p. 54-64.

167.   Morris, P.G. and M.N. Fornier, *Microtubule active agents: beyond the taxane frontier.* Clin Cancer Res, 2008. **14**(22): p. 7167-72.

168.   Rowinsky EK, C.E., *Novel agents that target tublin and related elements.* Semin Oncol. 2006 2006. **33**(4): p. 32.

169.   Rai, S.S. and J. Wolff, *Localization of the vinblastine-binding site on beta-tubulin.* J Biol Chem, 1996. **271**(25): p. 14707-11.

170.   Gerth, K., et al., *Epothilons A and B: antifungal and cytotoxic compounds from Sorangium cellulosum (Myxobacteria). Production, physico-chemical and biological properties.* J Antibiot (Tokyo), 1996. **49**(6): p. 560-3.

171.   Liu, J., et al., *In vitro and in vivo anticancer activities of synthetic (-)-laulimalide, a marine natural product microtubule stabilizing agent.* Anticancer Res, 2007. **27**(3B): p. 1509-18.

172.   Wilmes, A., et al., *Peloruside A synergizes with other microtubule stabilizing agents in cultured cancer cell lines.* Mol Pharm, 2007. **4**(2): p. 269-80.

173.   Schweppe, R.E., et al., *Deoxyribonucleic acid profiling analysis of 40 human thyroid cancer cell lines reveals cross-contamination resulting in cell line redundancy and misidentification.* J Clin Endocrinol Metab, 2008. **93**(11): p. 4331-41.

174.   Rao, A.S., et al., *Letter Re: Id1 gene expression in hyperplastic and neoplastic thyroid tissues.* J Clin Endocrinol Metab, 2005. **90**(10): p. 5906.

175.   Holting, T., et al., *Transforming growth factor-beta 1 is a negative regulator for differentiated thyroid cancer: studies of growth, migration, invasion, and adhesion of cultured follicular and papillary thyroid cancer cell lines.* J Clin Endocrinol Metab, 1994. **79**(3): p. 806-13.

176.   Liu, D., et al., *Genetic alterations in the phosphoinositide 3-kinase/Akt signaling pathway confer sensitivity of thyroid cancer cells to therapeutic targeting of Akt and*

mammalian target of rapamycin. Cancer Res, 2009. **69**(18): p. 7311-9.

177. Ishizaka, Y., et al., *Presence of aberrant transcripts of ret proto-oncogene in a human papillary thyroid carcinoma cell line.* Jpn J Cancer Res, 1989. **80**(12): p. 1149-52.

178. Ishizaka, Y., et al., *cDNA cloning and characterization of ret activated in a human papillary thyroid carcinoma cell line.* Biochem Biophys Res Commun, 1990. **168**(2): p. 402-8.

179. Castellone, M.D., et al., *Autocrine stimulation by osteopontin plays a pivotal role in the expression of the mitogenic and invasive phenotype of RET/PTC-transformed thyroid cells.* Oncogene, 2004. **23**(12): p. 2188-96.

180. Jossart, G.H., et al., *Molecular and cytogenetic characterization of a t(1;10;21) translocation in the human papillary thyroid cancer cell line TPC-1 expressing the ret/H4 chimeric transcript.* Surgery, 1995. **118**(6): p. 1018-23.

181. Jensen, K., et al., *Inhibition of gap junction transfer sensitizes thyroid cancer cells to anoikis.* Endocr Relat Cancer, 2011. **18**(5): p. 613-26.

182. Tanaka, J., et al., *Establishment and biological characterization of an in vitro human cytomegalovirus latency model.* Virology, 1987. **161**(1): p. 62-72.

183. Enomoto, T., et al., *Establishment of a human undifferentiated thyroid cancer cell line producing several growth factors and cytokines.* Cancer, 1990. **65**(9): p. 1971-9.

184. Fogh, J., J.M. Fogh, and T. Orfeo, *One hundred and twenty-seven cultured human tumor cell lines producing tumors in nude mice.* J Natl Cancer Inst, 1977. **59**(1): p. 221-6.

185. Fogh, J., W.C. Wright, and J.D. Loveless, *Absence of HeLa cell contamination in 169 cell lines derived from human tumors.* J Natl Cancer Inst, 1977. **58**(2): p. 209-14.

186. Lin, J.D., et al., *Establishment of xenografts and cell lines from well-differentiated human thyroid carcinoma.* J Surg Oncol, 1996. **63**(2): p. 112-8.

187. Aust, G., et al., *Human thyroid carcinoma cell lines and normal thyrocytes: expression and regulation of matrix metalloproteinase-1 and tissue matrix metalloproteinase inhibitor-1 messenger-RNA and protein.* Thyroid, 1997. **7**(5): p. 713-24.

188. Heldin, N.E., et al., *Aberrant expression of receptors for platelet-derived growth factor in an anaplastic thyroid carcinoma cell line.* Proc Natl Acad Sci U S A, 1988. **85**(23): p.

9302-6.

189.   Heldin, N.E., et al., *Coexpression of functionally active receptors for thyrotropin and platelet-derived growth factor in human thyroid carcinoma cells.* Endocrinology, 1991. **129**(4): p. 2187-93.

190.   Heldin, N.E. and B. Westermark, *Epidermal growth factor, but not thyrotropin, stimulates the expression of c-fos and c-myc messenger ribonucleic acid in porcine thyroid follicle cells in primary culture.* Endocrinology, 1988. **122**(3): p. 1042-6.

191.   neoplasia, A.i.t., *Mario Andreoli, Fabrizio Monaco, Jacob Robbins.* Vol. RC280T6 A28 1981 1981.

192.   Behr, T.M., et al., *Improved treatment of medullary thyroid cancer in a nude mouse model by combined radioimmunochemotherapy: doxorubicin potentiates the therapeutic efficacy of radiolabeled antibodies in a radioresistant tumor type.* Cancer Res, 1997. **57**(23): p. 5309-19.

193.   Carlomagno, F., et al., *Point mutation of the RET proto-oncogene in the TT human medullary thyroid carcinoma cell line.* Biochem Biophys Res Commun, 1995. **207**(3): p. 1022-8.

194.   Giannakakou, P., et al., *p53 is associated with cellular microtubules and is transported to the nucleus by dynein.* Nat Cell Biol, 2000. **2**(10): p. 709-17.

195.   Hood, K.A., et al., *Peloruside A, a novel antimitotic agent with paclitaxel-like microtubule- stabilizing activity.* Cancer Res, 2002. **62**(12): p. 3356-60.

196.   Laemmli, U.K., *Cleavage of structural proteins during the assembly of the head of bacteriophage T4.* Nature, 1970. **227**(5259): p. 680-5.

197.   Ed Harlow, D.L., *Antibodies: A Laboratory Manual.* 1988: Cold Spring Harbor Laboratory Press.

198.   Ngoka, L.C., *Sample prep for proteomics of breast cancer: proteomics and gene ontology reveal dramatic differences in protein solubilization preferences of radioimmunoprecipitation assay and urea lysis buffers.* Proteome Sci, 2008. **6**: p. 30.

199.   Smith, P.K., et al., *Measurement of protein using bicinchoninic acid.* Anal Biochem, 1985. **150**(1): p. 76-85.

200.   Szklarczyk, D., et al., *The STRING database in 2011: functional interaction networks of proteins, globally integrated and scored.* Nucleic Acids Res, 2011. **39**(Database issue): p. D561-8.

201.   Kuhn, M., et al., *STITCH: interaction networks of chemicals and proteins.* Nucleic Acids Res, 2008. **36**(Database issue): p. D684-8.

202.   Kuhn, M., et al., *STITCH 2: an interaction network database for small molecules and proteins.* Nucleic Acids Res, 2010. **38**(Database issue): p. D552-6.

203.   Kuhn, M., et al., *STITCH 3: zooming in on protein-chemical interactions.* Nucleic Acids Res, 2012. **40**(Database issue): p. D876-80.

204.   Kim, J.H., et al., *SP600125 overcomes antimitotic drug-resistance in cancer cells by increasing apoptosis with independence of P-gp inhibition.* Eur J Pharmacol, 2013.

205.   Ennis, B.W., et al., *Inhibition of tumor growth, angiogenesis, and tumor cell proliferation by a small molecule inhibitor of c-Jun N-terminal kinase.* J Pharmacol Exp Ther, 2005. **313**(1): p. 325-32.

206.   Kuntzen, C., et al., *Inhibition of c-Jun-N-terminal-kinase sensitizes tumor cells to CD95-induced apoptosis and induces G2/M cell cycle arrest.* Cancer Res, 2005. **65**(15): p. 6780-8.

207.   Miyamoto-Yamasaki, Y., et al., *Induction of endoreduplication by a JNK inhibitor SP600125 in human lung carcinoma A 549 cells.* Cell Biol Int, 2007. **31**(12): p. 1501-6.

208.   Moon, D.O., et al., *JNK inhibitor SP600125 promotes the formation of polymerized tubulin, leading to G2/M phase arrest, endoreduplication, and delayed apoptosis.* Exp Mol Med, 2009. **41**(9): p. 665-77.

209.   Kuntzen, C., V. Gulberg, and A.L. Gerbes, *Use of a mixed endothelin receptor antagonist in portopulmonary hypertension: a safe and effective therapy?* Gastroenterology, 2005. **128**(1): p. 164-8.

210.   Mingo-Sion, A.M., et al., *Inhibition of JNK reduces G2/M transit independent of p53, leading to endoreduplication, decreased proliferation, and apoptosis in breast cancer cells.* Oncogene, 2004. **23**(2): p. 596-604.

211.   Bykov, V.J., et al., *Reactivation of mutant p53 and induction of apoptosis in human*

tumor cells by maleimide analogs. J Biol Chem, 2005. **280**(34): p. 30384-91.

212. Bykov, V.J., et al., *Restoration of the tumor suppressor function to mutant p53 by a low-molecular-weight compound.* Nat Med, 2002. **8**(3): p. 282-8.

213. Yu, X., et al., *Allele-specific p53 mutant reactivation.* Cancer Cell, 2012. **21**(5): p. 614-25.

214. North, S., et al., *Restoration of wild-type conformation and activity of a temperature-sensitive mutant of p53 (p53(V272M)) by the cytoprotective aminothiol WR1065 in the esophageal cancer cell line TE-1.* Mol Carcinog, 2002. **33**(3): p. 181-8.

215. Lin, H.Y., et al., *Resveratrol induced serine phosphorylation of p53 causes apoptosis in a mutant p53 prostate cancer cell line.* J Urol, 2002. **168**(2): p. 748-55.

216. Christophorou, M.A., et al., *The pathological response to DNA damage does not contribute to p53-mediated tumour suppression.* Nature, 2006. **443**(7108): p. 214-7.

217. Lowe, S.W., E. Cepero, and G. Evan, *Intrinsic tumour suppression.* Nature, 2004. **432**(7015): p. 307-15.

218. Xue, W., et al., *Senescence and tumour clearance is triggered by p53 restoration in murine liver carcinomas.* Nature, 2007. **445**(7128): p. 656-60.

219. Joerger, A.C. and A.R. Fersht, *Structure-function-rescue: the diverse nature of common p53 cancer mutants.* Oncogene, 2007. **26**(15): p. 2226-42.

220. Joerger, A.C. and A.R. Fersht, *Structural biology of the tumor suppressor p53 and cancer-associated mutants.* Adv Cancer Res, 2007. **97**: p. 1-23.

221. Hupp, T.R. and D.P. Lane, *Allosteric activation of latent p53 tetramers.* Curr Biol, 1994. **4**(10): p. 865-75.

222. Sablina, A.A., et al., *Activation of p53-mediated cell cycle checkpoint in response to micronuclei formation.* J Cell Sci, 1998. **111 (Pt 7)**: p. 977-84.

223. Derry, W.B., L. Wilson, and M.A. Jordan, *Low potency of taxol at microtubule minus ends: implications for its antimitotic and therapeutic mechanism.* Cancer Res, 1998. **58**(6): p. 1177-84.

224. Ngan, V.K., et al., *Novel actions of the antitumor drugs vinflunine and vinorelbine on*

microtubules. Cancer Res, 2000. **60**(18): p. 5045-51.

225.   Giannakakou, P., et al., *Enhanced microtubule-dependent trafficking and p53 nuclear accumulation by suppression of microtubule dynamics.* Proc Natl Acad Sci U S A, 2002. **99**(16): p. 10855-60.

226.   Stewart, Z.A., L.J. Tang, and J.A. Pietenpol, *Increased p53 phosphorylation after microtubule disruption is mediated in a microtubule inhibitor- and cell-specific manner.* Oncogene, 2001. **20**(1): p. 113-24.

227.   Maclaine, N.J. and T.R. Hupp, *The regulation of p53 by phosphorylation: a model for how distinct signals integrate into the p53 pathway.* Aging (Albany NY), 2009. **1**(5): p. 490-502.

228.   Kodama, M., et al., *Requirement of ATM for rapid p53 phosphorylation at Ser46 without Ser/Thr-Gln sequences.* Mol Cell Biol, 2010. **30**(7): p. 1620-33.

229.   Bershadsky, A., et al., *Involvement of microtubules in the control of adhesion-dependent signal transduction.* Curr Biol, 1996. **6**(10): p. 1279-89.

230.   Wang, L.G., et al., *The effect of antimicrotubule agents on signal transduction pathways of apoptosis: a review.* Cancer Chemother Pharmacol, 1999. **44**(5): p. 355-61.

231.   Sablina, A.A., et al., *p53 activation in response to microtubule disruption is mediated by integrin-Erk signaling.* Oncogene, 2001. **20**(8): p. 899-909.

232.   Umeyama, T., et al., *Dynamics of microtubules bundled by microtubule associated protein 2C (MAP2C).* J Cell Biol, 1993. **120**(2): p. 451-65.

233.   Bratman, S.V. and F. Chang, *Mechanisms for maintaining microtubule bundles.* Trends Cell Biol, 2008. **18**(12): p. 580-6.

234.   Schiff, P.B. and S.B. Horwitz, *Taxol stabilizes microtubules in mouse fibroblast cells.* Proc Natl Acad Sci U S A, 1980. **77**(3): p. 1561-5.

235.   Thompson, W.C., L. Wilson, and D.L. Purich, *Taxol induces microtubule assembly at low temperature.* Cell Motil, 1981. **1**(4): p. 445-54.

236.   Hausmann, K., M. Linnenbach, and D.J. Patterson, *The effects of taxol on microtubular arrays: in vivo effects on heliozoan axonemes.* J Ultrastruct Res, 1983. **82**(2): p. 212-20.

237.   William T Beck, C.E.C.a.P.J.H., *Microtubule-Targeting Anticancer Drugs Derived from Plants and Microbes: Vinca Alkaloids, Taxanes, and Epothilones*, in *Holland-Frei Cancer Medicine*, K.D. Bast RC Jr, Pollock RE, Editor. 2000, BC Decker.

238.   Arthur, C.R., et al., *Autophagic cell death, polyploidy and senescence induced in breast tumor cells by the substituted pyrrole JG-03-14, a novel microtubule poison.* Biochem Pharmacol, 2007. **74**(7): p. 981-91.

239.   Klein, L.E., et al., *The microtubule stabilizing agent discodermolide is a potent inducer of accelerated cell senescence.* Cell Cycle, 2005. **4**(3): p. 501-7.

240.   Tierno, M.B., et al., *Microtubule binding and disruption and induction of premature senescence by disorazole C(1).* J Pharmacol Exp Ther, 2009. **328**(3): p. 715-22.

241.   Hayot, C., et al., *In vitro pharmacological characterizations of the anti-angiogenic and anti-tumor cell migration properties mediated by microtubule-affecting drugs, with special emphasis on the organization of the actin cytoskeleton.* Int J Oncol, 2002. **21**(2): p. 417-25.

242.   Liao, G., T. Nagasaki, and G.G. Gundersen, *Low concentrations of nocodazole interfere with fibroblast locomotion without significantly affecting microtubule level: implications for the role of dynamic microtubules in cell locomotion.* J Cell Sci, 1995. **108 (Pt 11)**: p. 3473-83.

243.   Schwartz, E.L., *Antivascular actions of microtubule-binding drugs.* Clin Cancer Res, 2009. **15**(8): p. 2594-601.

244.   Liu, S.M., K.E. Magnusson, and T. Sundqvist, *Microtubules are involved in transport of macromolecules by vesicles in cultured bovine aortic endothelial cells.* J Cell Physiol, 1993. **156**(2): p. 311-6.

245.   Waterman-Storer, C.M. and E. Salmon, *Positive feedback interactions between microtubule and actin dynamics during cell motility.* Curr Opin Cell Biol, 1999. **11**(1): p. 61-7.

246.   Zhou, X., J. Li, and D.F. Kucik, *The microtubule cytoskeleton participates in control of beta2 integrin avidity.* J Biol Chem, 2001. **276**(48): p. 44762-9.

247.   Bijman, M.N., et al., *Microtubule-targeting agents inhibit angiogenesis at subtoxic*

concentrations, a process associated with inhibition of Rac1 and Cdc42 activity and changes in the endothelial cytoskeleton. Mol Cancer Ther, 2006. **5**(9): p. 2348-57.

248. Bolden, J.E., M.J. Peart, and R.W. Johnstone, *Anticancer activities of histone deacetylase inhibitors.* Nat Rev Drug Discov, 2006. **5**(9): p. 769-84.

249. Mann, B.S., et al., *FDA approval summary: vorinostat for treatment of advanced primary cutaneous T-cell lymphoma.* Oncologist, 2007. **12**(10): p. 1247-52.

250. Li, D., N.D. Marchenko, and U.M. Moll, *SAHA shows preferential cytotoxicity in mutant p53 cancer cells by destabilizing mutant p53 through inhibition of the HDAC6-Hsp90 chaperone axis.* Cell Death Differ, 2011. **18**(12): p. 1904-13.

251. Schofield, A.V., R. Steel, and O. Bernard, *Rho-associated coiled-coil kinase (ROCK) protein controls microtubule dynamics in a novel signaling pathway that regulates cell migration.* J Biol Chem, 2012. **287**(52): p. 43620-9.

252. Ge, X., et al., *PCAF acetylates {beta}-catenin and improves its stability.* Mol Biol Cell, 2009. **20**(1): p. 419-27.

"You Can Run All Your Life,

But Not Go Anywhere"

M. Ness